ISSN 1023-9855

Thoracic Medicine

Volume 38 • Number 4 • December 2023

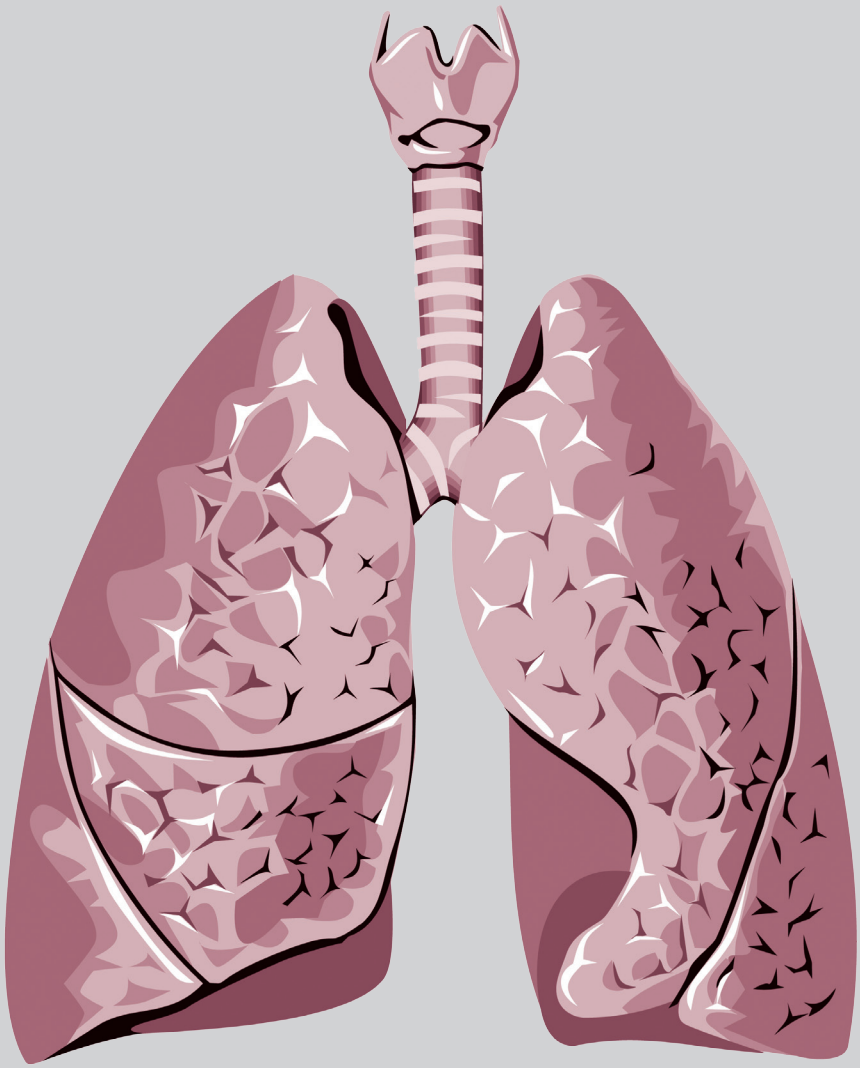

The Official Journal of

Taiwan Society of Pulmonary and Critical Care Medicine

Taiwan Society of Sleep Medicine

Taiwan Society for Respiratory Therapy

Taiwan Society of Tuberculosis and Lung Diseases

Thoracic Medicine

The Official Journal of
Taiwan Society of Pulmonary and Critical Care Medicine
Taiwan Society for Respiratory Therapy
Taiwan Society of Sleep Medicine
Taiwan Society of Tuberculosis and Lung Diseases

Thoracic Medicine

The Official Journal of
Taiwan Society of Pulmonary and Critical Care Medicine
Taiwan Society for Respiratory Therapy
Taiwan Society of Sleep Medicine
Taiwan Society of Tuberculosis and Lung Diseases

Volume 38
Number 4
December 2023

CONTENTS

High Mortality Rates of Pneumocystis jirovecii Pneumonia in Non-HIV-Positive Patients with Malignant Tumors: A Retrospective Observational Study

Kun-Tse Lin[1], Sheng-Hao Lin[1], Jun-Wei Lin[1], Kuo-Yang Huang[1]

Background: Pneumocystis jirovecii pneumonia (PJP) is a potentially life-threatening infection that occurs in severely immunocompromised patients. Polymerase chain reaction (PCR) testing of sputum samples may be a viable alternative to invasive testing for PJP. Lung cancer morbidity and mortality rates have always been among the highest worldwide, with lung cancer patients clinically infected with PJP having a particularly poor prognosis.

Methods: This retrospective observational study analyzed non-HIV-positive patients with PJP admitted to Changhua Christian Hospital from 2012 to 2022. Patients with PJP were defined as those with positive results from immunofluorescence quantitative PCR detection, chest radiography, or computed tomography (CT), or those with clinical symptoms and confirmation of PJP treatment during hospitalization. The patients and their data,including age, sex, use of intravenous and/or oral trimethoprim/sulfamethoxazole for PJP treatment, steroid treatment, and mortality, were collected from electronic medical records. Statistical analysis was performed using the Mann–Whitney test, Chi-square test, and Kaplan–Meier method.

Results: A total of 234 patients with PJP were identified, among whom 190 had no HIV. The non-HIV-positive patients with PJP were found to have the highest incidence of PJP and the highest mortality rates ($p=0.021$). Among patients with solid tumors, those with lung cancer had the highest incidence. In a comparison between lung and non-lung cancer patients, age was the only variable that differed significantly ($p=0.025$).

Conclusion: The current study showed that non-HIV-positive patients with PJP had an increased incidence of malignant tumors and high mortality rates. PJP is a risk factor for mortality in patients with malignant tumors. ***(Thorac Med 2023; 38: 271-280)***

Key words: *Pneumocystis jirovecii* pneumonia (PJP), *Pneumocystis carinii* pneumonia (PCP),distribution ratio, risk factors, mortality, outcome

[1]Division of Chest Medicine, Department of Internal Medicine, Changhua Christian Hospital, Changhua, Taiwan
Address reprint requests to: Dr. Kuo-Yang Huang, Division of Chest Medicine, Department of Internal Medicine, Changhua Christian Hospital, Changhua, Taiwan

Introduction

*Pneumocystis jirovecii*pneumonia (PJP), an opportunistic lung infection caused by human *Pneumocystis jiroveciivirus*, commonly occurs in premature and malnourished infants. In adults, it often develops in those with acquired immunodeficiency syndrome (AIDS) and cancer, or those using immunosuppressive agents leading to secondary immunodeficiency. In 1909, Chagas discovered *Pneumocystis* while studying trypanosomes. Dr. Carini also discovered it in infected rats around the same time. Initially classified as a protozoan, *Pneumocystis* was later found, through nucleic acid and biochemical analyses, to be more similar to fungi. Delanoes later confirmed that *Pneumocystis* was a pathogen mainly infecting the lungs, and named it *Pneumocystis carinii*[1]. Thereafter, it was renamed as*Pneumocystis jirovecii* to distinguish it from lung *Pneumocystis* infecting rats. PJP was found mostly in AIDS patients between 1980 and 2000. With the recent widespread use of immunosuppressive agents, detection rates of PJP in non-HIV patients, such as those with malignant tumors, transplant patients, and those with autoimmune diseases, have significantly increased. The overall mortality rate of non-HIV PJP patients is around 35%-55% [2-5], whereas that of AIDS PJP patients is 10%-20% [6].

PJP is characterized by its gradual onset, with shortness of breath and/or respiratory distress. This disease may present with fever, night sweats, weight loss, and dry cough, as well as hypoxia and respiratory failure [7]. Dry cough is not common in PJP given the thick viscosity of phlegm. PJP can be classified into mild, moderate (usually HIV-positive), or severe, based on symptoms and blood oxygen levels. Mild disease is characterized by shortness of breath during exercise, arterial oxygen pressure (PaO_2) >11.0 kPa, oxygen saturation (SaO_2) >96%, and chest radiography showing normal or minor changes. Moderate disease is characterized by mild shortness of breath during exercise with possible shortness of breath and fever at rest, PaO_2 of approximately 8.1-11.0 kPa, SaO_2 of 91%-96%, and chest radiography showing diffuse interstitial changes. Severe disease is characterized by shortness of breath and respiratory distress at rest, as well as fever and cough, with a PaO_2<8.0 kPa, SaO_2<91%, and chest radiography usually showing widespread interstitial changes and diffuse pulmonary shadowing [8].

Computed tomography (CT) remains the best radiological examination for diagnosing PJP, and should be considered in the early disease stages [9]. Although chest CT in patients with PJP usually shows bilateral centrally distributed ground-glass opacities (GGO), patchy and diffuse GGOs may also appear. Early PJP may present as diffuse GGO, which progresses to GGO and patchy consolidation, with solid changes dominating the late stage of the disease. Normal CT may help exclude PJP; however, the absence of radiation features specific to PJP does not completely rule it out [10-11].

P. jirovecii cultivation is quite challenging and is not part of a routine examination. Despite its poor sensitivity, microscopic examination is considered the gold standard for clinical differentiation of *P. jirovecii*[12]. Polymerase chain reaction (PCR) technology can rapidly detect the presence of *Pneumocystis*. However, failure to detect *Pneumocystis* DNA clinically could be due to an infection rate below the detection limit, and does not indicate organism absence. PCR testing of *P. jirovecii* is unable to differentiate between active or dead organisms; hence, the

results obtained from molecular biology techniques should be compared with the patient's clinical information to serve as an important reference for physicians [13-15]. When PJP is clinically suspected, treatment should not be delayed until a definitive diagnosis is confirmed. Bronchoscopic alveolar lavage (BAL) is the preferred PCR testing method. If BAL detects PJP, treatment should be initiated immediately. However, if BAL is negative, other samples, such as sputum, may be used to exclude the same. Considering that sputum sample PCR testing is less invasive than other techniques, it may be a feasible alternative to invasive examination [16].

Trimethoprim/sulfamethoxazole (TMP/SMX) are the drugs of choice for non-HIV patients with PJP [17]. For patients with normal renal function, the dosage of TMP–SMX should be 15 to 20 mg/kg per day intravenously or orally, divided into 3 or 4 doses. Patients should continue to receive treatment until their clinical condition stabilizes (e.g., PaO_2 ≥60 mmHg, respiratory rate<25) and their gastrointestinal function returns to normal.

With the recent increase in the use of immunosuppressive agents, PJP has been detected much more frequently in non-HIV infected patients who have malignant tumors, who underwent transplantation, or who have autoimmune disease. A recent study found that the incidence of PJP in patients with acute leukemia, chronic lymphocytic leukemia, or non-Hodgkin lymphoma was >45 cases/100,000 patients/year, whereas that in patients with solid tumors was <25 cases/100,000 patients/year [18]. Lung cancer is among the most common causes of death in patients with solid malignant tumors, and recent case reports have described PJP in lung cancer patients [3,19-20].

This study retrospectively analyzed the distribution and mortality rates of PJP in patients with various diseases reported in previous research, providing a reference for clinical application.

Methods

Study design and population

This study retrospectively analyzed the electronic medical records of patients admitted to Changhua Christian Hospital. Patients discharged with a diagnosis of PJP from January 2012 to December 2022 were included. HIV-positive patients were excluded. The distribution of non-HIV-positive patients with PJP and different diseases was statistically analyzed. Based on the classification of their main diseases, patients were divided into those with malignant tumors, autoimmune diseases, infectious diseases, diabetes mellitus (DM), or chronic kidney disease (CKD), and transplant patients.Given that patients with malignant tumorswere the highest proportion, they were further divided into those with solid and non-solid tumors. The number of patients with solid tumors was then statistically analyzed according to tumor type, including lung cancer, head and neck cancer, gastrointestinal tumors, breast cancer, prostate cancer, and other malignant tumors. Patients were then analyzed according to age, sex, treatment with intravenous and/or oral TMP–SMX for PJP, steroid treatment, and mortality (Figure 1).

Definition of PJP

PJP was considered positive when a patient satisfied the following 3 criteria: (1) positive P.jirovecii findings following real-time PCR or direct immunofluorescence testing of spontane-

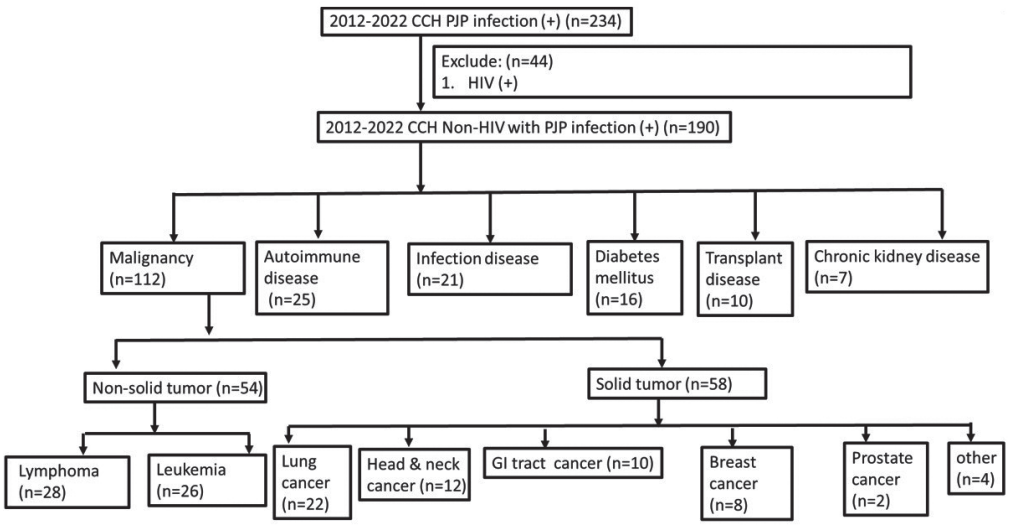

Fig. 1. Flowchart of study participant enrollment. Patients with *Pneumocystis jirovecii*pneumonia admitted to Changhua Christian Hospital from 2012-2022 were included, after excluding those with HIV. The number of diseases in patients with *Pneumocystis jirovecii*pneumonia is shown.

ous sputum, induced sputum, BAL fluid, or tissue samples; (2) presence of infiltrates in lung radiography or CT; and (3) clinical symptoms of PJP, and PJP treatment during hospitalization.All patients fulfilled the3 inclusion criteria.

Data collection

The patient number and clinical data forthe non-HIV-positive patients with PJP were collected from electronic medical records.Clinical data including age, sex, use of intravenous and/or oral TMP–SMX for PJP treatment, steroid treatment, and mortality were collected.

Statistical analysis

Normally distributed continuous variables were reported as means ± inter-quartile range, whereas non-normally distributed variables were reported as medians (range). The Mann–Whitney test was used to analyze continuous variables. Categorical variables were reported as numbers and percentages, andwere compared using the Chi-square test. Based on matched-pair data, conditional logistic regression models were used to evaluate independent risk factors for the development of PJP. A 2-tailed p value of <0.05 was considered statistically significant. The Kaplan–Meier method was used to create the survivorship curve.

Results

A total of 234 patients were diagnosed with PJP at our hospital from 2012 to 2021. Among them, 190 did not have HIV; 112 had malignancies (58.94%); 25 had autoimmune diseases (13.16%); 21 had infectious diseases (11.05%), of which 13 were due to infectiouslung disease (6.84%); 16 had DM (8.42%); 10 had transplant diseases (5.26%); and 7 had CKD (3.68%) (Figure 1, Supplementary Figure 1 and Supplementary Figure 2). The survival rates of these patients can be found in Table 1.

The patients were then analyzedbased on age, sex, receipt of intravenous and/or oral administration of TMP–SMX for PJP treatment, use of steroid treatment, and mortality. The mortality rate was the only factor that showed

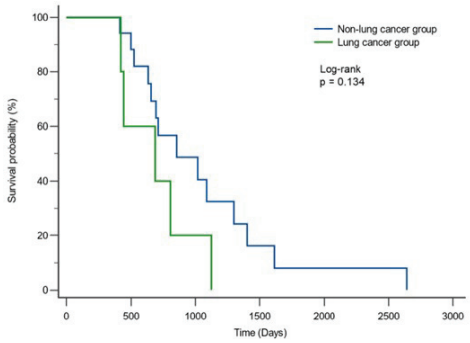

Fig. 2. Survival duration (from *Pneumocystis jirovecii*pneumonia diagnosis to death) of lung cancer and non-lung cancer groups.

a statistically significant difference (p = 0.043) (Table 1).

There were more cases with malignant tumors than without.Nevertheless, patients with and without malignant tumors were compared based on age, sex, administration of intravenous and/or oral TMP–SMX for PJP treatment, use of steroids, and mortality rates. We found a significant difference in mortality rates, (p = 0.021) between these 2 groups, with a higher mortality rate in the malignant tumor group, but no significant difference in other factors (Table 2 and Table 3).

Table 1. Comparison of Various Diseases in Patients with PJP Infection

	Malignancy (n=112)	Autoimmune disease (n=25)	Infectious disease (n=21)	Diabetes mellitus (n=16)	Transplant disease (n=9)	Chronic kidney disease (n=7)	*p*-value
Age	65.5 (56.5-73.5)	67 (58-80)	56 (44-80)	69 (64-83.5)	63 (57-68)	70 (63-77)	0.303
Gender							0.307
Male (%)	38 (33.9)	13 (52)	8 (38.1)	3 (18.8)	2 (22.2)	3 (42.9)	
Female (%)	74 (66.1)	12 (48)	13 (61.9)	13 (81.3)	7 (77.8)	4 (57.1)	
Antibiotics treatment (%)	108 (96.4)	25 (100)	20 (95.2)	15 (93.8)	9 (100)	7 (100)	0.838
Steroid therapy (%)	71 (63.4)	22 (88)	14 (66.7)	10 (62.5)	8 (88.9)	3 (42.9)	0.086
Mortality rate (%)	72 (64.3)	10 (40)	11 (52.4)	11 (68.8)	2 (22.2)	3 (42.9)	0.043

PJP: *Pneumocystis jirovecii*pneumonia

Table 2. Demographic Data of Various Diseases in Patients with *Pneumocystis Jirovecii*pneumonia who Had Malignant Tumors

Malignancy	Non-solid tumor (n=54)	Lung cancer (n=22)	Head and neck tumor (n=12)	GI tract cancer (n=10)	Breast cancer (n=8)	Prostate cancer (n=2)
Age	66.5 (52.0-74.0)	69.0 (62.0-79.0)	55.1 (4.0 -70.0)	65.5 (52.0-89.0)	67.8 (51.0-86.0)	53.4 (33.0-74.0)
Gender						
Male (%)	32 (59.3)	19 (86.4)	11 (91.7)	7 (70.0)	0 (0.0)	2 (100.0)
Female (%)	22 (40.7)	3 (13.6)	1 (8.3)	3 (30.0)	8 (100.0)	0 (0.0)
Antibiotics treatment (%)	52 (96.3)	22 (100.0)	12 (100.0)	10 (100.0)	8 (100.0)	2 (100.0)
Steroid therapy (%)	31 (57.4)	16 (72.7)	10 (83.3)	4 (40.0)	6 (75.0)	2 (100.0)
Mortality rate (%)	34 (63.0)	16 (72.7)	7 (58.3)	8 (80.0)	5 (62.5)	0 (0.0)

Table 3. Comparisonof Malignancy and Non-malignancy in PJP Patients

	Malignancy (n=112)	Non-malignancy (n=78)	*p*-value
Age	65.5 (56.5-73.5)	67 (57-79)	0.320
Gender			0.645
Male (%)	38 (33.9)	29 (37.2)	
Female (%)	74 (66.1)	49 (62.8)	
Antibiotics treatment (%)	108 (96.4)	76 (97.4)	0.696
Steroid therapy (%)	71 (63.4)	57 (73.1)	0.161
Mortality rate (%)	72 (64.3)	37 (47.4)	0.021

PJP: *Pneumocystis jirovecii*pneumonia

Analysis based on malignancy type showed that 54 (48.21%) and 58 patients (51.79%) had non-solid and solid tumors, respectively. Among the 58 patients with solid tumors, 22 (37.93%) had lung cancer, 12 (20.69%) had head and neck tumors, 10 (17.24%) had GI tract cancers, 8 (13.79%) had breast cancer, 2 (3.45%) had prostate cancer, and 4 (6.90%) had other types of cancer (Figure 1, Supplementary Figure 1 and Supplementary Figure 2).

Analysis wasthen conducted based on malignancy type, survival, and mortality. Ofthe 54 patients with non-solid tumors, 21 (38.89%) survived and 33 (61.11%) expired. Of the 58 patients with solid tumors, 20 (34.48%) survived and 38 (65.52%) expired(Figure 1, Supplementary Figure 1 and Supplementary Figure 2).

Given that lung cancer patients accounted for the highest number of patients with solid tumors, analysis of both lung cancer and non-lung cancer patients was conducted based on their age, sex, administration of intravenous and/or oral TMP–SMX for PJP treatment, steroid therapy, and mortality. Notably, we found that age was the only factor that showed a significant difference (p = 0.025) (Table 4). The length of survival (from PJP diagnosis to death)

Table 4. Comparisonof Lung Cancer and Other Cancers in PJP Patients with Malignancy

	Lung cancer with PJP infection (n=22)	Other cancer with PJP infection (n=36)	*p* -value
Age	69.0 (62.0-79.0)	62.5 (55.5-69.5)	0.025
Gender			0.066
Male (%)	19 (86.4)	23 (63.9)	
Female (%)	3 (13.6)	13 (36.1)	
Antibiotics treatment (%)	22 (100.0)	34 (94.4)	0.265
Steroid therapy (%)	16 (72.7)	24 (66.7)	0.631
Mortality rate (%)	16 (72.7)	22 (61.1)	0.371

PJP: *Pneumocystis jirovecii*pneumonia

of the lung cancer and non-lung cancer groups was calculated using the survival curve created using the Kaplan–Meier method (Figure 2).

Discussion

PJP, also known as PCP, is a potentially life-threatening infection that often occurs in patients with severe immunodeficiency, such as HIV-positive patients with a CD4 cell count of less than 200 cells/μL, those undergoing hematopoietic stem cell transplantation or solid organ transplantation, or those receiving chronic immunosuppressive therapies [22-23].

A total of 234 patients with PJP were treated at our hospital during the study period; 190 of the 234 patients did not have HIV. Our analysis showed a significant correlation between PJP and mortality rates for various diseases (p = 0.043), indicating PJP as a causative factor for death among non-HIV-positive patients. Moreover, our analysis of cases with and without malignant tumors identified PJP as a risk factor for death in patients with malignant tumors.

In addition, we noted that the incidence rate of PJP in patients with DM was relatively high, second only to that in patients with malignant tumors, autoimmune diseases, and lung infections. In addition, the mortality rate of PJP patients with DM was also high, reaching 68.75%. DM, a metabolic disease that occurs due to inflammation, involves a complex immune process. Insulin resistance caused by insulin signal inhibition can lead to a series of immune reactions that exacerbate the inflammatory state and lead to hyperglycemia. Congenital immune response defects (including neutrophil and macrophage dysfunction) and adaptive immune response dysfunction (including T cells) have been identified as weaknesses of the immune system that promote susceptibility to pathogens in patients with DM [24].

Our analysis of PJP patients with malignant tumors showed that the proportion of non-solid tumors to solid tumors was similar, at 48.21% and 51.79%, respectively. The mortality rate for patients with non-solid tumors was slightly lower than that for patients with solid tumors, at 61.11% and 65.52%, respectively, albeit not significantly.

Our analysis of the types of solid tumors in PJP patients also found that lung cancer was the most common, followed by head and neck tumors, gastrointestinal tract cancers, breast cancer, and prostate cancer. No significant difference in mortality rate was observed (p = 0.371), although those with lung cancer were significantly older (69.0 vs. 62.5 years; p = 0.025).

In 1980, Fossieck and Spagnolo [20] reported 5 cases of PJP associated with lung cancer, in which all patients received chemotherapy, 3 underwent radiation therapy, and 2 did not receive corticosteroids. Based on these findings, PJP in lung cancer can be considered to be associated with highly invasive chemotherapy and radiation therapy. Similarly, McAleese *et al*. [21] described a series of cases in which curative radiation therapy was associated with PJP in lung cancer patients. Recently, Lee et al.[10,24] found that long-term, high-dose steroid therapy and concurrent chemoradiotherapy are risk factors for PJP in lung cancer patients. However, the present study showed no significant difference between treatment with TMP–SMX and treatment with steroids, possibly due to the small sample size.

In HIV-positive patients, prophylaxis with TMP–SMX is highly effective in preventing PJP [25]. A recent meta-analysis also showed that TMP–SMX therapy reduces the incidence

and mortality rates of PJP in solid organ transplant recipients and in patients with hematological malignancies, indicating that prophylaxis for PJP is both necessary and effective for adult patients at highrisk [26]. Several studies have shown an increased risk of PJP in patients with solid tumors, although no clinical data support the routine use of PJP prophylaxis for lung cancer patients. However, given the high mortality rate associated with PJP, prophylaxis for PJP in high-risk patients with malignant tumors may be beneficial.

Conclusion

PJP is a potentially life-threatening infection commonly observed in patients with severe immune dysfunction. The current study found that non-HIV-positive patients with PJP had an increased prevalence of malignant tumors and that PJP was a risk factor for high mortality in patients with malignant tumors. Considering that cancer treatment often involves chemotherapy and radiation therapy, early detection and treatment of PJP can be helpful in improving patient survival.

Declarations

Ethical Approval and Consent to participate

The study was approved by the Institutional Review Board of Changhua Christian Hospital (approval no.: 220514). The Institutional Review Board waived the need for informed consent considering the retrospective nature of the data collected. The Declaration of Helsinki and its subsequent revisions were followed.

Data Availability Statement

Data are available from the corresponding author on reasonable request.

Competing interests

The authors declare no competing interests.

Authors' contributions

K.U.L and S.H.L. contributed to the research outline and design

K.U.L and K.Y.H. contributed to the data collection.

K.U.L., K.Y.H. and S.H.L. contributed to the data analysis.

K.Y.H., S.H.L., andJ.W.L.contributed to the data interpretation.

K.U.L., K.Y.H. and S.H.L. take responsibility for the content of the manuscript, including the data and analysis.

References

1. Edman JC, Kovacs JA, Masur H, *et al*. Ribosomal RNA sequence shows *Pneumocystis* carinii to be a member of the fungiexternal icon. Nature 1988; 334: 519-22.
2. Kovacs JA, Masur H. Evolving health effects of *Pneumocystis*: one hundred years of progress in diagnosis and treatment. JAMA 2009; 301: 2578-2585. doi: 10.1001/jama.2009.880.
3. Sepkowitz KA, Brown AE, Telzak EE, *et al*. *Pneumocystis* carinii pneumonia among patients without AIDS at a cancer hospital. JAMA 1992; 267: 832-837. doi: 10.1001/jama.1992.03480060078034.
4. Mansharamani NG, Garland R, Delaney D, *et al*. Management and outcome patterns for adult Pneumocystis carinii pneumonia, 1985 to 1995: comparison of HIV-associated cases to other immunocompromised states. Chest 2000; 118: 704-711. doi: 10.1378/chest.118.3.704.
5. Roblot F, Godet C, Le Moal G, *et al*. Analysis of underlying diseases and prognosis factors associated with Pneumocystis carinii pneumonia in immunocompromised

HIV-negative patients. Eur J Clin Microbiol Infect Dis 2002; 21: 523-531. doi: 10.1007/s10096-002-0758-5.

6. Pulvirenti J, Herrera P, Venkataraman P, *et al*. Pneumocystis carinii pneumonia in HIV-infected patients in the HAART era. AIDS Patient Care STDS 2003; 17: 261-265. doi: 10.1089/108729103322108139.
7. "Pneumocystis pneumonia | Fungal Diseases | CDC". *www.cdc.gov*. *2020-07-27*. Retrieved 2020-08-10.
8. Miller RF, Le Noury J, Corbett EL, *et al*. Pneumocystis carinii infection: current treatment and prevention. J AntimicrobChemother 1996;37(Suppl B): 33-53.https://doi.org/10.1093/jac/37.suppl_b.33.
9. Mu X-D, Jia P, Gao L, *et al*. Relationship between radiological stages and prognoses of Pneumocystis pneumonia in non-AIDS immunocompromised patients. Chin Med J 2016;129(17): 2020-5. https://doi.org/10.4103/0366-6999.189068.
10. Lee E, Kim E, Lee S, *et al*. Risk factors and clinical characteristics of Pneumocystis jirovecii pneumonia in lung cancer. Sci Rep 2019;9(1): 2094.https://doi.org/10.1038/s41598-019-38618-3.
11. Cereser L, Dallorto A, Candoni A, *et al*. Pneumocystis jirovecii pneumonia at chest high-resolution computed tomography (HRCT) in non-HIV immunocompromised patients: spectrum of findings and mimickers. Eur J Radiol 2019;116:116-27.https://doi.org/10.1016/j.ejrad.2019.04.025
12. Liu Y, Fahle GA, Kovacs JA. Inability to culture Pneumocystis jirovecii. MBio 2018; 9(3): e00939-18. https://doi.org/10.1128/mBio.00939-18.
13. Summah H, Zhu Y-G, Falagas ME, *et al*. Use of real-time polymerase chain reaction for the diagnosis of Pneumocystis pneumonia in immunocompromised patients: a meta-analysis. Chin Med J 2013;126: 1965-73.
14. Fan L-C, Lu H-W, Cheng K-B, *et al*. Evaluation of PCR in bronchoalveolar lavage fluid for diagnosis of Pneumocystis jirovecii pneumonia: a bivariate meta-analysis and systematic review. PLoS One2013;8:e73099. https://doi.org/10.1371/journal.pone.0073099.
15. Lu Y, Ling G, Qiang C, *et al*. PCR diagnosis of Pneumocystis pneumonia: a bivariate meta-analysis. J Clin Microbiol 2011;49:4361-3. https://doi.org/10.1128/JCM.06066-11.
16. Pennington K, Wilson J, Limper AH.Positive Pneumocystis jirovecii sputum PCR results with negative bronchoscopic PCR results in suspected pneumocystis pneumonia. Can Respir J 2018; 2018: 6283935. https://doi.org/10.1155/2018/6283935
17. Limper AH, Knox KS, Sarosi GA, *et al*. An official American Thoracic Society statement: Treatment of fungal infections in adult pulmonary and critical care patients. Am J Respir Crit Care Med 2011; 183: 96.
18. Fillatre P, Decaux O, Jouneau S, *et al*. Incidence of Pneumocystis jiroveci pneumonia among groups at risk in HIV-negative patients. Am J Med 2014 Dec; 127(12): 1242.e11-7, https://doi.org/10.1016/j.amjmed.2014.07.010 (2014).
19. Bollee G, Sarfati C, Thiery G, *et al*. Clinical picture of Pneumocystis jiroveci pneumonia in cancer patients. Chest 2007 Oct; 132(4): 1305-10. https://doi.org/10.1378/chest.07-0223 (2007).
20. Fossieck BE, Jr, Spagnolo SV. Pneumocystis carinii pneumonitis in patients with lung cancer. Chest 1980; 78(5): 721-2.
21. McAleese J, Mooney L, Walls GM, *et al*. Risk of death from *Pneumocystis jirovecii* after curative-intent radiotherapy for lung cancer. Clin Oncol (R Coll Radiol) 2018; 30(12): e81-2.
22. Cordonnier C, Cesaro S, Maschmeyer G, *et al*. Pneumocystis jirovecii pneumonia: still a concern in patients with haematological malignancies and stem cell transplant recipients. J AntimicrobChemother2016; 71(9): 2379-2385.
23. Maertens J, Cesaro S, Maschmeyer G, *et al*. ECIL guidelines for preventing Pneumocystis jirovecii pneumonia in patients with haematological malignancies and stem cell transplant recipients. J AntimicrobChemother2016; 71(9): 2397-2404.
24. Berbudi A,Rahmadika N, Tjahjadi AI, *et al*.Type 2 diabetes and its impact on the immune system. Curr Diabetes Rev 2020;16(5): 442-449. doi: 10.2174/1573399815666191024085838.
25. Kaplan JE, Benson C,Holmes KK, *et al*. Guidelines for prevention and treatment of opportunistic infections in HIV-infected adults and adolescents: recommendations from CDC, the National Institutes of Health, and the HIV Medicine Association of the Infectious Diseases Society of America. MMWR Recomm Rep 2009; 58(RR-4): 1-207. quiz CE201-204 (2009).
26. Green H, Paul M, Vidal L, *et al*. Prophylaxis of

Pneumocystis pneumonia in immunocompromised non-HIV-infected patients: systematic review and meta-analysis of randomized controlled trials. Mayo Clin Proc 2007; 82: 1052-1059. Doi : 10.4065/82.9.1052.

Does it Matter Where the Heart Stops? rCAST Score Performance in Predicting Outcomes of in-hospital Cardiac Arrest patients

Chao-Hsien Chen[1,2], Chieh-Jen Wang[2,3], I-Ting Wang[2,3], Sheng-Hsiung Yang[2,3], Chang-Yi Lin[2,3]

Objectives: The characteristics of patients with in-hospital cardiac arrest (IHCA) are generally considered to be different from those with out-of-hospital cardiac arrest (OHCA). The revised post-Cardiac Arrest Syndrome for Therapeutic hypothermia (rCAST) score has been proven to be a good predictive score for neurologic outcomes and mortality in OHCA patients who receive therapeutic temperature management (TTM); however, its application in IHCA patients has yet to be evaluated.

Methods: In this retrospective study, we enrolled adult post-cardiac arrest syndrome (PCAS) patients who had an IHCA and received TTM from 2017 to 2021 at our hospital. Their medical records were extracted to calculate the rCAST score and analyze their outcomes.

Results: A total of 37 patients were enrolled for analysis. The average rCAST score was 5.6±3.6, and 51.4% and 48.6% of the patients were classified into the low and moderate severity categories, respectively. The areas under the curves for the rCAST score were 0.780 (95% confidence interval [CI]: 0.614-0.899) to predict poor neurologic outcomes, and 0.809 (95% CI: 0.647-0.919) to predict mortality at day 28. Only those patients in the low severity category were associated with survival and favorable neurologic outcome benefits.

Conclusion: Our preliminary results suggest that the rCAST score had moderate accuracy in predicting poor neurologic outcomes and mortality at 28 days in IHCA patients receiving TTM. Further large-scale studies are warranted to confirm these findings. ***(Thorac Med 2023; 38: 281-288)***

Key words: Mortality, neurologic outcome, in-hospital cardiac arrest, post-cardiac arrest syndrome, rCAST, targeted temperature management

[1]Division of Pulmonary and Critical Care Medicine, Department of Internal Medicine, Taitung MacKay Memorial Hospital, Taitung, Taiwan. [2]Department of Medicine, MacKay Memorial College, New Taipei City, Taiwan. [3]Division of Pulmonary and Critical Care Medicine, Department of Internal Medicine, MacKay Memorial Hospital, Taipei City, Taiwan

Address reprint requests to: Dr. Chieh-Jen Wang, Division of Pulmonary, Department of Internal Medicine, MacKay Memorial Hospital, Taipei, Taiwan

Introduction

Sudden cardiac arrest is fatal if resuscitation is not initiated in a timely manner. Patients with cardiac arrest are classified as having an out-of-hospital cardiac arrest (OHCA) or an in-hospital cardiac arrest (IHCA), depending on where the cardiac arrest occurs [1,2]. Due to differences in care systems and the underlying pathogenesis, IHCA is generally considered to be distinct from OHCA [2]. The incidence of IHCA in different reports globally ranges from 1.2-17.2 per 1000 admissions [2-4]. Although the discharge survival rate of IHCA patients is better than that of OHCA patients [2, 4], the survival rate of IHCA patients to discharge is only 17.6% and the 1-year survival rate only 13.4% [5].

Studies by Bernard *et al*. and the HACA study group [6-7] showed that mild hypothermia (targeted temperature management [TTM] at 32~34℃) could significantly improve survival and neurologic outcomes in comatose patients with post-cardiac arrest syndrome (PCAS) due to OHCA. TTM is believed to reduce metabolism, inhibit inflammation and oxidative stress in the brain, and prevent further hypoxic-ischemic brain injury [8]. Although there is no direct evidence of the benefits of TTM for IHCA patients, the guidelines still suggest using TTM for patients with PCAS due to IHCA [9-10].

The early prediction of neurologic outcomes during TTM is difficult [11-12]. The revised post-Cardiac Arrest Syndrome for Therapeutic hypothermia (rCAST) score proposed by Nishikimi *et al*. [13] uses an app-based algorithm, which can be calculated easily using common laboratory data and clinical findings after the return of spontaneous circulation (ROSC) and before initiating TTM in OHCA patients. The rCAST score has been proven to have the potential to predict neurologic outcomes and mortality in OHCA patients receiving TTM in Japan and in Taiwan [13-14]. However, no study has yet evaluated the usefulness of the rCAST score in predicting neurologic outcomes and mortality in IHCA patients receiving TTM. Our institution has many years of experience in using TTM for PCAS patients, including those with OHCA and those with IHCA [15-16]. Therefore, the aim of this study was to use the medical records of past IHCA patients who received TTM at our institute to validate the usefulness of the rCAST score in predicting neurologic outcomes and mortality.

Material and Methods

Study design and patient selection

We conducted this retrospective study at MacKay Memorial Hospital (MMH), a medical center and first aid hospital with 2 campuses, 1 in Taipei City and 1 in New Taipei City, Taiwan, with a total of 749 and 872 beds, and 57 and 62 intensive care unit (ICU) beds, respectively. This study was approved by the Institutional Review Boards of MMH (approval no. 21MMHIS012e), and the need for written informed consent was waived.

We screened patients admitted to ICUs for TTM from July 2015 to July 2021. All adult PCAS patients due to IHCA who received TTM were included, but those who were aged < 18 years, who had an OHCA or traumatic cardiac arrest, who did not receive TTM, or who had any missing values needed to calculate the rCAST score, were excluded. Data were collected from electronic chart reviews, including the baseline patient profiles, comorbidities, resuscitation records, laboratory data, and hospi-

tal outcomes. The rCAST score was calculated using 5 factors collected before initiating TTM: the initial rhythm of the cardiac arrest, duration from cardiac arrest to ROSC, pH of arterial blood gas, lactate level, and motor response of the Glasgow Coma Scale (GCS) score [13]. The time of ROSC was defined as requiring chest compressions for not more than 20 consecutive minutes [17]. Based on their total rCAST score, the patients were further classified into low severity (rCAST ≤ 5.5), moderate severity (rCAST, 6-14), and high severity (rCAST ≥ 14.5) categories [13].

TTM at MMH is suggested for comatose PCAS patients without contraindications. The standard protocol is to give 4°C Ringer's lactate solution 30 ml/kg for induction, and use a surface cooling device (Arctic Sun Model 2000/5000 (Medivance, Louisville, CO) set at 33℃ for 24-48 hours. A rewarming rate of 0.15℃/hour is applied to a targeted body temperature of 36.5℃ after the hypothermia period. Details of the protocol have been described previously [14].

Outcome measurements and statistical analysis

The outcomes of interest in this study were neurologic function and mortality at 28 days or discharge. Neurologic function was classified according to the Glasgow–Pittsburgh cerebral performance categories (GP-CPC) [18-19] as good (GP-CPC 1-2: good cerebral performance, or moderate cerebral disability), or poor (GP-CPC 3-5: severe cerebral disability, coma, or death). Receiver operating characteristic (ROC) curve analysis was used to validate the rCAST score to predict outcomes in the IHCA patients. The accuracy of the score was classified, based on the area under the ROC curve (AUC), as high accuracy (AUC > 0.9), moderate accuracy (AUC 0.7 - 0.9), or low accuracy (AUC < 0.7) [20].

Categorical variables are presented as number (percentage), and continuous variables are presented as mean ± standard deviation or median (interquartile range), depending on whether or not they were normally distributed. Shapiro–Wilk's test was used to evaluate the normality of a continuous variable. Differences between categorical variables were assessed using the chi-squared test or Fisher's exact test, as indicated, and continuous variables were compared using the independent samples t-test if normally distributed, or the Mann-Whitney U test if non-normally distributed. A 2-sided p value < 0.05 was considered to indicate a statistically significant difference. All statistical analyses were performed using MedCalc 20.210 (MedCalc Software Ltd, Ostend, Belgium).

Results

Patients

In all, 214 PCAS patients admitted to the medical ICU during the study period were screened (Figure 1), and 173, including those aged less than 18 years, those who had an OHCA, and those who did not receive TTM, were excluded. Another 4 patients who did not have lactate values before initiating TTM, which were needed to calculate the rCAST score, were also excluded from the analysis. Finally, a total of 37 patients who had an IHCA and received TTM were enrolled in this study.

The mean age of the 37 patients was 65.5±14.3 years, and 70.3% were male. All of them had experienced cardiac arrests, but only 18.9% had an initial shockable rhythm. The average APACHE II score was 32.8±7.2, and

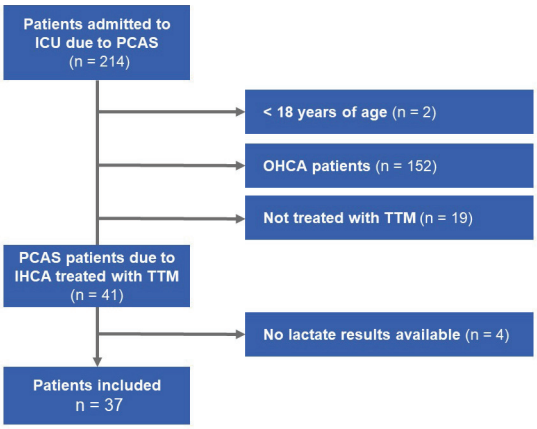

Fig. 1. Flowchart of patient selection. ICU: intensive care unit, IHCA: in-hospital cardiac arrest, OHCA: out-of-hospital cardiac arrest, PCAS: post-cardiac arrest syndrome, TTM: targeted temperature management.
Above: PCAS in IHCA patients treated with TTM (n = 41)

the average rCAST score was 5.6±3.6 (Table 1). There were no significant differences in age, sex, or comorbidities between those with good and those with poor neurologic outcomes, but the patients who survived were younger (54.2±17.1 vs. 67.6±12.9 years, p=0.0329) than those who died at 28 days. Although the APACHE II scores did not differ between the survivors and the non-survivors, or between those with good or poor neurologic outcomes, the patients with good neurologic outcomes (2.6±2.0 vs. 5.9±3.6, p=0.0310) and the survivors (2.5±1.7 vs. 6.1±3.6, p=0.0017) had significantly lower rCAST scores.

The AUCs for the rCAST scores to predict poor neurologic outcomes and mortality at 28 days were 0.780 (95% confidence interval [CI]: 0.614-0.899) (Figure 2A) and 0.809 (95% CI: 0.647-0.919) (Figure 2B), respectively. Based on the rCAST score, 19 patients (51.4%) were classified as having low severity, and 18 (48.6%) as having moderate severity (Table 2). The probability of an IHCA patient in the low severity category was 78.9% (95% CI: 54.4%-94.0%) for having a poor neurologic outcome, and 68.4% (95% CI: 43.5%-87.4%) for mortality at 28 days. The probability of a patient in the moderate severity category having both a poor neurologic outcome and mortality at 28 days was 100% (95% CI: 81.5%-100.0%).

Discussion

In this study, we found that the rCAST score had moderate accuracy in predicting a poor neurologic outcome and mortality at 28 days in IHCA patients receiving TTM. All of the patients classified into the moderate severity category died within 28 days after cardiac arrest.

The outcomes of IHCA patients are considered to be different from those of OHCA patients due to the underlying demographics, initial cardiac rhythm, etiology, and system of care [2, 4, 21]. Chen *et al*. retrospectively reviewed the etiology of 986 cardiac arrest patients over a 4-year period, and found that with regard to the etiology of cardiac arrest, OHCA patients had a more acute coronary syndrome (16% vs. 8%),

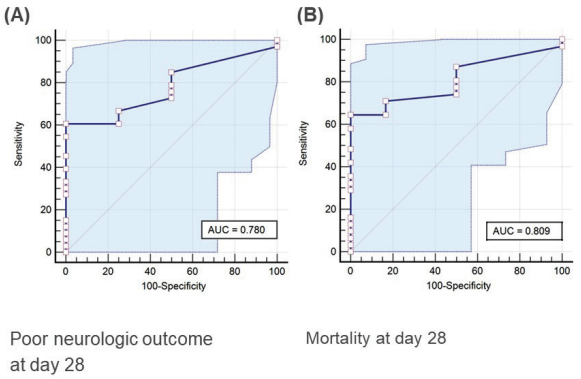

Fig. 2. Receiver operating characteristic curves of the rCAST score in predicting a poor neurologic outcome (A) or mortality (B) at day 28. Light blue areas represent the 95% confidence interval. AUC: area under the curve

Table 1. Patients' Characteristics and Differences Between Outcomes at Day 28

	All patients (n= 37)	Good neurologic outcome (n= 4)	Poor neurologic outcome (n= 33)	*p* value	Survival (n= 6)	Mortality (n= 31)	*p* value
Age, years	65.5±14.3	55.8±20.6	66.6±13.3	0.3786	54.2±17.1	67.6±12.9	0.0329
Sex, male/female	26/11 (70.3%/29.7%)	3/1 (75.0%/25.0%)	23/10 (69.7%/30.3%)	>0.9999	5/1 (83.3%816.7%)	21/10 (67.7%/32.3%)	0.6463
Co-morbidity							
Heart failure	13 (35.1%)	1 (25.0%)	12 (36.4%)	>0.9999	1 (16.7%)	12 (38.7%)	0.3945
Old stroke	4 (10.8%)	1 (25.0%)	3 (9.1%)	0.3804	1 (16.7%)	3 (9.7%)	0.5236
Diabetes	23 (62.2%)	1 (25.0%)	22 (66.7%)	0.1419	3 (50.0%)	20 (64.5%)	0.6534
CAD	10 (27.0%)	1 (25.0%)	9 (27.3%)	>0.9999	1 (16.7%)	9 (29.0%)	>0.9999
COPD/Asthma	2 (5.6%)	0 (0.0%)	2 (6.2%)	>0.9999	0 (0.0%)	2 (6.7%)	>0.9999
Malignancy	6 (16.7%)	0 (0.0%)	6 (18.8%)	>0.9999	0 (0.0%)	6 (20.0%)	0.5610
ESRD on hemodialysis	15 (40.5%)	2 (50.0%)	13 (39.4%)	>0.9999	3 (50.0%)	12 (38.7%)	0.6696
Witnessed	37 (100%)	4 (100%)	33 (100%)	NA	6 (100%)	31 (100%)	NA
Bystander chest compression	37 (100%)	4 (100%)	33 (100%)	NA	6 (100%)	31 (100%)	NA
Bystander defibrillation	6 (16.2%)	2 (50.0%)	4 (12.1%)	0.1152	2 (33.3%)	4 (12.9%)	0.2448
Initial rhythm, shockable	7 (18.9%)	2 (50.0%)	5 (15.2%)	0.1547	2 (33.3%)	5 (16.1%)	0.3155
Duration of resuscitation effort, minutes	12.0 (8.0-31.3))	15.5 (2.0-54.0)	12.0 (8.0-31.3)	0.6950	7.5 (2.0-29.0)	15.0 (8.5-31.8)	0.2563
Motor GCS score < 2	20 (54.1%)	4 (100%)	16 (48.5%)	0.1094	6 (100%)	14 (45.2%)	0.0220
Serum pH	7.33±0.18	7.38±0.06	7.32±0.19	0.2005	7.40±0.11	7.31±0.19	0.2802
Serum lactate, mg/dL	47.9 (32.4-83.7)	54.2 (36.3-86.9)	47.4 (32.4-83.7)	0.8449	43.2 (21.8-56.5)	47.9 (34.8-92.0)	0.4836
rCAST score	5.6±3.6	2.6±2.0	5.9±3.6	0.0310	2.5±1.7	6.1±3.6	0.0017
APACHE II	32.8±7.2	31.8±2.8	32.9±7.6	0.5675	31.5±4.4	33.0±7.7	0.6477
PCI after resuscitation	1 (2.7%)	1 (25.0%)	0 (0.0%)	0.1081	1 (16.7%)	0 (0.0%)	0.1622

Data are presented as mean ± standard deviation, median (interquartile range), or number (percentage). APACHE: acute physiology and chronic health evaluation, COPD: chronic obstructive pulmonary disease, CAD: coronary artery disease, ESRD: end-stage renal disease, GCS: Glasgow Coma Scale, NA: not applicable, PCI: percutaneous coronary intervention.

Table 2. Using rCAST Severity Category to Predict the Probability of Poor Neurologic Outcomes or Mortality at Day 28

(n = 37)	Number of patients	Probability of poor neurologic outcome	Probability of hospital mortality
Low severity category	19	78.9% (54.4%-94.0%)	68.4% (43.5%-87.4%)
Moderate severity category	18	100.0% (81.5%-100.0%)	100.0% (81.5%-100.0%)
High severity category	0	NA	NA

Data are presented as probability (95% confidence interval). NA: not applicable

but IHCA patients had more respiratory failure (22% vs. 12%) [21]. Andersson *et al*. retrospectively analyzed 799 ROSC patients admitted to ICUs, and found that the IHCA patients were older, less frequently male, had more comorbidities, more often had an initially non-shockable rhythm, had more witnessed arrests, and had shorter delay times [22]. Epidemiology studies have reported survival advantages in IHCA patients [2, 4, 23], including a survival rate of 23.3% in IHCA patients compared to 9.0% in OHCA patients in the United States in 2020 [2]. However, Høybye *et al*. found that the survival benefits diminished after adjusting for cardiac arrest characteristics [23]. Andersson *et al*. also found that cardiac arrest characteristics, rather than location of the arrest, were independent predictors of the outcome [22].

Although TTM is suggested for IHCA patients based on current guidelines [9-10], some retrospective studies [16, 24-25] have reported that TTM in IHCA patients was not associated with significant benefits in survival or neurological outcomes compared to TTM in OHCA patients. However, these studies [16, 24-25] were limited by the low implementation rates of TTM, and possibly high selection bias. In contrast, Blanc *et al*. reported that targeted hypothermia was associated with better 90-day neurological outcomes (adjusted odds ratio: 2.40, 95% CI: 1.17-13.03, p=0.03) in IHCA patients with a non-shockable rhythm compared to targeted normothermia [26]. To address these inconsistencies, Polderman suggested that prospective randomized-controlled trials should be considered to clarify the effect of TTM in IHCA patients [27]; however, this may be impractical.

The rCAST score was first proposed by Nishikimi *et al*., and was simplified from the original CAST score, which consists of 8 factors, and was developed at 4 hospitals in Japan using logistic regression and decision tree algorithms [13, 28]. The rCAST score was later validated retrospectively using data from the Japanese Association for Acute Medicine, with an AUC of 0.892 to predict a poor neurologic outcome and 0.832 to predict mortality at 30 days [13]. We previously validated the rCAST score with OHCA patients at our hospital [14], and found that the rCAST score had a similar predictive value in Taiwan. However, the cutoff values proposed by Nishikimi *et al*. [13] did not show significant discrimination ability [14]. In this study, we found that the rCAST score had moderate accuracy in predicting a poor neurologic outcome and mortality in IHCA patients, in contrast with the rCAST scores of the OHCA patients. The distribution of the rCAST scores and severity categories were different from the original study of Nishikimi *et al* [13]. This may

be due to the higher rate of witnessed cardiac arrests, shorter time delay, higher rate of bystander chest compression, and shorter duration of resuscitation due to the setting of IHCA, compared to the OHCA patients at our institute during the same period [14]. Future research is needed to determine an appropriate cutoff value to distinguish which IHCA patients are more likely to benefit from TTM.

To the best of our knowledge, this study is the first to evaluate the usefulness of the rCAST score in PCAS patients due to IHCA; however, several limitations should be noted. First, the retrospective nature of this study may have resulted in missing values and selection bias with regard to which patients received TTM, which was decided by the physician in charge. Only 4 patients were excluded due to missing data in our cohort, so this may not have had a large effect on our results. Second, the number of enrolled patients was relatively small. Further studies with more participants are warranted. Finally, no patients were classified as having a high degree of severity. However, all of the patients in the moderate severity category died, which may imply that a higher rCAST score would also be associated with a poor outcome. Even with these limitations, the results of this study shed light on the early prediction of outcomes in IHCA patients.

Conclusion

Our preliminary results suggest that the rCAST score has moderate accuracy in predicting a poor neurologic outcome and mortality at 28 days in IHCA patients receiving TTM. Further large-scale studies are warranted to confirm our findings.

References

1. Wittwer MR, Zeitz C, Beltrame JF, *et al*. Providing a simple and consistent solution for the definition of in- versus out-of-hospital cardiac arrest. Resuscitation 2020; 156: 51-2.
2. Tsao CW, Aday AW, Almarzooq ZI, *et al*. Heart disease and stroke statistics-2022 update: a report from the American Heart Association. Circulation 2022; 145: e153-e639.
3. Penketh J, Nolan JP. In-hospital cardiac arrest: the state of the art. Crit Care 2022; 26: 376.
4. Gräsner JT, Herlitz J, Tjelmeland IBM, *et al*. European Resuscitation Council Guidelines 2021: epidemiology of cardiac arrest in Europe. Resuscitation 2021; 161: 61-79.
5. Schluep M, Gravesteijn BY, Stolker RJ, *et al*. One-year survival after in-hospital cardiac arrest: a systematic review and meta-analysis. Resuscitation 2018; 132: 90-100.
6. Bernard SA, Gray TW, Buist MD, *et al*. Treatment of comatose survivors of out-of-hospital cardiac arrest with induced hypothermia. N Engl J Med 2002; 346: 557-63.
7. The Hypothermia After Cardiac Arrest Study Group. Mild therapeutic hypothermia to improve the neurologic outcome after cardiac arrest. N Engl J Med 2002; 346: 549-56.
8. Holzer M. Targeted temperature management for comatose survivors of cardiac arrest. N Engl J Med 2010; 363: 1256-64.
9. Nolan JP, Sandroni C, Böttiger BW, *et al*. European Resuscitation Council and European Society of Intensive Care Medicine Guidelines 2021: Post-resuscitation care. Resuscitation 2021; 161: 220-69.
10. Panchal AR, Bartos JA, Cabañas JG, *et al*. Part 3: Adult basic and advanced life support: 2020 American Heart Association guidelines for cardiopulmonary resuscitation and emergency cardiovascular care. Circulation 2020; 142: S366-468.
11. Hawkes MA, Rabinstein AA. Neurological prognostication after cardiac arrest in the era of target temperature management. Curr Neurol Neurosci Rep 2019; 19: 10.
12. Sandroni C, D'Arrigo S, Cacciola S, *et al*. Prediction of good neurological outcome in comatose survivors of

cardiac arrest: a systematic review. Intensive Care Med 2022; 48: 389-413.
13. Nishikimi M, Ogura T, Nishida K, *et al*. External validation of a risk classification at the emergency department of post-cardiac arrest syndrome patients undergoing targeted temperature management. Resuscitation 2019; 140: 135-41.
14. Chen C-H, Wang C-J, Wang I-T, *et al*. Does one size fit all? External validation of the rCAST score to predict the hospital outcomes of post-cardiac arrest patients receiving targeted temperature management. J Clin Med 2023; 12: 242.
15. Wang CJ, Yang SH, Lee CH, *et al*. Therapeutic hypothermia application vs standard support care in post resuscitated out-of-hospital cardiac arrest patients. Am J Emerg Med 2013; 31: 319-25.
16. Wang CJ, Yang SH, Chen CH, *et al*. Targeted temperature management for in-hospital cardiac arrest: 6 years of experience. Ther Hypothermia Temp Manag 2020; 10: 153-8.
17. Jacobs I, Nadkarni V, Bahr J, *et al*. Cardiac arrest and cardiopulmonary resuscitation outcome reports: update and simplification of the Utstein templates for resuscitation registries: a statement for healthcare professionals from a task force of the International Liaison Committee on Resuscitation (American Heart Association, European Resuscitation Council, Australian Resuscitation Council, New Zealand Resuscitation Council, Heart and Stroke Foundation of Canada, InterAmerican Heart Foundation, Resuscitation Councils of Southern Africa). Circulation 2004; 110: 3385-97.
18. Brain Resuscitation Clinical Trial I Study Group. Randomized clinical study of thiopental loading in comatose survivors of cardiac arrest. N Engl J Med 1986; 314: 397-403.
19. Cummins RO, Chamberlain DA, Abramson NS, *et al*. Recommended guidelines for uniform reporting of data from out-of-hospital cardiac arrest: the Utstein Style. A statement for health professionals from a task force of the American Heart Association, the European Resuscitation Council, the Heart and Stroke Foundation of Canada, and the Australian Resuscitation Council. Circulation 1991; 84: 960-75.
20. Akobeng AK. Understanding diagnostic tests 3: Receiver operating characteristic curves. Acta Paediatr 2007; 96: 644-7.
21. Chen N, Callaway CW, Guyette FX, *et al*. Arrest etiology among patients resuscitated from cardiac arrest. Resuscitation 2018; 130: 33-40.
22. Andersson A, Arctaedius I, Cronberg T, *et al*. In-hospital versus out-of-hospital cardiac arrest: Characteristics and outcomes in patients admitted to intensive care after return of spontaneous circulation. Resuscitation 2022; 176: 1-8.
23. Høybye M, Stankovic N, Holmberg M, *et al*. In-hospital vs. out-of-hospital cardiac arrest: patient characteristics and survival. Resuscitation 2021; 158: 157-65.
24. Chan PS, Berg RA, Tang Y, *et al*. Association between therapeutic hypothermia and survival after in-hospital cardiac arrest. JAMA 2016; 316: 1375-82.
25. Nichol G, Huszti E, Kim F, *et al*. Does induction of hypothermia improve outcomes after in-hospital cardiac arrest? Resuscitation 2013; 84: 620-5.
26. Blanc A, Colin G, Cariou A, *et al*. Targeted temperature management after in-hospital cardiac arrest: an ancillary analysis of HYPERION trial data. Chest 2022; 162(2): 356-66.
27. Polderman KH, Varon J. Confusion around therapeutic temperature management hypothermia after in-hospital cardiac arrest? Circulation 2018; 137: 219-21.
28. Nishikimi M, Matsuda N, Matsui K, *et al*. A novel scoring system for predicting the neurologic prognosis prior to the initiation of induced hypothermia in cases of post-cardiac arrest syndrome: the CAST score. Scand J Trauma Resusc Emerg Med 2017; 25: 49.

Importance of Identifying Chronic Pulmonary Aspergillosis During Treatment of Nontuberculous Mycobacterium Lung Disease – A Case Report

Yu-Song Tang[1], Chau-Chyun Sheu[1,2], Hung-Ling Huang[1,3,4]

Chronic pulmonary aspergillosis (CPA) following nontuberculous mycobacterial lung disease (NTM-LD) has been observed increasingly worldwide in recent years. Identification of CPA in patients with NTM-LD is crucial because the prognosis is worse than that for patients with NTM-LD alone. The complexity and similarities of these concurrent diseases is a clinical challenge, and treatments for both diseases might conflict due to the complicated interaction of multi-drug use.

This study reported the case of an older man with a low body mass index, previous tuberculosis infection with fibrocavitary lung lesions, and chronic obstructive pulmonary disease under inhaled and oral corticosteroid treatment who developed CPA with deteriorating symptoms after receiving months of effective antimicrobial treatment for *Mycobacterium kansasii* lung disease. The patient's general condition improved after treatment for CPA. This case demonstrated that CPA can develop during treatment for NTM-LD, especially in patients with certain risk factors, and that prompt treatment of CPA is required. ***(Thorac Med 2023; 38: 289-296)***

Key words: Chronic pulmonary aspergillosis, *Mycobacterium kansasii* lung disease, nontuberculous mycobacterial lung disease, treatment, voriconazole

Introduction

Chronic pulmonary aspergillosis (CPA), a progressive deteriorating parenchymal lung disease, can occur in patients with preexisting cavitary lesions, structural lung diseases, or subtle immune defects [1]. As CPA develops in preexisting or new and expanding bronchopulmonary cavities or nodules, it becomes a potential complication of Mycobacterium tuberculosis (TB) and nontuberculous mycobacteria (NTM). Concomitant infection of CPA and NTM lung disease (NTM-LD) has gradually become a clinical concern as novel techniques for detect-

[1]Division of Pulmonary and Critical Care Medicine, Department of Internal Medicine, Kaohsiung Medical University Hospital, Kaohsiung Medical University, Kaohsiung, Taiwan. [2]Department of Internal Medicine, School of Medicine, College of Medicine, Kaohsiung Medical University, Kaohsiung, Taiwan. [3]Department of Internal Medicine, Kaohsiung Municipal Ta-Tung Hospital, Kaohsiung, Taiwan. [4]Graduate Institute of Medicine, College of Medicine, Kaohsiung Medical University, Kaohsiung, Taiwan.
Address reprint requests to: Dr. Hung-Ling Huang, Department of Internal Medicine, Kaohsiung Medical University Hospital, Kaohsiung Medical University No. 100, Tzyou First Road, Kaohsiung City, Taiwan

ing the diseases have developed and associated risk factors have been identified.

Up to 93% of patients with CPA receive a diagnosis of preexisting pulmonary TB in high TB endemic areas [2]. However, in countries with a lower incidence rate of TB, pulmonary NTM is the second leading cause of CPA (14.9%), following pulmonary TB (15.3%) [3]. One study found a higher incidence of *Aspergillus*-related diseases in patients with bronchiectasis and NTM diseases [4]. Kunst *et al*. conducted a case-control study of patients with bronchiectasis and observed that patients with NTM diseases had a higher positivity rate of *Aspergillus* serology (radioallergosorbent test [RAST], total serum immunoglobulin [Ig]E and *Aspergillus* precipitins) when compared with controls (33.3% vs. 9.8%, $p=0.005$). Furthermore, the radiological features of *Aspergillus*-related lung disease, including multiple nodules, focal consolidation, a tree-in-bud appearance, and mycetoma formation, were more common among patients with NTM diseases than among controls (20% vs. 0%, $p=0.003$). Geurts *et al*. reported that 63.8% of patients with NTM-LD had positive *Aspergillus* IgG, and 37.8% yielded *A. fumigatus*, indicating that coinfection with *A. fumigatus* was common in patients with NTM-LD [5]. Two retrospective studies, in Japan and Denmark, respectively, reported a coincidence rate of NTM infections of approximately 11% and 8.2%, which complicated cases of CPA, respectively [6-7].

CPA is diagnosed when the following criteria are satisfied: (a) compatible clinical symptoms of CPA, (b) radiological findings, (c) a positive serum *Aspergillus* precipitin test (using an *A. fumigatus* IgG ELISA kit), isolation of *Aspergillus* spp. from respiratory samples (e.g., sputum, transtracheal aspirate, or bronchial aspiration fluid), or an immunological response to *Aspergillus* spp. and the exclusion of alternative diagnoses [8-10].

NTM refers to members of the genus Mycobacterium other than *M. tuberculosis complex*, and *M. leprae*, and they are ubiquitous in the environment worldwide [11]. NTM have been known to cause disease in humans for over 70 years [12]. NTM-LD occurs when aerosolized droplets containing mycobacteria are inhaled by a susceptible host [13]. A diagnosis of NTM-LD was proposed by the American Thoracic Society and the Infectious Disease Society of America in their jointly published guidelines in 2007, and in 2020, as follows: (a) clinical symptoms of NTM-LD; (b) radiographic images that include bronchiectasis, nodular lesions, cavitary lesions, and parenchymal consolidation; (c) microbiological data from (1) at least 2 positive cultures from sputum, (2) a positive culture with bronchoscopic wash or lavage, or (3) a transbronchial, or other lung biopsy, with a positive culture for NTM or compatible histopathological features, and (d) exclusion of other disorders [14].

The global prevalence of NTM-LD appears to vary widely in areas with low TB endemicity. In the United States and Japan, prevalence rates of 23-37 and 33-65 cases per 100 000 people, respectively, have been reported [11]. A trend toward an increasing incidence rate has been observed in TB-endemic countries [15-16]. In Taiwan, from 2005 to 2013, Lin *et al*. found that the age-adjusted incidence rate of NTM-LD increased from 5.3 to 14.8 per 100 000 people per year. Meanwhile, the age-adjusted incidence rate of confirmed TB cases decreased from 63.4 to 50.1 per 100,000 people per year, and the age-adjusted incidence rate of NTM–TB coinfection was from 1.2 to 1.8 per 100 000

people per year. The proportion of NTM–TB coinfections in patients with confirmed TB was 2.8%. Among them, male and older patients had a significantly higher incidence of NTM diseases (the incidence rate ratio (IRR) of the men with NTM–TB coinfection was 1.9, and the IRR of patients with NTM–TB coinfection aged > 74 years was 12.5, compared with that of patients aged < 45 years) [15]. A retrospective study in Taiwan found that patients with previous pulmonary TB and those with chronic obstructive pulmonary disease (COPD) had a 1.31- and 1.17-fold higher risk for NTM-LD, respectively [16].

Identification of *Aspergillus*-related lung disease is crucial because the prognosis among undetected cases is poor. Case series from Japan (n=42) and South Korea (n=43) have revealed that the 1-, 5- and 10-year survival rates of patients with CPA are 63%-74%, 15%-50% and 26%, respectively [2, 17]. One study conducted in the United Kingdom that evaluated 387 patients with CPA revealed 1-, 5- and 10-year survival rates of 86%, 62%, and 47%, respectively [18].

The present study examined the case of a patient with *Mycobacterium kansasii (M. kansasii)*-LD with bronchiectasis and fibrocavitary lesions who subsequently developed pulmonary aspergillosis after 6 months of anti–*M. kansasii* treatment.

Case Presentation

A 70-year-old man visited our chest outpatient department (OPD) after experiencing productive cough for 3 months and intermittent hemoptysis with exertional dyspnea for several days. The patient was a heavy smoker (>30 pack-years) with a low body mass index (BMI) (17.7 kg/m^2) and engaged in fruit-tree farming. A review of his medical history revealed previous diagnoses of old TB, bronchiectasis, asthma–COPD overlapping syndrome (ACOS), and prescriptions of Seretide and Spiriva. Oral corticosteroid (prednisolone 10 mg/day) had been prescribed for 2 months before the patient visited the OPD due to the acute exacerbation of ACOS. The initial chest radiograph (CXR) indicated bronchiectasis and fibrosis with emphysema (Fig. 1A), and chest computed tomography (CT) showed multiple fibrocavitary lesions in the right lung and nodules and multiple consolidative patches with bronchiectasis in the bilateral lungs (Fig. 1B). The sputum acid-fast stain (AFS) was positive and yielded M. kansasii. The patient's laboratory data revealed leukocytosis (white blood cell count: 15770/uL) with elevated C-reactive protein (134.1 mg/L). Serum galactomannan test (GM test) results and *Aspergillus* immunoglobulin titers were within normal ranges (0.092 for the GM test [normal range: <0.5 index], 27.2 for *A. fumigatus* [normal range: <40 μmol/h], and 22.2 for A. niger [normal range: <24 μmol/h]).

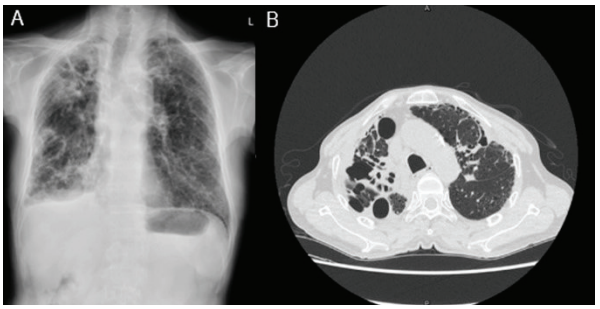

Fig. 1. Initial chest radiograph and high-resolution computed tomography images of Mycobacterium kansasii lung disease. The posteroanterior radiograph of the chest in Panel A shows bronchiectasis and fibrocavitary lesions with emphysema in both lungs. High-resolution computed tomography scan of the chest in Panel B shows fibrocavitary lesions in the right lung and nodules and consolidative patches with bronchiectasis in the bilateral lungs.

M. kansasii–LD was diagnosed, and the patient received anti-*M. kansasii* treatment with regimens of isoniazid 300 mg/day, rifampin 450 mg/day, and ethambutol 15 mg/kg/day. After receiving the effective anti-*M. kansasii* treatment for 3 months, the patient gradually recovered to his baseline condition, and sputum AFS with culture also indicated negative reversion. Anti-*M. kansasii* treatment was planned to be maintained for a total of 12 months for full treatment.

After 9 months of anti-*M. kansasii* treatment totally, the patient experienced progressive dyspnea on exertion and increased sputum levels with low-grade afternoon fever for 1 month. CXR revealed progressive right-lung infiltration (Fig. 2A), and laboratory data indicated leukocytosis (white blood cell count: 14960/uL) with elevated C-reactive protein (257.8 mg/L). The patient was admitted for treatment of pneumonia. However, the symptoms improved little, and the CXR follow-up showed no resolution of infiltration after 2 weeks of broad-spectrum antibiotic treatment. Chest CT was performed and disclosed multiple cavitary nodular lesions in the right lung with aspergilloma in the right upper lobe (Fig. 2B). GM testing of the bronchoalveolar lavage (BAL) fluid via the right upper lobe (RB 3) was 0.578 (normal range: <0.5 index), with positive serum *A. fumigatus*–specific IgG (108 μmol/h). The final BAL culture report also yielded *A. fumigatus*; newly developed CPA was thus diagnosed.

A drug susceptibility test indicated that *A. fumigatus* was susceptible to voriconazole (minimal inhibitory concentration = 2). Since drug–drug interactions between rifampicin and voriconazole were considered, we discontinued anti-*M. kansasii* medication, and voriconazole was administered thereafter. The patient suffered from epigastria and mild blurred vision after voriconazole use. The blurred vision subsided spontaneously after 1 week and epigastralgia was relieved by antacid. The patient was discharged and continued to receive CPA treatment at the OPD. There were no relapsing side effects or others such as hepatitis, and no QT prolongation was noted during the period of treatment. After 6 months of CPA treatment, images showed resolution of the cavitary lesion with aspergilloma (Fig. 2C), and the follow-up serum *Aspergillus* IgG titer declined gradually (Fig. 3). We also regularly followed up on the

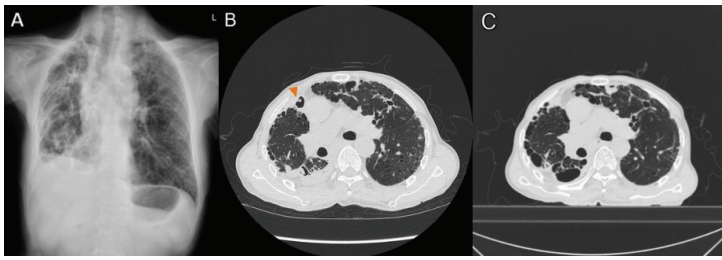

Fig. 2. Chest radiograph and high-resolution computed tomography images showing suspected pulmonary aspergillosis before and after treatment. The posteroanterior radiograph of the chest in Panel A shows progressive right-lung infiltration. The high-resolution computed tomography scan of the chest in Panel B shows multiple nodular lesions in the right lung with aspergilloma in the cavity of the right upper lobe (arrowhead). Panel C shows disappearance of aspergilloma with improvements in bilateral lung infiltration after voriconazole use for 6 months

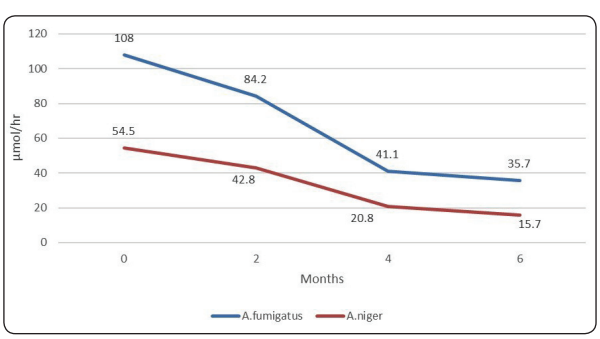

Fig. 3. Gradual decline of the Aspergillus IgG titer. IgG titers of A. fumigatus and A. niger declined gradually after treatment with voriconazole.

sputum AFS with culture for 1 year, and no relapse of *M. kansasii*–LD was noted.

Discussion

We reported a case of CPA that developed during effective anti-*M. kansasii* treatment. Clinicians should be aware of the potential concomitance of CPA and NTM. In past reports, CPA has developed about 1.5-7 years after the diagnosis of NTM-LD [6, 19-23]. The causative relationship between NTM and CPA is not well elucidated, but hypotheses have been proposed to explain the correlation between them. Patients with NTM-LD usually receive long-term broad-spectrum antibiotics that increase the risk of fungal colonization due to selective pressure, which may eventually lead to *Aspergillus* lung infection, especially in patients with underlying structural lung diseases [10]. Moreover, NTM-LD results in destructive lung lesions, particularly lung cavitation, which leads to a higher incidence of CPA [24]. In a retrospective study, Takeda and colleagues found that cavitary NTM infection and steroid use were independent risk factors for the development of CPA [6].

Whether through systemic or inhalation use, a prednisolone dosage of 10 mg/day is significantly associated with CPA [6]. Long-term inhaled corticosteroid use can impair the host immune system, including both innate (phagocyte) and adaptive (lymphocyte) immunity [25], which inhibits the killing of fungi. Corticosteroids also increase *Aspergillus* colonization and the growth of *Aspergillus* hyphae [25, 26]. A retrospective report demonstrated that 7.2% of patients with NTM-LD had newly developed CPA during NTM-LD treatment; old age, male sex, low BMI, COPD, systemic steroids use, M. abscessus complex as the etiologic organism, and NTM-LD fibrocavitary lesions are the greatest risk factors [22].

The incidence of different NTM species with pulmonary aspergillosis is unclear. Many studies have reported that the *M. avium* complex (MAC) is the most common NTM group associated with CPA [20, 21]. In Taiwan, the prevalence and incidence of both NTM isolates and NTM-LD increases annually; the most common species are MAC followed by M. abscessus [27]. The incidence rate of the third leading species, *M. kansasii*, has increased more in southern Taiwan than in northern Taiwan [16]. Nevertheless, fibrocavitary *M. kansasii*–LD combined with old age, male sex, low BMI, and a history of COPD were all risk factors for CPA in our patient.

A higher mortality rate was observed in groups with NTM-LD and CPA than in groups with NTM-LD only [22, 28-29]. In a retrospective study, Zoumot *et al*. investigated MAC infection in patients ($n=52$) with noncystic fibrosis and bronchiectasis, and compared the clinical characteristics of the survivors and non-survivors. CPA was significantly more common in non-survivors than in survivors (87.5% vs. 12.5%, respectively; $p < 0.001$) [28]. In another retrospective study, Fukushima *et al*. reported CPA to be an independent risk factor for mortality in patients ($n=75$) with MAC lung disease (OR: 8.552, 95% CI: 1.335-54.770) [29].

Triazole (itraconazole or voriconazole) use for at least 6 months is the first-line antifungal treatment for CPA [8]. However, we encountered a clinical challenge when treating NTM-LD concomitant with CPA due to the drug–drug interaction between rifampicin and triazole [10]. Rifampicin is a key drug in standard antimycobacterial regimens for patients with MAC and *M. kansasii* infection. However, rifamycin is a

strong CYP3A4 inducer, and the co-administration of rifamycin and triazole can significantly lower the effect of the antifungal agent, which can increase the possibility of treatment failure [30]. As an alternative to antifungal agents, amphotericin B is not suitable for long-term clinical use due to nephrotoxicity. Echinocandins may be an alternative due to their fewer drug–drug interactions and lower toxicity [31], but they can only be administered intravenously. A high dose of posaconazole taken orally and combined with therapeutic drug monitoring (TDM) may also be considered for long-term therapy [32].

TDM for voriconazole concentration in the blood may ensure safe and effective treatment. A prospective, randomized trial of TDM during voriconazole therapy in 108 patients with a diagnosis of invasive fungal infections yielded a significantly lower discontinuation rate due to adverse events (4% vs. 17%; $p=0.02$) and a higher response rate (81% vs. 57%; $p=0.04$) in patients who received TDM compared to those who did not [33]. According to the recommended guidelines, alternative agents in antimycobacterial regimens can be substituted with rifampicin [34-35], although caution should be exercised in balancing the benefits and risks.

Some indicators associated with a poor prognosis with CPA have been reported [18, 36]. A retrospective study by Lowes *et al*. revealed preexisting NTM-LD as a key predictor of high mortality among patients with CPA (hazard ratio [HR]: 2.07, 95% CI: 1.22-3.52). Other predictors included prior COPD, pleural involvement, bilateral cavitary disease or aspergillomas, low BMI, and low albumin [18]. Another retrospective study found that systemic corticosteroid use (HR: 3.32, 95% CI: 1.23–9.51) and C-reactive protein levels higher than 5 mg/dL (HR: 8.96, 95% CI: 2.15-62.9) were independently associated with high overall mortality among patients with CPA after pulmonary NTM [36].

In this report, we shared our experience with diagnosing and treating a patient with CPA after NTM-LD. NTM-LD itself is a risk factor for the development of CPA, which may take place during the lengthy antibiotics treatment for NTM-LD. Clinicians should be aware of newly developed CPA when treating NTM-LD, especially when combined with other risk factors in male patients, older patients, or patients with low BMI, previous TB infection, a history of COPD, or systemic or inhaled corticosteroid use, and particularly when a deteriorating clinical condition occurs suddenly during effective anti-NTM treatment. The prognosis in patients with concomitant NTM-LD and CPA is worse than in patients with NTM-LD alone, so obtaining the correct diagnosis and providing prompt antifungal treatment is essential.

References

1. Bongomin F, Asio LG, Baluku JB, *et al*. Chronic pulmonary aspergillosis: notes for a clinician in a resource-limited setting where there is no mycologist. J Fungi (Basel) 2020; 6(2).
2. Nam HS, Jeon K, Um SW, *et al*. Clinical characteristics and treatment outcomes of chronic necrotizing pulmonary aspergillosis: a review of 43 cases. Int J Infect Dis 2010; 14(6): e479-82.
3. Smith NL, Denning DW. Underlying conditions in chronic pulmonary aspergillosis including simple aspergilloma. Eur Respir J 2011; 37(4): 865-72.
4. Kunst H, Wickremasinghe M, Wells A, *et al*. Nontuberculous mycobacterial disease and *Aspergillus*-related lung disease in bronchiectasis. Eur Respir J 2006; 28(2): 352-7.
5. Geurts K, Zweijpfenning SMH, Pennings LJ, *et al*. Nontuberculous mycobacterial pulmonary disease and

Aspergillus co-infection: Bonnie and Clyde? Eur Respir J 2019; 54(1).

6. Takeda K, Imamura Y, Takazono T, *et al*. The risk factors for developing of chronic pulmonary aspergillosis in nontuberculous mycobacteria patients and clinical characteristics and outcomes in chronic pulmonary aspergillosis patients coinfected with nontuberculous mycobacteria. Med Mycol 2016; 54(2): 120-7.
7. Klinting FP, Laursen CB, Titlestad IL. Incidence of chronic pulmonary aspergillosis in patients with suspected or confirmed NTM and TB - A population-based retrospective cohort study. J Fungi (Basel) 2022; 8(3).
8. Denning DW, Cadranel J, Beigelman-Aubry C, *et al*. Chronic pulmonary aspergillosis: rationale and clinical guidelines for diagnosis and management. Eur Respir J 2016; 47(1): 45-68.
9. Patterson TF, Thompson GR, 3rd, Denning DW, *et al*. Practice guidelines for the diagnosis and management of aspergillosis: 2016 update by the Infectious Diseases Society of America. Clin Infect Dis 2016; 63(4): e1-e60.
10. Phoompoung P, Chayakulkeeree M. Chronic pulmonary aspergillosis following nontuberculous mycobacterial infections: an emerging disease. J Fungi (Basel) 2020; 6(4).
11. Cowman S, van Ingen J, Griffith DE, *et al*. Non-tuberculous mycobacterial pulmonary disease. Eur Respir J 2019; 54(1).
12. Feldman WH, Hutchinson D, *et al*. Pathogenicity studies of tubercle bacilli, type avium, from a human infection. Am J Pathol. 1948; 24(3): 696.
13. Piersimoni C, Scarparo C. Pulmonary infections associated with non-tuberculous mycobacteria in immunocompetent patients. Lancet Infect Dis 2008; 8(5): 323-34.
14. Griffith DE, Aksamit T, Brown-Elliott BA, *et al*. An official ATS/IDSA statement: diagnosis, treatment, and prevention of nontuberculous mycobacterial diseases. Am J Respir Crit Care Med 2007; 175(4): 367-416.
15. Lin CK, Yang YH, Lu ML, *et al*. Incidence of nontuberculous mycobacterial disease and coinfection with tuberculosis in a tuberculosis-endemic region: A population-based retrospective cohort study. Medicine (Baltimore) 2020; 99(52): e23775.
16. Huang HL, Cheng MH, Lu PL, *et al*. Epidemiology and predictors of NTM pulmonary infection in Taiwan - a retrospective, five-year multicenter study. Sci Rep 2017; 7(1): 16300.
17. Ohba H, Miwa S, Shirai M, *et al*. Clinical characteristics and prognosis of chronic pulmonary aspergillosis. Respir Med 2012; 106(5): 724-9.
18. Lowes D, Al-Shair K, Newton PJ, *et al*. Predictors of mortality in chronic pulmonary aspergillosis. Eur Respir J 2017; 49(2).
19. Ishikawa S, Yano S, Kadowaki T, *et al*. [Clinical analysis of non-tuberculous mycobacteriosis cases complicated with pulmonary aspergillosis]. Kekkaku 2011; 86(9): 781-5.
20. Furuuchi K, Ito A, Hashimoto T, *et al*. Risk stratification for the development of chronic pulmonary aspergillosis in patients with Mycobacterium avium complex lung disease. J Infect Chemother 2018; 24(8): 654-9.
21. Kobashi Y, Fukuda M, Yoshida K, *et al*. Chronic necrotizing pulmonary aspergillosis as a complication of pulmonary Mycobacterium avium complex disease. Respirology 2006; 11(6): 809-13.
22. Jhun BW, Jung WJ, Hwang NY, *et al*. Risk factors for the development of chronic pulmonary aspergillosis in patients with nontuberculous mycobacterial lung disease. PLoS One 2017; 12(11): e0188716.
23. Fukushima K, Kida H. New/different look at the presence of *Aspergillus* in mycobacterial pulmonary diseases. Long-term retrospective cohort study. Microorganisms 2021; 9(2).
24. Fowler SJ, French J, Screaton NJ, *et al*. Nontuberculous mycobacteria in bronchiectasis: prevalence and patient characteristics. Eur Respir J 2006; 28(6): 1204-10.
25. Lionakis MS, Kontoyiannis DP. Glucocorticoids and invasive fungal infections. Lancet 2003; 362(9398): 1828-38.
26. Ng TT, Robson GD, Denning DW. Hydrocortisone-enhanced growth of *Aspergillus* spp.: implications for pathogenesis. Microbiology (Reading) 1994; 140 (Pt 9): 2475-9.
27. Lai CC, Tan CK, Chou CH, *et al*. Increasing incidence of nontuberculous mycobacteria, Taiwan, 2000-2008. Emerg Infect Dis 2010; 16(2): 294-6.
28. Zoumot Z, Boutou AK, Gill SS, et al. Mycobacterium avium complex infection in non-cystic fibrosis bronchiectasis. Respirology 2014; 19(5): 714-22.

29. Fukushima K, Kitada S, Abe Y, *et al*. Long-term treatment outcome of progressive mycobacterium avium complex pulmonary disease. J Clin Med 2020; 9(5).
30. Drayton J, Dickinson G, Rinaldi MG. Coadministration of rifampin and itraconazole leads to undetectable levels of serum itraconazole. Clin Infect Dis 1994; 18(2): 266.
31. Kohno S, Izumikawa K, Ogawa K, *et al*. Intravenous micafungin versus voriconazole for chronic pulmonary aspergillosis: a multicenter trial in Japan. J Infect 2010; 61(5): 410-8.
32. Dekkers BGJ, Bakker M, van der Elst KCM, *et al*. Therapeutic drug monitoring of posaconazole: an update. Curr Fungal Infect Rep 2016; 10: 51-61.
33. Park WB, Kim NH, Kim KH, *et al*. The effect of therapeutic drug monitoring on safety and efficacy of voriconazole in invasive fungal infections: a randomized controlled trial. Clin Infect Dis 2012; 55(8): 1080-7.
34. Daley CL, Iaccarino JM, Lange C, *et al*. Treatment of nontuberculous mycobacterial pulmonary disease: an official ATS/ERS/ESCMID/IDSA clinical practice guideline. Eur Respir J 2020; 56(1).
35. Haworth CS, Banks J, Capstick T, *et al*. British Thoracic Society guidelines for the management of non-tuberculous mycobacterial pulmonary disease (NTM-PD). Thorax 2017; 72(Suppl 2): ii1-ii64.
36. Naito M, Kurahara Y, Yoshida S, *et al*. Prognosis of chronic pulmonary aspergillosis in patients with pulmonary non-tuberculous mycobacterial disease. Respir Investig 2018; 56(4): 326-31.

A Huge Ancient Schwannoma at the Middle Mediastinum: Case Report

Shuo-Ying Dai[1], Cheng-Lin Wu[4], Ren-Hao Chan[3], Jenq-Chang Lee[3], Ying-Yuan Chen[2]

Schwannoma is the most common mediastinal peripheral nerve sheath tumor, and is usually located at the posterior mediastinum. Ancient schwannoma, an uncommon variant of schwannoma, is a slow-growing benign tumor with the degenerative features of cyst formation, calcification, hemorrhage and hyalinization. Due to the pleomorphism of ancient schwannomas, they are difficult to diagnose based on clinical presentation, imaging studies, and histopathological reviews of core biopsy alone. Here, we reported the case of a huge middle mediastinal ancient schwannoma accidently found by chest X-ray, that had not been diagnosed in 2 attempts at core biopsy. Surgical pathology finally confirmed this ancient schwannoma after video-assisted thoracic surgery. Successful surgical tumor removal can provide not only an accurate pathological diagnosis, but also radical treatment to prevent unexpected events in the future. ***(Thorac Med 2023; 38: 297-302)***

Key words: Ancient schwannoma, neurilemoma, mediastinal tumor, video-assisted thoracic surgery

Introduction

The mediastinal schwannoma, or so-called neurilemoma, accounts for 9% of all schwannomas, and is the most common mediastinal peripheral nerve sheath tumor [1-2]. Although they occur mostly in the posterior mediastinum, peripheral nerve sheath tumors in all compartments of the mediastinum could generate into schwannomas. The ancient schwannoma, as a slow-growing benign tumor with the degenerative features of cyst formation, calcification, hemorrhage and hyalinization, is 1 of these variants [3]. To our knowledge, this is the first case report of a huge middle mediastinal ancient schwannoma accidently found by chest X-ray, that was undiagnosed in 2 attempts at core biopsy. The surgical pa-thology after video-assisted thoracic surgery (VATS) finally confirmed this ancient schwannoma.

[1]Division of Thoracic Surgery, Department of Surgery, Yuan's General Hospital, Kaohsiung, Taiwan. [2]Division of Thoracic Surgery, [3]Division of Colorectal Surgery, Department of Surgery, [4]Department of Pathology, National Cheng Kung University Hospital, Tainan, Taiwan.
Address reprint requests to: Dr. Ying-Yuan Chen, Department of Surgery National Cheng Kung University Hospital 138 Shengli Rd., North District Tainan 704302, Taiwan.

Case Report

The patient was a 59-year-old man with a relatively normal health status previously, who also was a never-smoker. He was diagnosed with rectosigmoid adenocarcinoma as a result of colonoscopy, and a 6.5-cm left perihilar mass was found on chest X-ray in a health check-up in 2021. He denied chest tightness, dyspnea, hemoptysis, fever, or other discomfort.

Chest computed tomography (CT) with contrast medium disclosed a large middle mediastinal tumor, 6.4 x 6.2 cm in size, near the aortopulmonary window, with a well-defined border and mild central enhancement (Figure 1). Magnetic resonance imaging (MRI) with contrast medium further revealed a smoothly encapsulated, heterogeneously enhancing left mediastinal mass, with foci of T1 hyperintensity, and a suspected hemorrhagic component. The T2-weighted image exhibited marked signal intensity (Figure 2). MRI also disclosed that the mass had not invaded the peripheral organs, including the pulmonary artery.

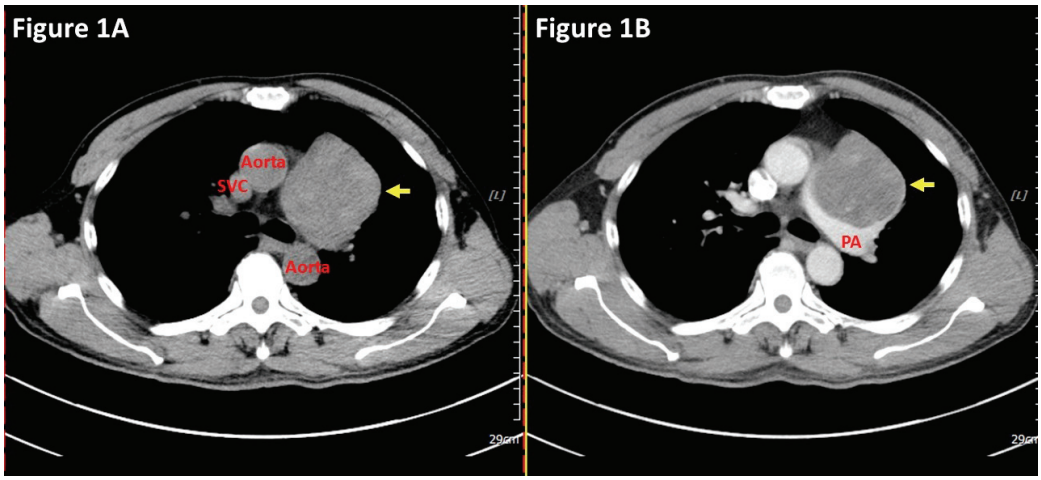

Fig. 1. Chest computed tomography (A) with contrast medium (B) disclosed a large mid-dle mediastinal tumor (yellow arrow), 6.4 x 6.2 cm in size, near the aortopulmonary window, with a well-defined border and mild central contrast enhancement. PA, pulmonary artery; SVC, superior vena cava.

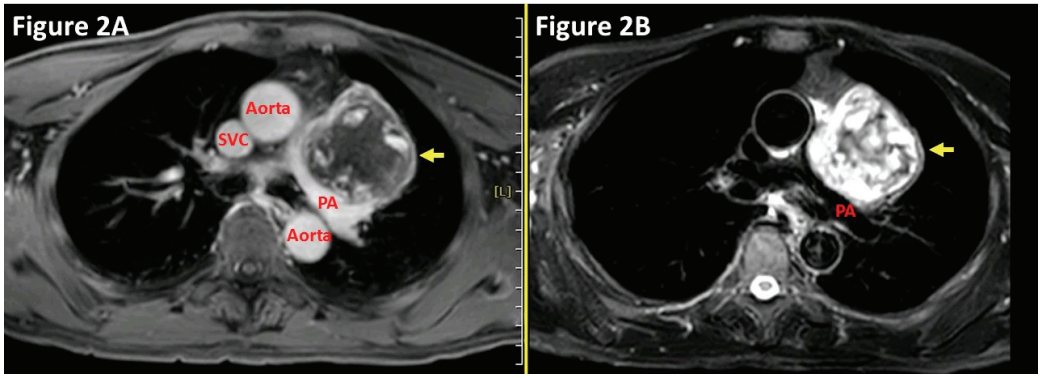

Fig. 2. Magnetic resonance imaging with contrast medium further demonstrated a smoothly encapsulated, heterogeneously enhanced mediastinal mass (yellow arrow) with foci of T1 hyperintensity (A), and involvement of a suspected hemorrhagic component. The T2-weighted image exhibited marked signal intensi-ty (B). PA, pulmonary artery; SVC, superior vena cava.

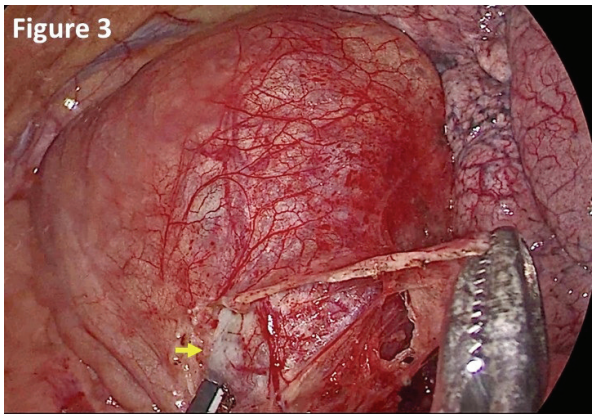

Fig. 3. The operation revealed a well-encapsulated greyish large mediastinal mass (yellow arrow) anterior to the left pulmonary hilum, without pulmonary or vessel invasion.

CT-guided biopsy revealed fibrosis, and the second attempt at CT-guided biopsy also presented fibrosis with hemorrhage. Due to a suspected benign process of the mediastinal tumor, the patient first underwent anterior resection for his rectosigmoid cancer on August 31, 2021. The surgical pathologic stage was IIIA (T2aN1), and he completed adjuvant chemotherapy smoothly in the following year, without local recurrence or distal metastasis.

During the 1-year follow-up, serial chest CTs showed no interval change in this mediastinal tumor. The patient finally underwent VATS excision of the mediastinal mass through the left hemithorax. Intraoperatively, we noticed a well-encapsulated, greyish, large mediastinal mass anterior to the left pulmonary hilum (Figure 3). After incising the mediastinal pleura overlaying it, the tumor was easily dissected, except for the interface between the tumor and the pericardium. Partial pericardiectomy was performed to ensure the integrity of tumor removal, and to also exclude tumor invasion into the pulmonary vessels. Eventually, the huge middle mediastinal tumor was removed simply using a VATS approach.

Surgical pathology finally confirmed an ancient schwannoma with hemorrhagic necrosis and calcification. It was a well-encapsulated nodular tumor grossly, measuring 6.5 x 6.0 x 5.0 cm in size and 84.3 gm in weight, with gray and firmly cut surfaces, and multiple cystic and hemorrhagic change (Figure 4). Microscopically, there were the typical histological char-

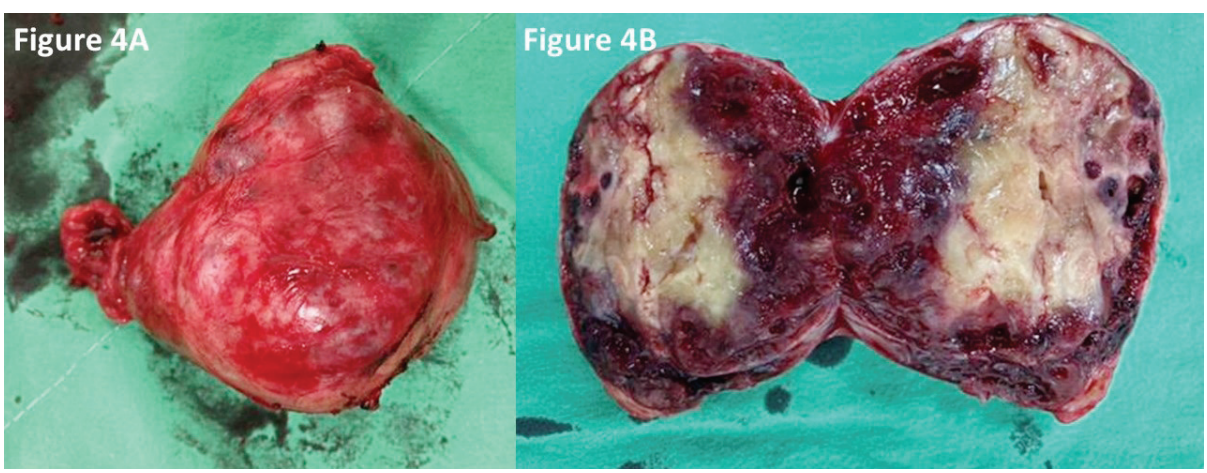

Fig. 4. The specimen was a well-encapsulated nodular tumor (A), measuring 6.5 x 6.0 x 5.0 cm in size and 84.3 gm in weight, with gray and firm cut surfaces, and multiple cystic and hemorrhagic change (B).

acteristics of schwannoma, including Antoni A, fascicles of compact spindle-shaped cells with nuclear palisading, and Antoni B, scattered hypocellular areas with haphazardly arranged spindle cells in a loosely textured matrix (Figure 5). The degenerative features, pleomorphic nuclei with hyperchromasia and atypia, except mitosis, contributed to this being an "ancient schiwannoma". The tumor cells were reactive to S-100, but not pan-cytokeratin (AE1/AE3) stains in the immunohistochemistry (Figure 6).

The chest tube was removed on postoperative day 1, and the patient was dis-charged smoothly the next day, without hoarseness or choking episodes. At the 1 month postoperative clinical follow-up, the patient presented without event, and the chest X-ray showed a clear lung field with no signs of mediastinal tumors.

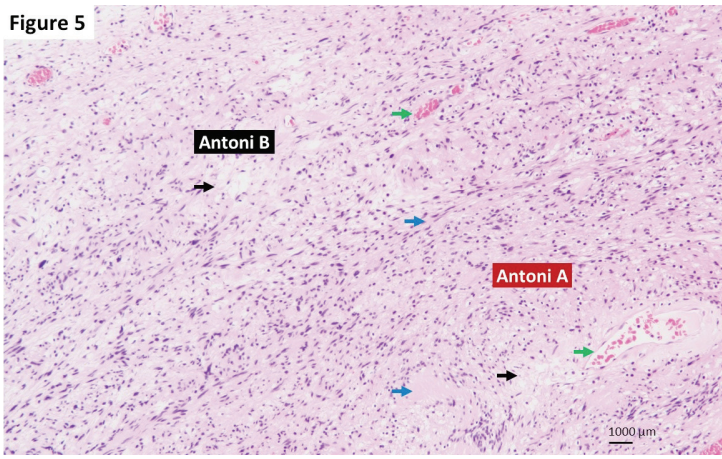

Fig. 5. Histological sections: Microscopy 10x magnification: Hematoxylin and Eosin stain revealed typical histological characteristics of schwannoma, including Antoni A, fascicles of compact spindle-shaped cells with nuclear palisading, and Antoni B, scattered hypocellular areas with haphazardly arranged spindle cells in a loosely textured matrix. There were also some degenerative features, such as calcification, cystic change (black arrow), hemorrhage (green arrow), diffuse fibrosis and hyalinization (blue arrow).

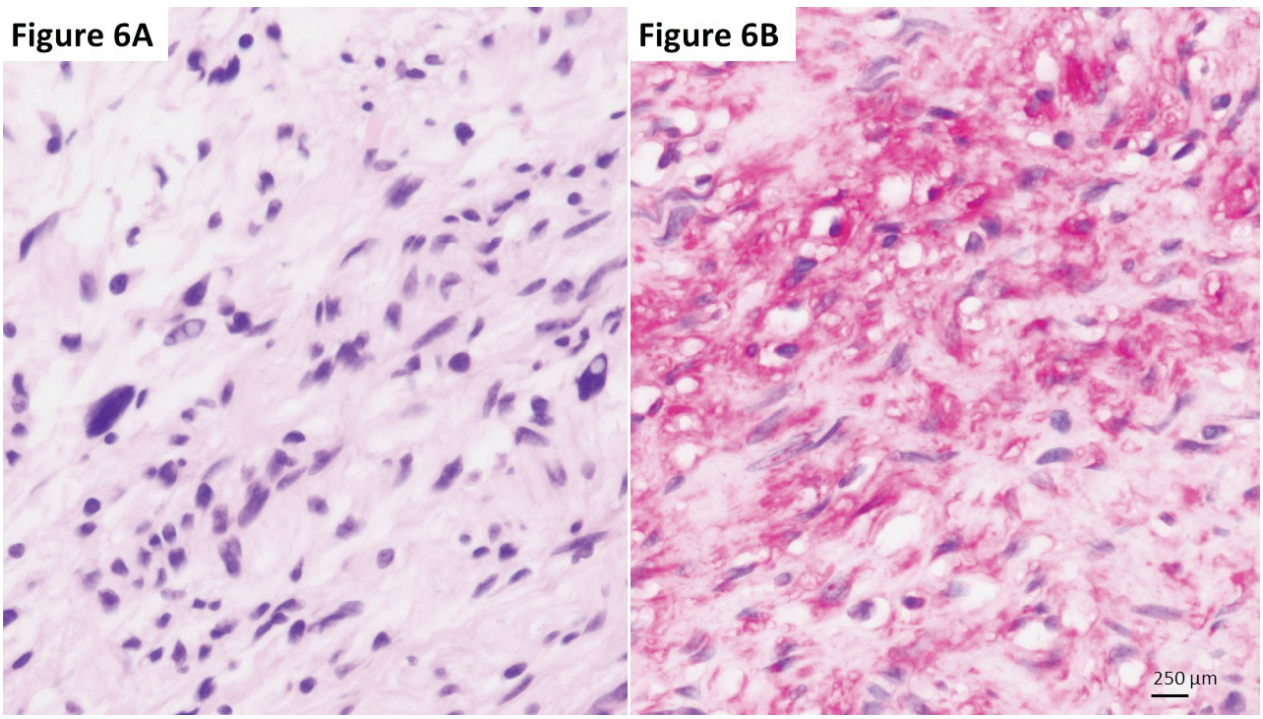

Fig. 6. Histological sections: Microscopy 40x magnification: Hematoxylin and Eosin stain revealed pleomorphic nuclei with hyperchromasia and atypia, without mitosis (A). The tumor cells were reactive to S100 stains in immunohistochemistry (B).

Discussion

Although mediastinal schwannomas often occur in the posterior mediastinum, any compartment of the mediastinum could be the origin of these peripheral nerve sheath tumors [3]. Most mediastinal schwannomas originated from the intercostal nerve or sympathetic chain in the posterior mediastinum; vagus nerve-related middle mediastinal schwannomas comprised only 2% of all mediastinal schwannomas [4,5]. An ancient schwannoma originating from the middle mediastinum is rare, and to our knowledge, this is the first reported case in the literature.

Grossly, a schwannoma is well demarcated and lobulated with central calcification, hemorrhage and mild enhancement in CT scans. It may exhibit hyperintensity in T2-weighted MRI images [6]. In immunostaining, all variants of schwannomas are diffusely and strongly positive for S-100 protein, and there are 2 cellular patterns histologically: Antoni type A areas show a dense spindle cell pattern with nuclear palisading; and Antoni type B areas show loose myxomatous changes, less orderly than in Antoni A areas, and are composed of cystic areas, vascular thickening, and hemorrhage [1]. Schwannomas, consisting of either an Antoni type A or type B area, or a combination of both with varying proportions, present no clinical differences. The typical histological characteristics of "ancient" schwannoma are increased cellularity and atypia; however, some areas with degenerative features, such as diffuse fibrosis, cystic change, hematoma, calcification, hyalinization and hyperchromasia without atypia, might be noted [3,7-8].

Due to the pleomorphism of ancient schwannomas, they are difficult to diagnose based on clinical presentation and imaging studies alone, even after histopathological reviews of the core biopsy [6,9]. Some cases of ancient schwannoma were misdiagnosed as fibrosarcoma or malignant peripheral nerve sheath tumors, and some were even treated as an inflammatory disease before surgical pathological diagnosis [6]. The pathological examination emphasizes positive immunostaining of S-100 for the neural origin, in addition to an absence of mitoses to exclude malignant change [7].

Most ancient schwannomas in the mediastinum had benign, slow-growing, asymptomatic courses, but there were still some sporadic cases with extrinsic compression symptoms, intrathoracic bleeding, or even malignant transformation [6,10-11]. Although rare, mediastinal ancient schwannomas should be taken into consideration, since these tumors could occur in any compartment of the mediastinum. VATS complete tumor resection is highly recommended for a defi-nite diagnosis in cases with a huge mediastinal tumor, even stationary during follow-up. Successful surgical tumor removal can not only provide an accurate pathological diagnosis, but is also a radical treatment to prevent unexpected events in the future.

References

1. Marchevsky AM, Balzer B. Mediastinal tumors of peripheral nerve origin (so-called neurogenic tumors). Mediastinum 2020; 4: 32.
2. Shanmugasundaram G, Thangavel P, Venkataraman B, *et al*. Incidental ancient schwannoma of the posterior mediastinum in a young male: a rare scenario. BMJ Case Rep 2019 May 10; 12(5): e227497.
3. Micovic MV, Zivkovic BM, Zivanovic JD. Ancient olfactory schwannoma - case report and literature review. Turk Neurosurg 2017; 27(4): 656-651.
4. Dy P, Lajom C, Sanchez J. Middle mediastinal

schwannoma concealed by asthma and GORD. BMJ Case Rep 2018 Mar 13; 2018: bcr2017223795.

5. Rammos KS, Rammos SK, Foroulis CN, *et al*. Schwannoma of the vagus nerve, a rare middle mediastinal neurogenic tumor: case report. J Cardiothorac Surg 2009 Nov 26; 4: 68.
6. Quartey B, Lenert J, Deb SJ, *et al*. Giant posterior mediastinal ancient schwannoma requiring thoracoabdominal resection: a case report and literature review. World J Oncol 2011; 2(4): 191-194.
7. Ho CF, Wu PW, Lee TJ, *et al*. "Ancient" schwannoma of the submandibular gland: a case report and literature review. Medicine (Baltimore) 2017; 96(51): e9134.
8. Ratnagiri R, Mallikarjun S. Retroperitoneal ancient schwannoma: two cases and review of literature. J Cancer Res Ther 2014; 10(2): 368-70.
9. Vera-Sirera B, Fernades-Ciacha L, Floria LM, *et al*. Palatal ancient schwanno-ma: optical, immunohistochemical and ultrastructural study with literature re-view. Eur Arch Otorhinolaryngol 2017; 274(12): 4195-4202.
10. Nakashima C, Harada H, Shibata S. Mediastinal ancient schwannoma causing intrathoracic bleeding. Ann Thorac Cardiovasc Surg 2022; 28(1): 75-78.
11. Chu YC, Yoon YH, Han HS, *et al*. Malignant transformation of intrathoracic ancient neurilemmoma in a patient without Von Recklinghausen's disease. J Korean Med Sci 2003 Apr; 18(2): 295-8.

Silicosis Presenting with Exudative Pleural Effusion and Parietal Pleural Nodule Diagnosed by Medical Thoracoscopy: A Case Report and Literature Review

Chi-Wei Lin[1], Che-Chia Chang[1], Jing-Lan Liu[2], Shu-Yi Huang[1], Yu-Ching Lin[1,3,4], Chieh-Mo Lin[1,5,6]

Chronic silicosis is a common form of silicosis, which is a fibrotic pulmonary disease induced by inhalation of respiratory crystalline silica. In addition to pulmonary nodular opacities, pleural involvement such as visceral pleural invagination and pleural thickening are well documented in chronic silicosis. Pleural effusion is a less common presentation of silicosis, but it has been reported as the primary presentation in a few cases. There is also increasing evidence that exposure to silica is associated with the formation of exudative pleural effusion. However, evidence for the use of medical thoracoscopy for the diagnosis of silicosis remains limited.

Here, we reported the case of a 74-year-old male with decades of exposure to various kinds of dust. He was a former smoker with chronic obstructive pulmonary disease under medication control. He reported exertional dyspnea lasting for months, and chest X-ray showed blunting of the right costophrenic angle. His exudative pleural effusion was drained, but the cause was still unknown after laboratory studies. A thoracoscopy was performed, which revealed several whitish pleural nodules. A pathological examination showed silicotic nodules, and thus silicosis was diagnosed. ***(Thorac Med 2023; 38: 303-309)***

Key words: silicosis, pleural nodules, thoracoscopy, exudative pleural effusion

Introduction

To determine the etiology of pleural effusion, Light's criteria are used to screen for a probable exudate. The pleural effusion in patients positive for Light's criteria is classified as an exudate after heart failure and liver cirrhosis have been ruled out [1]. The most common causes of exudative pleural effusion are malignancy, bacterial pneumonia, and pulmonary

[1]Department of Pulmonary and Critical Medicine, Chang Gung Memorial Hospital, Chiayi, Taiwan. [2]Department of pathology, Chiayi Chang Gung Memorial Hospital. [3]Department of Medicine, College of Medicine, Chang Gung University, Taoyuan, Taiwan. [4]Department of Respiratory Care, Chang Gung University of Science and Technology, Chiayi Campus, Chiayi, Taiwan. [5]Graduate Institute of Clinical Medical Sciences, College of Medicine, Chang Gung University, Taoyuan City, Taiwan. [6]Department of Nursing, Chang Gung University of Science and Technology, Chiayi Campus, Puzi City, Chiayi County, Taiwan.
Address reprint requests to: Dr. Chieh-Mo Lin, Department of Pulmonary and Critical Medicine, Chang Gung Memorial Hospital, No 8, West Section, Chiapu Road, Putzu City, Chiayi, Taiwan.

embolism. The differential diagnosis for pleural effusion can generally be obtained by biochemical analysis, fluid culture, and cytology; however, if the etiology remains undetermined, a thoracoscopic examination and parietal pleural biopsy are indicated. For malignant pleural effusion, the sensitivity of thoracoscopy is 92.9%, which is significantly better than the 64.3% for thoracentesis [2]. In an Italian retrospective observational study, malignancy accounted for 62% of histological diagnoses, followed by unspecified pleural inflammation and tuberculosis, which accounted for 28.6% and 6% of the histological diagnoses, respectively [3]. Less common histological diagnoses include rheumatological diseases, sarcoidosis, and pleural fibroma [4-5].

Silicosis is a pneumoconiosis induced by silica, and it is classified as acute, chronic, or accelerated depending on the latency from exposure to diagnosis [6]. Chronic silicosis typically either remains asymptomatic or has nonspecific manifestations such as cough, dyspnea, and incidental findings in a chest radiograph [7]. The diagnosis of silicosis is made clinically by thoracic imaging and a history of dust exposure. If the clinical diagnosis cannot be confidently made, pathological findings are pursued. The tissue for diagnosis is typically obtained from surgical lung biopsy or transbronchial lung biopsy.

Silica exposure may cause exudative pleural effusion with or without silicosis [8]. Silica exposure can be proven by the identification of silica particles in pleural effusion labeled previously as idiopathic pleural effusion [8]. In rare instances, pleural effusion may be the initial clinical presentation of silicosis [9]. We report the case of a patient with silicosis who presented with exudative pleural effusion and was diagnosed by thoracoscopic biopsy.

Case Report

A 74-year-old male presented with chronic obstructive pulmonary disease (COPD), diabetes mellitus and essential hypertension. He was a former smoker who had quit smoking for 1 year. As a retired civil engineer, he had been intermittently exposed to different types of dust for decades. He reported aggravated dyspnea on exertion for a number of months prior to this presentation. A laboratory examination showed a normal white blood cell (WBC) count (5700/μL) with normal differential counts, hemoglobin (14.6 g/dL), creatinine (0.94 mg/dL), lactate dehydrogenase (LDH) (220.7 U/L), and total protein (6.2 g/dL). A chest radiograph showed blunting of the right costophrenic angle (Figure 1); an echo-guided thoracentesis yielded a small amount of yellowish monocyte-predominant exudative pleural effusion with an LDH of 164 U/L, total protein of 4.6 g/dL, and a WBC count of 8867/μL, which mainly consisted of mononuclear cells (99%). Bacterial and mycobacterial cultures of the pleural fluid were negative.

A chest computed tomography (CT) scan (Figure 2) showed bilateral smooth thickening of the interlobular septa, some discrete tiny centrilobular nodules, mediastinal lymphadenopathy with calcification, and pleural effusion on the right side. There were no lung parenchymal nodules, masses, or consolidations.

A medical thoracoscopy of the right chest (Figure 3) revealed multiple small whitish nodules at the mid- to upper parietal pleura, and small pearl-like nodules at the costophrenic angle; a pathological examination (Figure 4) of the whitish nodules revealed granulomas with a whorled collagen core surrounded by dust-

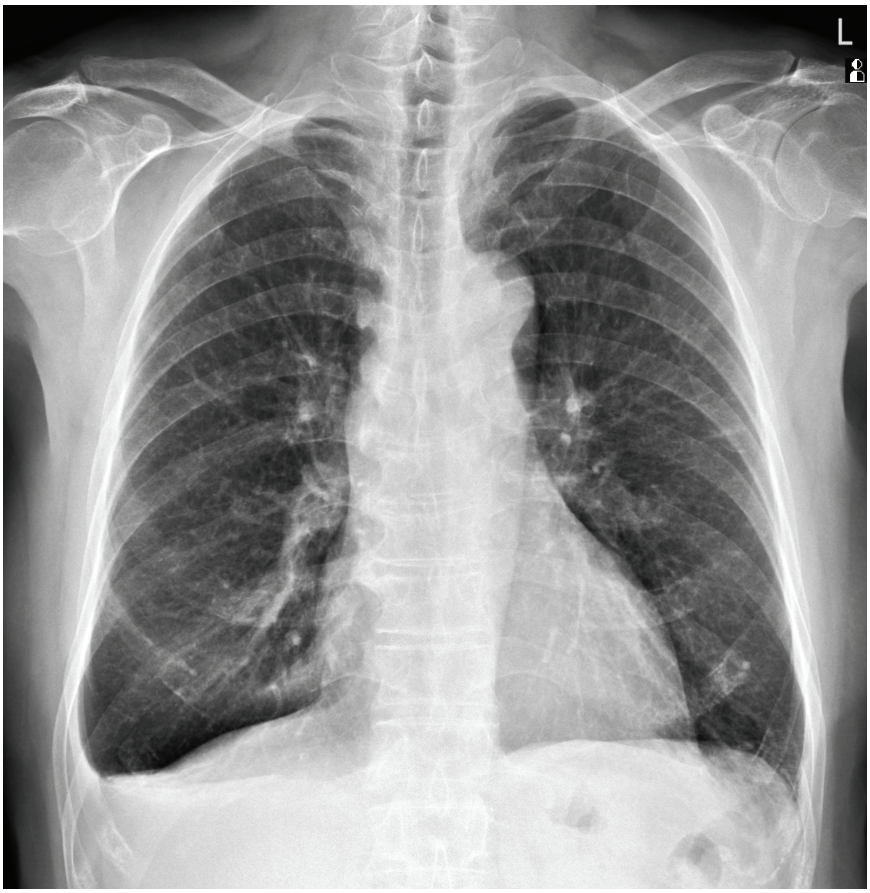

Fig. 1. Chest radiograph of the patient showing blunting of the right costophrenic angle.

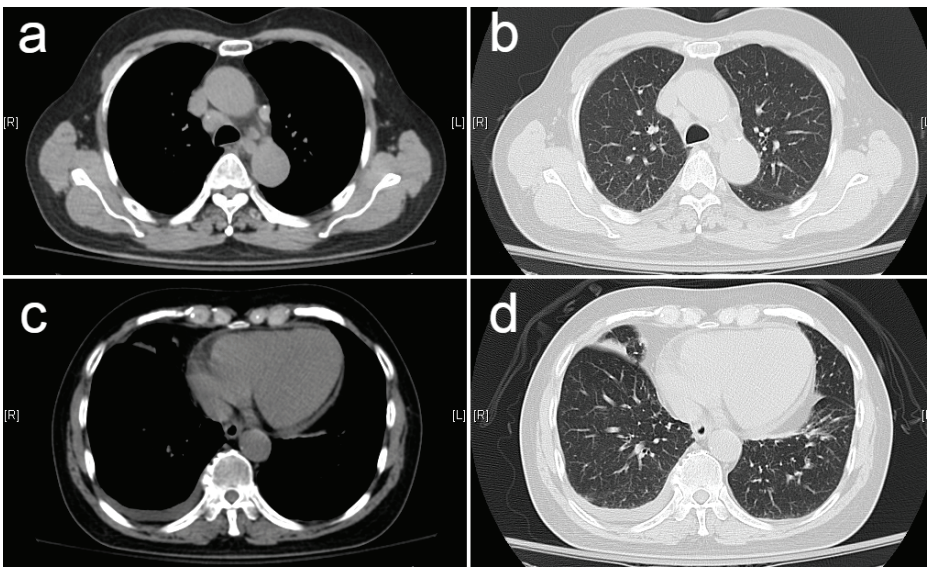

Fig. 2. a. Chest CT scan showing mediastinal lymphadenopathy with calcification. b. Tiny nodules in bilateral upper lungs. c, d. Pleural effusion in the right pleural cavity.

Fig. 3. One of the whitish nodules in the parietal pleura revealed by thoracoscopy.

laden macrophages. Acid-fast stain, periodic acid-Schiff stain and Grocott's methenamine silver stain were all negative. A polarized light examination confirmed birefringent silica particles in the macrophages. After undergoing thoracoscopy, the patient developed subcutaneous emphysema at his right chest wall and right neck. A follow-up chest radiograph revealed regression of the emphysema, and the patient was discharged from the hospital 3 days after the procedure. Transbronchial needle aspiration of the mediastinal lymph nodes also showed pneumoconiosis lymphadenopathy, consistent with silicosis. Therefore, silicosis was diagnosed.

As the patient had no further exposure to dust and he had well-controlled COPD, we provided only medical surveillance for his silicosis. After 6 months, there were no signs of further progression of the patient's pleural effusion, or other pulmonary disorders.

Discussion

Pathogenesis

Silicosis is a respirable crystalline silica-induced occupational lung disease. Occupations associated with silica exposure include quarrying, drilling, pottery and porcelain work, sandblasting, and engineering of stone counter tops [6]. High exposure to silica can lead to acute silicosis, which has a poor prognosis [7].

After deposition in the alveoli, silica is phagocytosed by alveolar macrophages. The

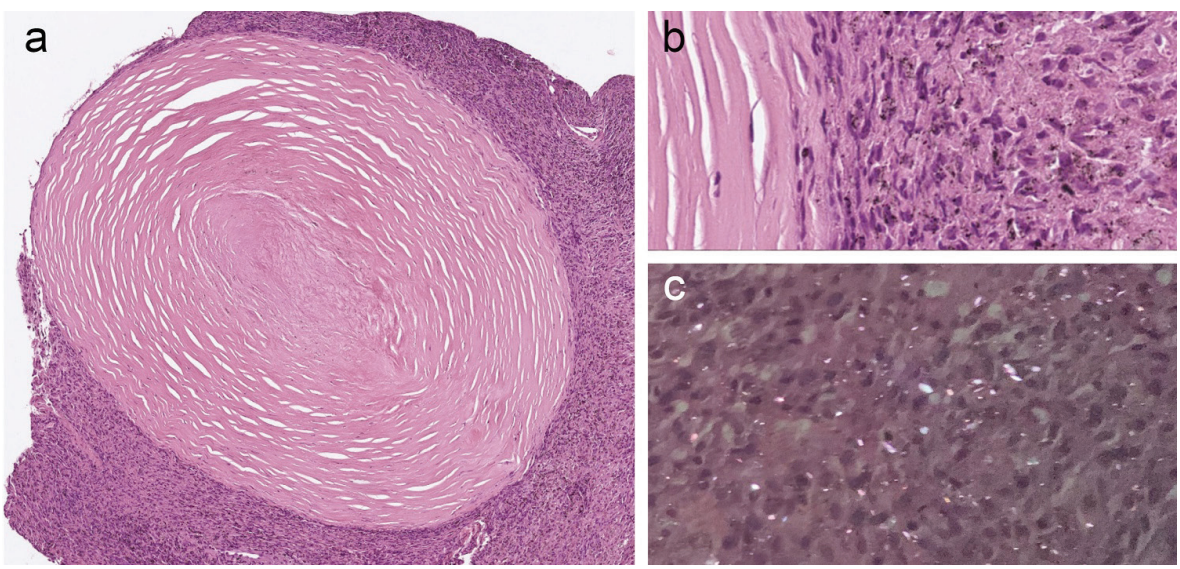

Fig. 4. a. Collagen whorl consistent with silicotic nodules in the pleural biopsy. b. Magnification of Figure 4a, which shows dust-laden macrophages. c. Polarized light examination confirmed the presence of birefringent silica particles.

silica causes damage to the phagosome, and subsequent release of the phagosome contents [10]. As a result, NOD-, LRR- and pyrin domain-containing protein 3 (NALP3) is activated and an inflammasome forms, leading to inflammation and fibrosis [10].

Silica exposure, such as that which occurs in the context of breast silicone implant rupture, leads to silicon granuloma, which manifests as cutaneous nodules or lymphadenopathy. In a case reported by Vo, *et al*., silicone drained into the pleural cavity, causing pleural nodularity and pleural thickening [11]. Exposure to silica nanoparticles is thought to cause pleural effusion; this is based on the presence of silica nanoparticles in the pleural effusion of both patients and experimental rats with a history of exposure [8]. In addition, silica particles have been identified in some cases of pleural effusion which were initially considered idiopathic [8].

The pathogenesis of pleural effusion caused by silicosis remains unclear. In our case, silica-containing macrophages were identified in the parietal pleural biopsy, indicating that the translocation of silica particles to the pleural space may be the initial event. In the case of asbestos fibers, particle translocation to the pleural cavity can occur through primary translocation across the visceral pleura or through secondary translocation via the bloodstream [12]. Since crystalline silica deposition in other organs is less documented, primary translocation may be the preferred route for silicosis. Following the translocation of silica to the pleural cavity, an inflammatory reaction is initiated, leading to the formation of granulomas, silicotic nodules, and pleural effusion. Due to the rarity of pleural effusion and parietal pleural lesions caused by silicosis, and the chronic nature of the disease, the translocation of silica to the pleural cavity may occur by chance, or be dose-related, while the inflammatory process may be time-related.

Clinical Course and Imaging

Silicosis is classified as acute, accelerated, or chronic [7], and the classification is primarily determined by the latency of the pulmonary response to silica exposure. Chronic pulmonary silicosis has a latency of 10 to 30 years. It is pathologically characterized by the presence of silicotic nodules, which are composed of a whorled collagen core surrounded by dust-laden macrophages and fibroblasts [6,13]. Using imaging studies, simple silicosis and complicated silicosis -- the 2 subgroups of chronic silicosis -- are further differentiated. The primary radiology findings for simple silicosis are upper lung nodular opacities [7]. If there are conglomerate nodules in a chest CT or large opacities in a chest radiograph, complicated silicosis is diagnosed, and the prognosis is poor due to secondary infection and progressive lung function impairment [6].

It is worth summarizing the differences between silicosis and asbestosis, the pneumoconiosis caused by asbestos fibers. Asbestosis is primarily caused by direct toxic effects from insulation materials containing asbestos fibers [14]. Due to the persistence of these fibers in the lungs, chronic inflammation and fibrosis develop over time [15]. In contrast to other pneumoconioses, the main radiological finding of asbestosis is lower lobe-predominant peripheral fibrosis, which may be radiologically consistent with usual interstitial pneumonia (UIP) [14]. The pathologic findings of asbestosis are also similar to UIP, except for the presence of asbestos bodies [15]. In addition, pleural effusion, which is uncommon in other pneumoconioses, is a common early manifestation of asbestos

exposure, and after a latency of many years, pleural plaques may develop [14].

Chronic silicosis may have pleural involvement, with pleural thickening being more common than pleural effusion [9]. In 2005, Arakawa, *et al*. reported 110 deceased patients with chronic silicosis; pleural findings included pleural thickening, pleural effusion, and pleural invagination [16]. In that study, radiological evidence of pleural effusion was found in 34.5% of the patients, but only 10.9% of the patients had pleural effusions that were attributed to silicosis. The remaining causes of pleural effusion included pneumonia, heart failure, hypoalbuminemia, pneumothorax, and abdominal malignancy [16]. In contrast to the case series mentioned above, there have been few case reports in which silicosis presents with pleural effusion. To the best of our knowledge, there have been only 4 cases, of which 3 were reviewed in a case report published in 2015, and 1 was reported in 2022 [9,17,18]. Notably, the case reported by Okamoto *et al* in 2022 was diagnosed by the presence of a silicon compound in the pleural fluid cell block of the patient's exudative pleural effusion [18].

Thoracoscopy

Few reported cases of silicosis with pleural involvement have been confirmed by thoracoscopy. In the aforementioned study by Arakawa, *et al*. [16], 58% and 60% of patients had pleural thickening on a chest CT and autopsy, respectively. Most (57 of 66) of the pleural thickening involved both visceral and parietal pleura in the form of adhesion. Seven of the 66 cases only had visceral pleural involvement, while 2 of the 66 cases only had parietal pleural thickening. In the cases reported by Salith, *et al*. in 2015 and by al-Kassimi in 1992, pleural biopsies showed both inflammation and mesothelial cell hyperplasia [17,19]. Another case of a systemic lupus erythematosus patient with silicosis and pleural silicotic nodules was reported in 2019; that case was the only incidence of biopsy-proven silicotic nodules in the parietal pleura identified in our literature review [20].

Pleural nodules are a common finding during medical thoracoscopy. In an observational study, pleural nodules were seen in 86 of 106 patients who underwent a medical thoracoscopy due to pleural effusion [21]. The causes of pleural nodules included primary pulmonary malignancies, primary pleural malignancies, metastases, hematological malignancies, tuberculosis, asbestos-related pleural disease, sarcoidosis, and parasitic infections [22]. The size, shape, contour, and color of pleural nodules can vary, and a thoracoscopic biopsy of the pleural nodules is necessary to make a diagnosis. In contrast, pleural plaques refer to sharply circumscribed raised whitish or pale-yellow lesions which are formed by collagen fibers with or without calcification. Typical pleural plaques are associated with asbestos exposure and are easily identified with either a chest radiograph or CT. While some isolated pleural plaques may be related to tuberculosis, trauma, or hemothorax, multiple plaques are regarded as markers of asbestos exposure [23]. The parietal pleural lesion observed in our case was white and raised; however, the margin was not sharp, and the lesion was neither calcified nor identifiable on CT. Thus, the lesion was classified as a pleural nodule.

Conclusion

In our case, the initial finding was exudative pleural effusion, and the whitish nodule was subsequently noted during a medical thoracos-

copy. A thoracoscopic biopsy yielded silicotic nodules, and so silicosis was diagnosed based on the imaging, chest CT findings, pleural biopsy plus mediastinal lymph node aspiration, and patient history of exposure to dust.

This case highlights that pneumoconiosis and silicosis are parts of a differential diagnosis for exudative pleural effusions and whitish hyaline pleural nodules. In addition, this is a rarely reported case with biopsy-proven silicotic nodules in the parietal pleura.

References

1. Broaddus CV, Light RW. Pleural effusion. In: Murray and Nadel's textbook of Respiratory Medicine (7th ed., Vol. 2), Elsevier, 2022: 1498-1523.
2. Martinez-Zayas G, Molina S, Ost DE. Sensitivity and complications of thoracentesis and thoracoscopy: a meta-analysis. Eur Respir Rev 2022; 31: 220053.
3. Valsecchi A, Arondi S, Marchetti G. Medical thoracoscopy: analysis on diagnostic yield through 30 years of experience. Ann Thorac Med 2016; 11: 177-82.
4. Hansen M, Faurschou P, Clementsen P. Medical thoracoscopy, results and complications in 146 patients: a retrospective study. Respir Med 1998 Feb; 92(2): 228-32.
5. Blanc FX, Atassi K, Bignon J, *et al*. Diagnostic value of medical thoracoscopy in pleural disease: a 6-year retrospective study. Chest 2002 May; 121(5): 1677-83.
6. Krefft S, Wolff J, Rose C. Silicosis: an update and guide for clinicians. Clin Chest Med 2020 Dec; 41(4): 709-722.
7. Leung CC, Yu ITS, Chen W. Silicosis. Lancet 2012; 379: 2008-18.
8. Bielsa S, Guitart A, Esquerda A, *et al*. Some pleural effusions labeled as idiopathic could be produced by the inhalation of silica. Pleura Peritoneum 2022; 7(1): 27–33.
9. Salih M, Aljarod T, Ayan M, *et al*. Pulmonary silicosis presents with pleural effusion. Case Rep Med 2015; 2015: 543070.
10. Adamcakova J, Mokra D. New insights into pathomechanisms and treatment possibilities for lung silicosis. Int J Mol Sci 2021; 22(8): 4162.
11. Vo K, Kilgore M, Scheel J. Intrapleural silicone granuloma mimicking pleural malignancy. Radiol Case Rep 2021 Oct 9; 16(12): 3824-3828.
12. Miserocchi G, Sancini G, Mantegazza F, *et al*. Translocation pathways for inhaled asbestos fibers. Environ Health 2008; 7, 4.
13. Weisenberg E. Silicosis 2021. PathologyOutlines.com. https://www.pathologyoutlines.com/topic/lungnontumorsilicosis.html.
14. Elicker BM, Webb WR. Pneumoconioses. In: Fundamentals of High-Resolution Lung CT (2nd ed.). Wolters Kluwer, 2018, 227-235.
15. Liu G, Cheresh P, Kamp DW. Molecular basis of asbestos-induced lung disease. Annu Rev Pathol 2013 Jan 24; 8: 161-87.
16. Arakawa H, Honma K, Saito Y, *et al*. Pleural disease in silicosis: pleural thickening, effusion, and invagination. Radiology 2005; 236: 685–693.
17. Zeren EH, Colby TV, Roggli VL. Silica-induced pleural disease: an unusual case mimicking malignant pleural effusion. Chest 1997; 112: 1436-38.
18. Okamoto S, Kobayashi I, Moriyama H, *et al*. Silicosis-related pleural effusion diagnosed using elemental analysis of the pleural fluid cell block: a case report. Respir Med Case Rep 2022 May 11; 37: 101665.
19. al-Kassimi FA. Pleural effusion in silicosis of the lung. Br J Ind Med 1992 Jun; 49(6): 448-50.
20. Tsuchiya K, Toyoshima M, Fukada A, *et al*. Lupus pleuritis with silicotic nodules in the parietal pleura. Intern Med 2018 May 1; 57(9): 1277-1280.
21. Liu XT, Dong XL, Zhang Y, *et al*. Diagnostic value and safety of medical thoracoscopy for pleural effusion of different causes. World J Clin Cases 2022 Apr 6; 10(10): 3088-3100.
22. Di Mango AL, Zanetti G, Marchiori E. Thymoma metastasis: differential diagnosis of pleural nodules and masses. Lung India 2018 Jul-Aug; 35(4): 369-370.
23. American Thoracic Society. Diagnosis and initial management of nonmalignant diseases related to asbestos. Am J Respir Crit Care Med 2004 Sep 15; 170(6): 691-715.

Unusual Trachea–Carotid Artery Fistula Bleeding Rescued by Endovascular Stent: Case Report

Yi-An Li[1], Hung-Lung Hsu[2], Cheng-Hung How[1]

A tracheoarterial fistula (TAF) is an uncommon but devastating complication of tracheostomy. Its appropriate management remains debatable. In the case of tracheostomy bleeding, it is necessary to treat the TAF and plan immediate surgery for hemostasis. Herein, we describe the case of an 82-year-old woman with a trachea–carotid artery fistula at an unusual site who was treated successfully by inserting an endovascular stent to control bleeding and maintain airway patency. ***(Thorac Med 2023; 38: 310-314)***

Key words: tracheostomy, fistula (carotid artery), carotid artery, endovascular stent

Introduction

In Taiwan, in addition to intubation with an endotracheal tube, tracheostomy is used to secure the airway in patients who cannot be weaned off ventilators, or in cases in which it is difficult to maintain airway hygiene [1]. The incidence of tracheoarterial fistula (TAF) in patients who underwent tracheostomy is estimated to be 0.6%–0.7% [2], with a peak incidence occurring between 3 days and 6 weeks after the procedure[3]. TAF is a rare but lethal complication of tracheostomy, necessitating an emergency surgery. The mortality rate associated with TAF is approximately 46%-100% [4].

Case Report

An 82-year-old woman was hospitalized 2 months previous to this admission for aspiration pneumonia and a non-ST elevation myocardial infarction event with coronary artery disease after percutaneous occlusive balloon angioplasty with stenting. During that admission, she underwent tracheostomy as ventilator weaning was difficult and she frequently choked with aspiration. Subsequently, she was discharged but continued to be on ventilator support at home. Unfortunately, her caregiver reported a sudden onset of massive tracheostomy bleeding after changing position, which cause the patient to

[1]Division of Thoracic Surgery, Department of Surgery, Far Eastern Memorial Hospital. [2]Division of Cardiovascular Surgery, Cardiovascular Medical Center, Far Eastern Memorial Hospital.
Address reprint requests to: Dr. Cheng-Hung How, Division of Thoracic Surgery, Department of Surgery, Far Eastern Memorial Hospital, No. 21, Sec. 2, Nanya S. Road, Banciao District, New Taipei City 220, Taiwan (Republic of China).

become unconscious.

The family contacted the emergency medical technician. The patient experienced out-of-hospital cardiac arrest on her way to the hospital. Following cardiopulmonary resuscitation upon arrival at the emergency department, the patient's spontaneous circulation was restored, and the tracheostomy wound bleeding was controlled via digital compression and hyperinflation of the tracheostomy tube cuff.

In our hybrid endovascular operating room, the tracheostomy tube was shifted to an oral endotracheal tube under general anesthesia. We attempted to explore and localize the bleeding site but failed to stop her massive bleeding. We then performed diagnostic digital subtraction angiography to identify the injured vessel, which was at the root of the common carotid artery near the lower part of the tracheostomy wound (Figure 1A, B). We performed balloon occlusion surgery (Figure 2A; Medtronic, Visi-Pro Balloon, eV3 10 mm/40 mm), which successfully stopped the bleeding temporarily. Then, an endograft stent was inserted (Figure 2B) (Bentley, BeGraft, 9 mm/37 mm) to cover the fistula, which instantaneously interrupted the extravasation, as noted on the angiogram. The patient was sufficiently stable to be transferred to the intensive care unit, and she survived (Figure 3A,B).

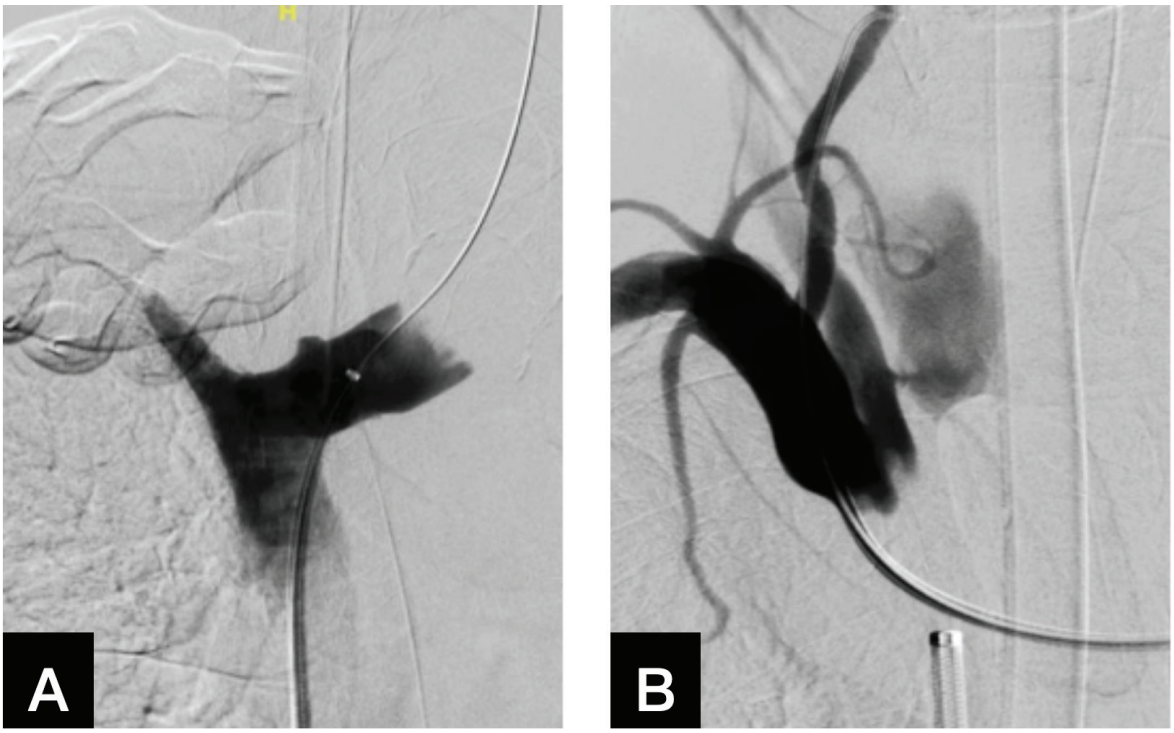

Fig. 1. (A). Digital compression to control the bleeding; (B). Extravasation over the root of the right common carotid artery.

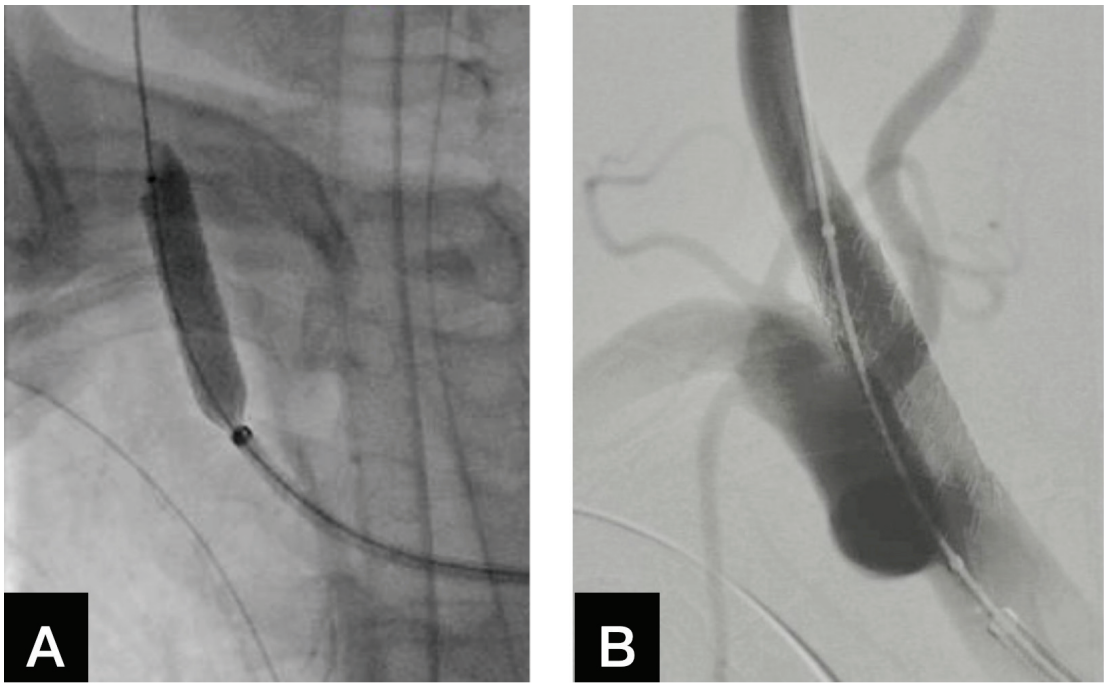

Fig. 2. (A). Balloon occlusion; (B). Endograft insertion.

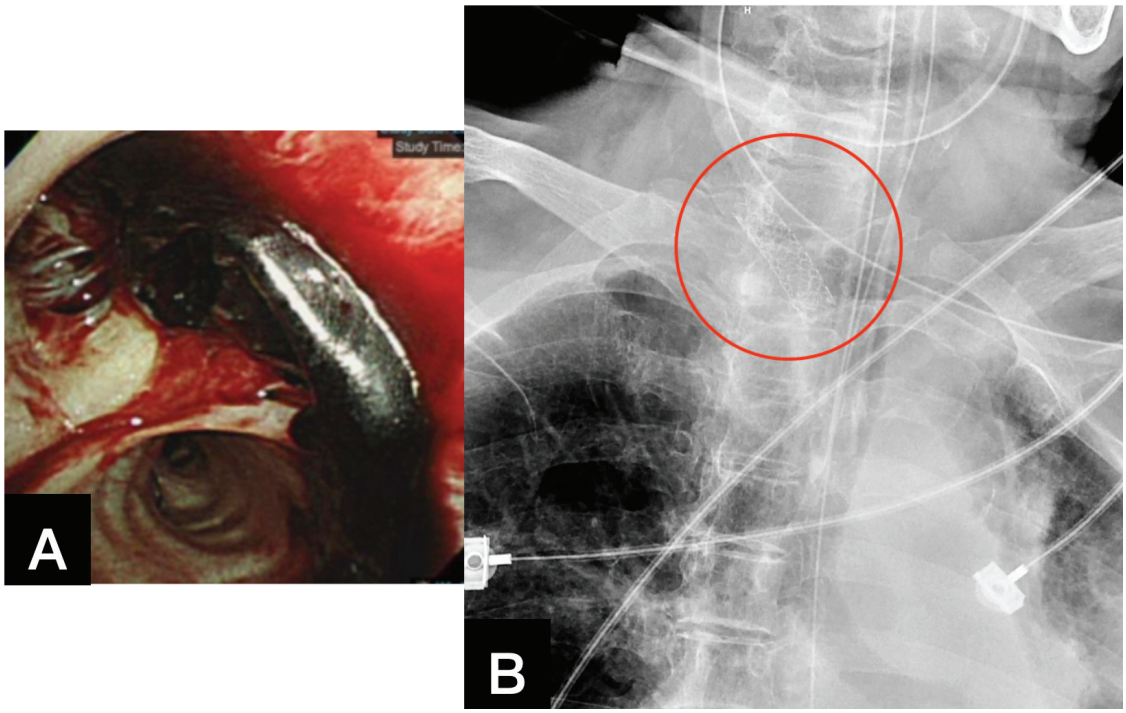

Fig. 3. (A). Removal of endobronchial blood clots using flexible bronchoscopy; (B). Follow-up chest X-ray on postoperative day 1.

Discussion

Unlike most cases in which TAFs represent trachea-innominate artery fistulas owing to their anatomic location near the anterior wall of the trachea, our patient had an injury at the right common carotid artery, which is an unusual site for a TAF (carotid artery, inferior thyroid artery, etc.) [5]. The involvement of our patient's common carotid artery might be due to her thin physique.

The risk factors for TAF formation include a pressure sore with advanced necrosis from high tracheostomy tube cuff pressure, mucosal trauma from a malpositioned cannula tip, low tracheal incision, high-lying brachiocephalic trunk, excessive neck movement, radiotherapy, and prolonged intubation. The use of excessive and continuous cuff pressure may result in erosion or necrotic changes in the intercartilaginous ligaments and tracheal cartilages, causing perforation between the vessels and tracheal wall. Tracheostoma infection, hypotension, malnutrition, and corticosteroid use may also be risk factors for TAF [2-5]. Since our patient had choking and aspiration, the accumulation of saliva over the trachea might also have facilitated inflammation progression and deterioration of wound healing. The poor nutrition status and low body weight of the patient resulted in the lack of soft-tissue protection; this might have exacerbated the vessel erosion.

Prompt diagnosis is crucial; flexible bronchoscopy, arteriography, and computed tomography angiography with 3-dimensional reconstruction may help us detect and locate the lesion. Sentinel bleeding and early hemoptysis imply the clinical occurrence of TAF [4-5].

Three emergency procedures have been proposed for controlling TAF bleeding immediately before achieving definite hemostasis through surgery [6]. The first procedure is securing the airway. Flexible bronchoscopy can be performed through the tracheostomy tube. The second procedure is overinflating the cuff of the tracheostomy tube to ensure temporary external compression of the wounded vessel, which may stop the bleeding in 85% of cases. Finally, digital compression can be performed around the tracheostomy incision.

From the experience of others, the massive bleeding is an obstacle to bronchoscope inspection. It is important to arrange the bronchoscope examination to occur after a proper hemostasis procedure (e.g. endograft or surgery) has been performed, which can provide further evaluation of the airway condition.

Emergency surgery is central to TAF management. Median sternotomy is the most common conventional approach. Although evidence suggests ligation of the injured artery, reconstruction, or endograft bypass, the optimal surgical method for TAF remains controversial [6]. In some studies, endografts have been used only as a bridge to surgical excision of the involved vessels to prevent local infection that may cause further erosion and recurrence [2,4-5]. There are still risks associated with graft infections regarding the location of the trachea and innominate artery and the possibility of stent graft fracture, for which subsequent surgery should be planned initially [7]. However, data regarding the use of endovascular stent graft repair as the first-line treatment instead of surgery remain inadequate. Long-term follow-up data are also insufficient or even lacking and must be collected for a better understanding.

Prevention is the key to managing vascular injury complications. From the procedure-related perspective, we recommend using the

Bjork flap to enhance the surrounding soft tissue of the tracheostoma to minimize the risk of adjacent vascular injury. It helps to suture an inverted U-shaped flap of the trachea to the skin edge, which can create a clear ostomy and reduce the chances of insertion into the false lumen; it may also protect vessels such as the high-riding innominate artery [8]. All healthcare staff involved in patient care, including nurses, caregivers, and respiratory therapists, must ensure that a long flexible tube is connected to the tracheostomy tube, which allows complete flexibility. Tracheal cuff pressure must be monitored regularly; if any visible blood or palpable pulsations are found around the tracheostomy, immediate action must be taken [6]. This is necessary to reduce iatrogenic causes.

A TAF is a rare but lethal complication, and prompt diagnosis and emergency intervention for hemostasis are crucial to saving a patient's life. We believe that preventing TAF through daily tracheostomy care and considering its severity are the best approaches. We must always be aware of any type of tracheostomy bleeding and identify the bleeding site. In our case, inserting the endograft stent proved to be an effective and lifesaving method, although the TAF was detected at an unusual site. However, further data on complications as well as limitations and improvement of patient management must be collected in the future to provide better care for patients with TAF.

Acknowledgments

We would like to thank Dr. Hung-Lung Hsu, the cardiovascular surgeon, for stent-grafting support; and the critical care unit for providing postoperative care to our patient. We also want to thank www.enago.tw for initial language editing.

References

1. Chen HC, Song L, Chang HC, *et al*. Factors related to tracheostomy timing and ventilator weaning: findings from a population in Northern Taiwan. Clin Respir J 2018; 12: 97-104.
2. Scalise P, Prunk SR, Healy D, *et al*. The incidence of tracheoarterial fistula in patients with chronic tracheostomy tubes: a retrospective study of 544 patients in a long-term care facility. Chest 2005; 128: 3906-9.
3. Hsu YC, Huang YC, Hsu CW. Tracheo-carotid artery fistula: an unusual cause of tracheostomy bleeding. QJM 2016; 109: 209-10.
4. Reger B, Neu R, Hofmann HS, *et al*. High mortality in patients with tracheoarterial fistulas: clinical experience and treatment recommendations. Interact Cardiovasc Thorac Surg 2018; 26: 12-7.
5. Grant CA, Dempsey G, Harrison J, *et al*. Tracheo-innominate artery fistula after percutaneous tracheostomy: three case reports and a clinical review. Br J Anaesth 2006; 96: 127-31.
6. Sihag S, Wright CD. Prevention and management of complications following tracheal resection. Thorac Surg Clin 2015; 25: 499-508.
7. Yogo A, Komori M, Yano Y, *et al*. A case of trachea-innominate artery fistula successfully treated with endovascular stent of the innominate artery. J Gen Fam Med 2017; 18: 162-4.
8. Dalati HA, Jabbr MS, Kassouma J. High-riding brachiocephalic (innominate) artery during surgical tracheostomy. BMJ Case Rep 2018; 2018: bcr2017221802.

Lung Cancer with Small Bowel Metastasis and Perforation in A Chemotherapy-Naïve Patient: A Case Report

Chung-Chi Yu[1], Jung-Yueh Chen[1,2]

Lung cancer is a leading cause of cancer-related death worldwide. Most patients diagnosed with lung cancer were at an advanced stage. However, small bowel metastasis is rare in patients with lung cancer. We reported a rare case of lung cancer with small bowel metastasis presenting with hollow organ perforation before treatment for cancer. CT of the abdomen disclosed free air accumulation at the peritoneal cavity. A tumor invasion-related perforation at 100 cm proximal to the ileocecal valve was seen in an emergency abdominal laparotomy. The histopathologic report revealed squamous cell carcinoma. ***(Thorac Med 2023; 38: 315-319)***

Key words: Lung cancer; small bowel metastasis; hollow organ perforation; chemotherapy

Introduction

Lung cancer is the most common cancer in the world, accounting for 19.4% of all cancer-related deaths [1]. Most patients diagnosed with lung cancer were at an advanced stage. When lung cancer metastasizes, the most common sites include the brain, bone, liver, adrenal glands, contralateral lung, and distant lymph nodes [1-2]. The gastrointestinal (GI) tract is an uncommon metastasis site in primary lung cancer, with an incidence rate of less than 0.2%, and the small intestine is the most frequently involved organ in the GI tract, due to its abundant blood supply [3-4]. Squamous cell carcinoma and adenocarcinoma were the most commonly reported histological types of lung cancer with GI tract metastasis [3,6]. Early diagnosis of small bowel metastasis is difficult, due to a lack of clinically apparent symptoms [5]. Perforation is the most common presentation of small bowel metastasis, followed by hemorrhage and obstruction [3]. However, the clinical presentation of symptomatic small intestinal metastasis is extremely rare. This report presents a rare case of small bowel metastasis from primary squamous cell carcinoma of the lung, complicated by hollow organ perforation.

[1]Department of Internal Medicine, E-Da Hospital, Kaohsiung, Taiwan. [2]School of Medicine, College of Medicine, I-Shou University, Kaohsiung, Taiwan.
Address reprint requests to: Dr. Jung-Yueh Chen, Department of Internal Medicine, E-Da Hospital No.1, Yida Road, Jiao-su Village, Yan-chao District, Kaohsiung 824, Taiwan.

Case Presentation

A 65-year-old male patient, a heavy smoker, presented with progressive shortness of breath and dry cough for 4 weeks, with no other discomfort. He had a medical history of hypertension and coronary artery disease status after 2 stents had been inserted in February 2018. Right-side fixed wheezing and bilateral lower lung crackles were noted by auscultation. Plain radiograph of the chest revealed a right upper lung cavitary mass. Computed tomography (CT) of the chest revealed a thick-wall cavitary lesion in the right upper lung area (Figure 1), a spiculated lesion in the left upper lung area, a necrotic mass-like lesion in the supraclavicular and mediastinal region of the right chest wall, and a nodular lesion on the right-side adrenal gland. Squamous cell carcinoma was proven by endobronchial biopsy. Bone scan revealed multiple active bone lesions at the right scapula, lower cervical spine, sternum, ribs and left proximal femur area, which indicated bone metastasis. No metastasis was found by brain magnetic resonance imaging. The patient's cancer stage was T4N3M1c (stage IVB).

Palliative radiotherapy for the right upper lung tumor and right main bronchi was started first, because severe right-side bronchial stenosis from tumor invasion presented a high risk of respiratory compromise. Systemic chemotherapy was scheduled after port-a-cath insertion. However, 2 weeks after admission and before chemotherapy began, the patient experienced a sudden onset of severe diffuse abdominal pain and dyspnea. At physical examination, the patient had diffuse abdominal tenderness, muscle guarding and rebound pain. Emergency CT of the abdomen revealed free air accumulation in the peritoneal cavity, which suggested hollow organ perforation (Figure 2). A tumor invasion-related perforation at 100 cm proximal to the

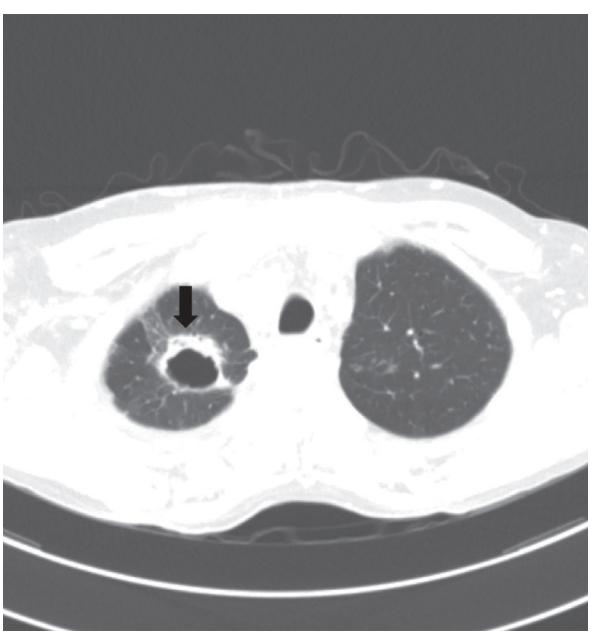

Fig. 1. Chest CT of a thick-wall cavitary lesion at the right upper lung area (arrow).

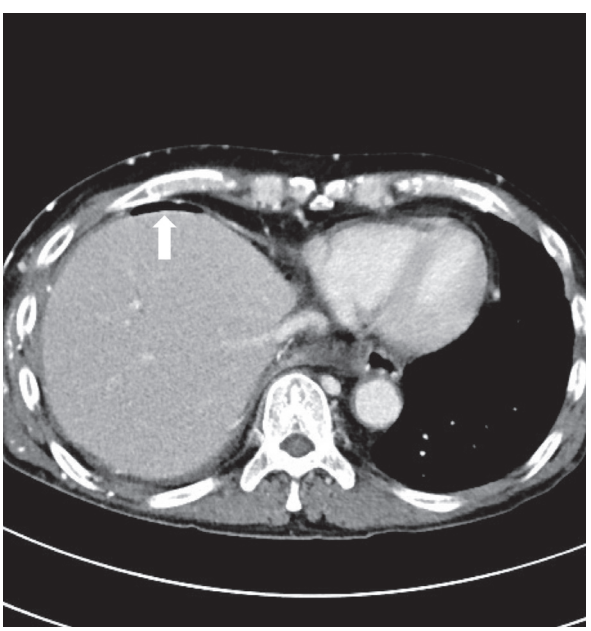

Fig. 2. Abdominal CT of free air accumulation at the right-side subphrenic area (arrow).

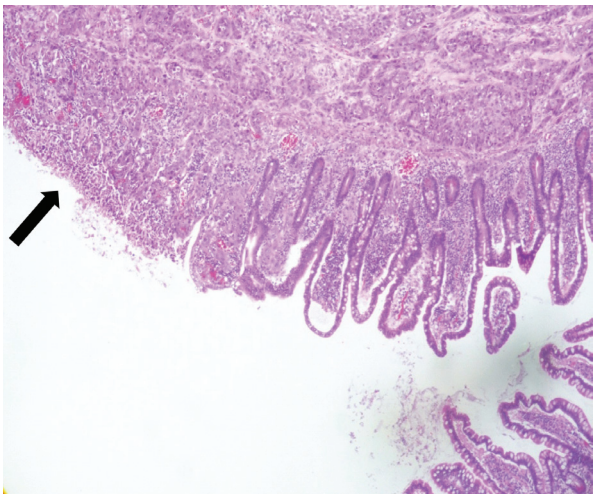

Fig. 3. Microscopic finding from resected jejunum showed transmural infiltration of neoplastic squamous epithelial cells in the small intestine (arrow).

ileocecal valve was seen in an emergency abdominal laparotomy. The histopathologic report revealed squamous cell carcinoma (Figure 3). Surgical intestinal tumor resection and end-to-end anastomosis were performed, though the patient's condition continued to deteriorate. The patient passed away 5 days after surgery, due to septic shock.

Discussion

The incidence rate of GI tract metastasis is less than 0.2% [3-4], but the actual incidence rate is much higher, based on the results of autopsy series [7]. The reason for this is that the majority of patients with gastrointestinal metastases are asymptomatic, and the metastasis is not clinically apparent [5,7].

The small intestine is the most frequently involved organ in the GI tract, followed by the colon and stomach [3,4,9]. Metastasis may reach the small bowel by the hematogenous or lymphatic route, or by direct invasion or contiguous spread.

Common symptoms are abdominal pain, gastro-intestinal bleeding, obstruction, nausea, vomiting, perforation, and peritonitis [3,8]. However, most patients have no obvious clinical symptoms, and the median time from primary lung cancer diagnosis to GI tract metastasis was 4 to 6 months [3,6]. Small bowel tumors are likely to initially present with serious clinical complications such as perforation, which often leads to death.

Small bowel metastasis may occur in any histological type of lung cancer, but the most common type was squamous cell carcinoma, followed by adenocarcinoma and small cell carcinoma [3,5-6,8-9]. The high incidence of squamous cell carcinoma and adenocarcinoma were due to their high prevalence in primary lung cancer. Squamous cell carcinoma also had

a higher incidence of small bowel perforation. Intestinal perforation occurred more commonly after chemotherapy; it induced necrosis of the tumor, resulting in the loss of bowel wall integrity [8-9]. But in other studies [3,6], there was no significant difference in the risks of perforation between patients with or without chemotherapy.

When patients with lung cancer have new-onset GI symptoms (abdominal pain, nausea, vomiting, anemia, hematochezia, melena, constipation or other changes in bowel habits), particularly those that cannot be explained by primary lung cancer or undergoing chemotherapy or radiotherapy, GI tract metastasis should be considered. Abdominal CT has a high value in diagnosing gastrointestinal metastasis [6,8,10]. Imaging features of a metastatic small bowel lesion include single or multiple polypoid intraluminal mass lesions or focal bowel wall thickening. Metastasis to the small intestine may not always be well detected on a CT scan, but the scan is good at showing some of the problems that a tumor can cause, like perforation or obstruction. Endoscopy, gastroenterography, push enteroscopy, and positron emission tomography-CT also aid the diagnosis of GI metastasis [6,8-9].

The prognosis of small bowel metastasis has been very poor, often less than 3 months, particularly in patients with jejunum metastasis [3,8-9]. Prognostic factors related to a clinically poor outcome include synchronous metastases, extra-gastrointestinal metastases, perforation of gastrointestinal metastasis, and a lack of abdominal surgery intervention. Surgical resection with primary end-to-end anastomosis may be the optimal treatment to prevent life-threatening complications, especially in patients with small bowel involvement, which can lead to perforation [3-4,11].

Symptomatic small bowel metastases are rare in lung cancer; when found, most have severe complications and a high mortality rate, even with prompt surgical therapy. Our patient was chemotherapy-naïve and had no evidence of GI bleeding before perforation. The clinical presentations in this patient were very rare and difficult to predict. In patients with lung cancer and new-onset GI symptoms, more attention should be paid to metastasis. Abdominal CT also has a good diagnostic rate for GI tract metastasis, but when no lesion is detected and metastasis is still highly suspected, other imaging studies should be considered to detect and prevent life-threatening conditions, especially small bowel metastases.

References

1. Mao Y, Yang D, He J, *et al*. Epidemiology of lung cancer. Surg Oncol Clin N Am 2016; 25: 439-45.
2. Perisano C, Spinelli MS, Graci C, *et al*. Soft tissue metastases in lung cancer: a review of the literature. Eur Rev Med Pharmacol Sci 2012; 16(14): 1908-14.
3. Hu Y, Feit N, Huang Y, *et al*. Gastrointestinal metastasis of primary lung cancer: an analysis of 366 cases. Oncol Lett 2018; 15: 9766-9776.
4. Kim MS, Kook EH, Ahn SH, *et al*. Gastrointestinal metastasis of lung cancer with special emphasis on a long-term survivor after operation. J Cancer Res Clin Oncol 2009; 135: 297-301.
5. McNeill PM, Wagman LD, Neifeld JP. Small bowel metastases from primary carcinoma of the lung. Cancer 1987 Apr 15; 59(8): 1486-9.
6. Kim SY, Ha HK, Park S *et al*. Gastrointestinal metastasis from primary lung cancer: CT findings and clinicopathologic features. AJR Am J Roentgenol 2009; 193: W197-201.
7. Yoshimoto A, Kasahara K, Kawashima A. Gastrointestinal metastases from primary lung cancer. Eur J Cancer 2006; 42: 3157-60.

8. Berger A, Cellier C, Daniel C, *et al*. Small bowel metastases from primary carcinoma of the lung: clinical findings and outcome. Am J Gastroenterol 1999; 94: 1884.
9. Yang C-J, Hwang J-J, Kang W-Y, *et al*. Gastrointestinal metastasis of primary lung carcinoma: clinical presentations and outcome. Lung Cancer 2006; 54(3): 319-323.
10. Jasti R, Carucci LR. Small bowel neoplasms: a pictorial review. Radiographics 2020 Jul-Aug; 40(4): 1020-1038.
11. Giulio R, Alessandro M, Elena R, *et al*. Primary lung cancer presenting with gastrointestinal tract involvement: clinicopathologic and immunohistochemical features in a series of 18 consecutive cases. J Thorac Oncol 2007 Feb; 2(2): 115-20.

Granulomatosis with Polyangiitis: A Case report and Review of the Literature

Kung-Yang Wang[1], Ching-Yao Yang[1]

Granulomatosis with polyangiitis (GPA), formerly called Wegener granulomatosis, is a rare vasculitis affecting the small vessels. It commonly involves the upper respiratory tract, lungs and kidneys, which lead to dyspnea, hemoptysis or hematuria. The damage to the organs can be fatal. Though the exact mechanisms leading to GPA are not well understood, anti-neutrophil cytoplasmic antibodies are considered to be associated with the inflammation in GPA. The diagnosis of GPA is based on clinical presentation, laboratory findings and image studies. The 2022 American College of Rheumatology and European Alliance of Associations for Rheumatology recently developed revised classification criteria for GPA. Treatment consists of an induction phase and a maintenance phase with glucocorticoid or immunosuppressive agents such as cyclophosphamide, rituximab or methotrexate. GPA is a rare disease in Taiwan. Here, we reported the case of a patient with GPA, who presented with bilateral lung cavitary nodules and consolidations. The diagnosis was proven by echo-guided lung biopsy. The patient showed a good response to cyclophosphamide pulse therapy and was under maintenance therapy with rituximab and oral prednisolone. ***(Thorac Med 2023; 38: 320-324)***

Key words: Granulomatosis with polyangiitis, anti-neutrophil cytoplasmic antibodies

Introduction

Granulomatosis with polyangiitis (GPA), formerly called Wegener granulomatosis [1], is a rare vasculitis affecting the small vessels, and involves granulomas. Patients present with non-specific symptoms of fever, malaise, anorexia, weight loss and myalgia [2], and may be misdiagnosed initially. GPA also commonly affects specific organs such as the upper respiratory tract, lungs and kidneys [3], which leads to dyspnea, hemoptysis or hematuria. The organs with affected blood vessels may sustain fatal damage. The exact mechanisms leading to GPA are not well understood. It is now widely presumed that anti-neutrophil cytoplasmic antibodies (ANCA) are associated with the inflammation in GPA [3]. The diagnosis of GPA is based on

[1]Department of Internal Medicine, National Taiwan University Hospital, Taipei, Taiwan.
Address reprint requests to: Dr. Ching-Yao Yang, Department of Internal Medicine, National Taiwan University Hospital and National Taiwan University College of Medicine, No. 7, Chung Shan S. Rd., Zhongzheng Dist., Taipei 100, Taiwan.

clinical presentation, laboratory findings and image studies. ANCA plays a major role in the diagnosis, but negative ANCA does not exclude GPA [4]. Treatment consists of an induction phase and a maintenance phase with glucocorticoid and immunosuppressive agents such as cyclophosphamide, rituximab or methotrexate.

GPA is a rare disease; the annual incidence of GPA in Taiwan was 0.37 per million patient-years from 1997 to 2008 [5]. We report the case of a patient with GPA, who presented with bilateral lung cavitary nodules and consolidations. The diagnosis was proved by echo-guided lung biopsy. The patient showed a good response to cyclophosphamide pulse therapy and was under maintenance therapy with rituximab and oral prednisolone.

Fig. 1. A: Chest radiograph on 20 June 2022.

Case Presentation

A 70-year-old woman visited our hospital in June 2022 due to intermittent productive cough for 2 months. Decreased appetite, easily fatigued, and body weight loss during the previous 1 month (48 kg to 46 kg) were also reported. She was an ex-smoker (0.5 pack per day for 35 years), and had hypertension and type 2 diabetes mellitus under medical control. In addition, she was a hepatitis B carrier with stable liver function tests. She did not have a remarkable occupational exposure or travel history, and did not breed any pets at home. She denied recent usage of health supplements or Chinese herbal medicine.

An abnormal chest radiograph was noted in a local clinic initially, so she was referred to our hospital. Bilateral cavitary nodules and consolidations with mediastinal and bilateral hilar lymphadenopathies were found in the chest radiograph (Figure 1A) and computed tomography (CT) (Figure 1B) on 20 June 2022. Her laboratory tests showed leukocytosis (11.7 k/μL), proteinuria, and a urine protein-creatinine ratio of 2200 mg/g. Echo-guided biopsy was performed, and the pathology reports revealed mostly necrotizing inflammation with scanty multinucleated giant cells. Laboratory surveys for autoimmune diseases showed a positive cytoplasmic anti-neutrophil cytoplasmic antibody (c-ANCA, 5.8I U/mL), elevated C-reactive protein (17.39 mg/dL), erythrocyte sedimentation rate (100 mm/hr), IgG (2044.43 mg/dL), IgA (693.69 mg/dL) and a decreased IgM level (44.14 mg/dL). Sputum culture yielded Klebsiella pneumoniae and Acinetobacter johnsonii, but tissue culture and acid-fast stain from the lung biopsy showed negative findings.

Taken together, GPA was diagnosed, and methylprednisolone 10 mg Q8H (~0.6 mg/kg/day) was initiated on 1 July 2022, as well as cy-

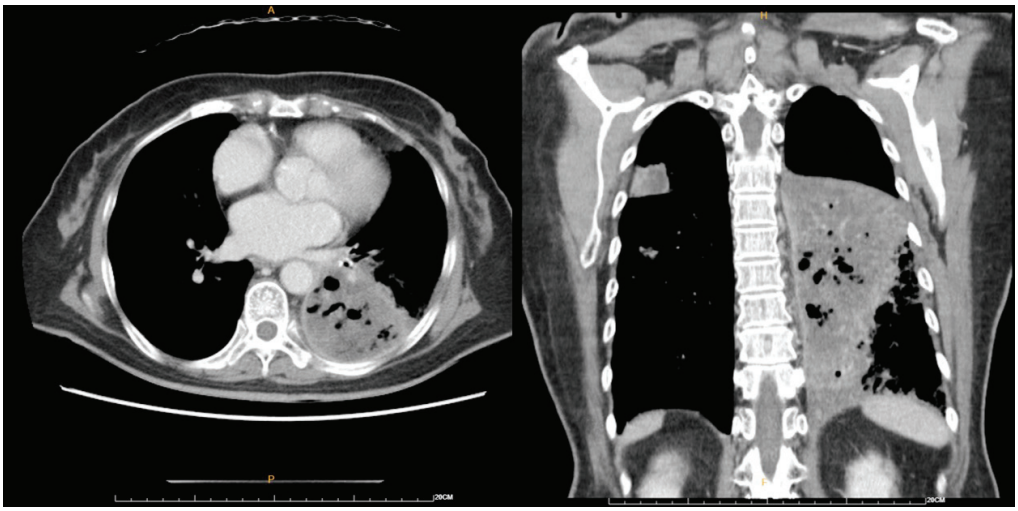

Fig. 1. B: Computed tomography on 20 June 2022.

clophosphamide pulse therapy (400 mg) treatment (cycle 1 = 2 July 2022, cycle 2 = 9 August 2022). Glucocorticoid was shifted to oral prednisolone 20 mg/day beginning on 9 July 2022. Follow-up chest radiographs (Figure 2) showed resolution of lung nodules and consolidations. Weekly rituximab (500 mg) was then initiated on 22 September 2022. A total of 4 cycles of rituximab were scheduled, and oral prednisolone 20 mg/day was maintained as treatment at the outpatient clinic.

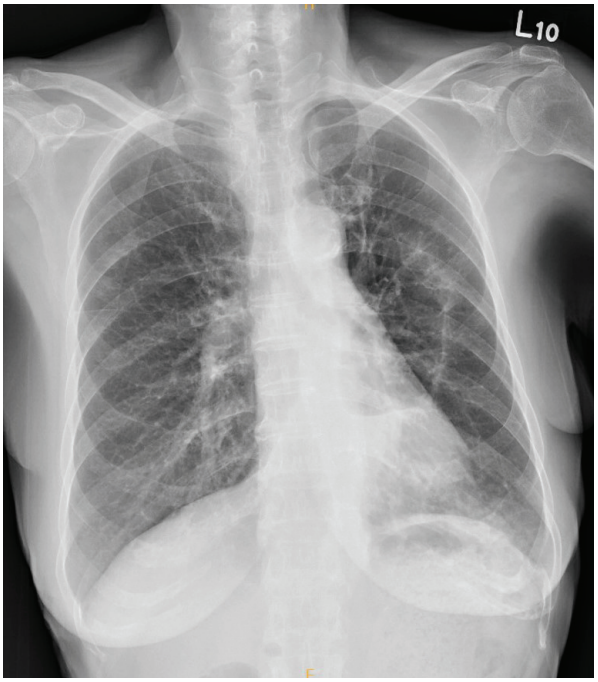

Fig. 2. Follow-up chest radiograph on 6 September 2022.

Discussion

GPA is 1 of the ANCA–associated vasculitis (AAV) disorders [6]. The prevalence of GPA ranges from 2.3 to 146.0 cases per million persons, with an incidence of 0.4 to 11.9 cases per million person-years [7]. The incidence varies depending upon geography. GPA mainly affects regions of the world in which the population is predominantly of European ancestry and is rarely observed in East Asia [8].

GPA usually presents with non-specific symptoms including fever, malaise, weight loss, polyarthralgia, and myalgia. It could be misdiagnosed as an infection or malignancy [9]. Prodromal symptoms may last for weeks to months without evidence of specific organ involvement [10].

Clinical features in organs included nasal septal perforation, saddle-nose deformity, conductive or sensorineural hearing loss, subglottic stenosis, orbital pseudotumor, scleritis, episcleritis, uveitis, lung nodules, infiltrations, cavitary lesions, alveolar hemorrhage, segmental necrotizing glomerulonephritis, and vasculitic neuropathy [3].

Various diagnostic criteria of GPA have been proposed, including organ involvement, abnormal imaging, biopsy and positive c-ANCA [11-12]. The Canadian Vasculitis Research Network recently proposed recommendations for diagnosis. A high-quality, antigen-specific immunoassay for proteinase 3-ANCA and myeloperoxidase-ANCA is the preferred method of ANCA detection over indirect immunofluorescence (IIF) detection of cytoplasmic staining ANCA and perinuclear staining of ANCA for patients in whom there is clinical suspicion of ANCA-associated vasculitis. Tissue biopsy should be considered in cases of suspected AAV to confirm the diagnosis [13-14]. Also, the 2022 American College of Rheumatology and European Alliance of Associations for Rheumatology developed revised classification criteria for GPA. A scoring system consisting of clinical, laboratory, imaging, and biopsy criteria should be used with a patient with a diagnosis of small- or medium-vessel vasculitis; an alternate diagnosis of mimicking vasculitis should be excluded. The patient could be classified as having GPA if the cumulative score was ≥5 points [15].

The treatment strategy depends on the severity of the disease. Organ or life-threatening features include active glomerulonephritis, pulmonary hemorrhage, cerebral vasculitis, progressive peripheral or cranial neuropathy, orbital pseudotumor, scleritis, gastrointestinal bleeding due to vasculitis, and cardiac disease due to vasculitis (pericarditis, myocarditis) [16]. The therapeutic recommendation involves the use of immunosuppressive agents with an induction and a maintenance phase. Glucocorticoid plus either cyclophosphamide or rituximab are often administered at the onset of induction therapy. A dosage of intravenous methylprednisolone pulses (500-1000 mg/day for 1-3 days) were suggested for patients with life-threatening conditions [17-18], and prednisone at 0.5 mg/kg/day (or its equivalent) was suggested for non-life-threatening conditions.

A glucocorticoid tapering protocol should be initiated within 2 weeks of induction therapy. In patients who achieve remission after induction therapy, rituximab (500-1000 mg, every 4–6 months) is recommended as maintenance therapy [19]. In most patients, maintenance therapy should be continued for 12 to 24 months after stable remission has been induced [20]. Patients should be closely followed up after cessation of therapy, since most relapses of GPA occur within the first 12 to 18 months [21]. Those with a non-severe disease relapse should be treated with an increased dose of glucocorticoid, and there should be a re-induction of either cyclophosphamide or rituximab in conjunction with glucocorticoid in those with an organ- or life-threatening condition [22].

Conclusion

GPA is an AAV disorder and typically affects the respiratory and renal systems. With combined treatment of immunosuppressive agents, our patient showed a good response.

Conflicts of interest

All authors declared no conflicts.

References

1. Singer O, McCune WJ. Update on maintenance therapy for granulomatosis with polyangiitis and microscopic polyangiitis. Cur Opin Rheumatol (Review) May 2017; 29 (3): 248-53.
2. Kitching AR, Anders HJ, Basu N, *et al*. ANCA-associated vasculitis. Nat Rev Dis Primers. 27 Aug 27 2020; 6(1): 71. Epub 2020.
3. Seo P, Stone JH. The antineutrophil cytoplasmic antibody-associated vasculitides. Am J Med 2004; 117: 39.
4. Hagen EC, Daha MR, Hermans J, *et al*. Diagnostic value of standardized assays for anti-neutrophil cytoplasmic antibodies in idiopathic systemic vasculitis. EC/BCR Project for ANCA Assay Standardization. Kidney Int. 1998; 53(3): 743.
5. Wu CS, Hsieh CJ, Peng YS, *et al*. Antineutrophil cytoplasmic antibody-associated vasculitis in Taiwan: A hospital-based study with reference to the population-based National Health Insurance database. J Microbiol Immunol Infect 2015; 48: 477-82.
6. Garlapati P, Qurie A. Granulomatosis with polyangiitis. StatPearls [Internet] 2021 Jan.
7. Kitching AR, Anders HJ, Basu N, *et al*. ANCA-associated vasculitis. Nat Rev Dis Primers 2020; 6: 71.
8. Watts RA, Scott DG, Jayne DR, *et al*. Renal vasculitis in Japan and the UK--are there differences in epidemiology and clinical phenotype? Nephrol Dial Transplant 2008; 23: 3928.
9. Comarmond C, Cacoub P. Granulomatosis with polyangiitis (Wegener): clinical aspects and treatment. Autoimmun Rev 2014 Nov; 13(11): 1121-5.
10. Falk RJ, Hogan S, Carey TS, *et al*. Clinical course of anti-neutrophil cytoplasmic autoantibody-associated glomerulonephritis and systemic vasculitis. The Glomerular Disease Collaborative Network. Ann Intern Med 1990; 113: 656.
11. Leavitt RY, Fauci AS, Bloch DA, *et al*. The American College of Rheumatology 1990 criteria for the classification of Wegener's granulomatosis. Arthritis Rheum 1990 Aug; 33(8): 1101-7.
12. DeRemee RA, McDonald TJ, Harrison EG, *et al*. Wegener's granulomatosis. Anatomic correlates, a proposed classification. Mayo Clin Proc 1976 Dec; 51(12): 777-81.
13. Mendel A, Ennis D, Go E, *et al*. CanVasc Consensus Recommendations for the Management of Antineutrophil Cytoplasm Antibody-associated Vasculitis: 2020 Update. J Rheumatol 2021; 48: 555-66.
14. Damoiseaux J, Csernok E, Rasmussen N, *et al*. Detection of antineutrophil cytoplasmic antibodies (ANCAs): a multicentre European Vasculitis Study Group (EUVAS) evaluation of the value of indirect immunofluorescence (IIF) versus antigen-specific immunoassays. Ann Rheum Dis 2017; 76: 647-53.
15. Robson JC, Grayson PC, Ponte C, *et al*. 2022 American College of Rheumatology/European Alliance of Associations for Rheumatology Classification Criteria for Granulomatosis With Polyangiitis. Arthritis Rheumatol 2022 Mar; 74(3): 393-399.
16. Chung SA, Langford CA, Maz M, *et al*. 2021 American College of Rheumatology/Vasculitis Foundation Guideline for the Management of Antineutrophil Cytoplasmic Antibody-Associated Vasculitis. Arthritis Care Res (Hoboken) 2021; 73(8): 1088. Epub 2021 Jul 8.
17. McGeoch L, Twilt M, Famorca L, *et al*. CanVasc Recommendations for the management of antineutrophil cytoplasm antibody-associated vasculitides. J Rheumatol 2016; 43: 97-120.
18. Stone JH, Merkel PA, Spiera R, *et al*. Rituximab versus cyclophosphamide for ANCA-associated vasculitis. N Engl J Med 2010; 363: 221-32.
19. Guillevin L, Pagnoux C, Karras A, *et al*. Rituximab versus azathioprine for maintenance in ANCA-associated vasculitis. N Engl J Med 2014; 371(19): 1771.
20. Charles P, Perrodeau É, Samson M, *et al*. Long-term rituximab use to maintain remission of antineutrophil cytoplasmic antibody-associated vasculitis: a randomized trial. Ann Intern Med 2020; 173(3): 179. Epub 2020 Jun 2.
21. Hogan SL, Falk RJ, Chin H, *et al*. Predictors of relapse and treatment resistance in antineutrophil cytoplasmic antibody-associated small-vessel vasculitis. Ann Intern Med 2005; 143(9): 621.
22. Miloslavsky EM, Specks U, Merkel PA, *et al*. Outcomes of nonsevere relapses in antineutrophil cytoplasmic antibody-associated vasculitis treated with glucocorticoids. Arthritis Rheumatol 2015; 67(6): 1629.

Successful Remission of a Large Post-intubation Tracheal Rupture with Conservative Management – A Case Report

Hsin-Wei Lin[1], Yen-Hsiang Tang[2], Yu-Hui Yang[3], Hsin-Pei Chung[1]

Iatrogenic tracheal rupture is a rare but life-threatening complication that can occur during an endotracheal intubation procedure. An iatrogenic rupture might be due to any one of various factors, including stylet-induced tracheal injury and an incorrect endotracheal tube size. The treatment strategy for iatrogenic tracheal rupture is challenging, and depends on the laceration length, size, location, and underlying disease. Surgical repair is often required for a large rupture, while conservative management is considered sufficient for small and stable lacerations. Mediastinitis, and even death could occur if the rupture cannot be handled properly.

We present the case of a 67-year-old woman with heart failure, who was diagnosed with a large tracheal rupture after emergency endotracheal intubation. She received conservative treatment for the tracheal rupture, rather than surgical repair, and bronchoscopic examination on the 8th day after intubation showed the rupture was healing. The patient was successfully extubated later. Therefore, conservative management may be considered for large post-intubation tracheal ruptures in a high-risk surgical candidate. ***(Thorac Med 2023; 38: 325-329)***

Key words: tracheal rupture, endotracheal intubation, endotracheal tube cuff

Introduction

Tracheal rupture is a rare complication of endotracheal intubation, and has occurred in only 0.005% of intubation attempts [1]. The causes of iatrogenic tracheal rupture are varied, and include stylet-induced tracheal injury and an incorrect endotracheal tube size. Due to its rarity, tracheal rupture is difficult to detect; however, it can be a life-threatening event. A tracheal rupture might lead to immediate death due to asphyxia, and with a delayed diagnosis, mediastinitis, and even death may occur. Surgical intervention remains the gold standard treatment for lacerations larger than 2 cm. But conservative management is considered to be a safe choice for clinically stable patients without complications, which means there is no

[1]Section of Pulmonary Medicine, Department of Internal Medicine, MacKay Memorial Hospital, Tamsui Branch.
[2]Section of Critical Care Medicine, Department of Internal Medicine, MacKay Memorial Hospital, Tamsui Branch.
[3]Division of Thoracic Surgery, Department of Surgery, MacKay Memorial Hospital, Tamsui Branch.
Address reprint requests to: Dr. Hsin-Pei Chung, MacKay Memorial Hospital, Tamsui Branch No. 45, Minsheng Rd., Tamsui District, New Taipei City 25160, Taiwan.

pneumomediastinum, mediastinitis or esophageal lacerations [2]. We present the case of a 67-year-old woman with a history of heart failure who successfully underwent conservative treatment for a large post-intubation tracheal rupture.

Case Report

A 67-year-old woman with a history of heart failure visited our emergency department because of shortness of breath for 3 days. She was alert on arrival at the emergency room, but lost consciousness after receiving contrast media for a computed tomography (CT) scan. An echocardiogram revealed ventricular tachyarrhythmias. Cardioversion and cardiopulmonary resuscitation (CPR) were performed immediately. She returned to spontaneous circulation after 17 minutes of resuscitation. During CPR, a 7.5 French endotracheal tube (ETT) was inserted under laryngoscopic guidance. She was successfully intubated at the first attempt. The length of the insertion was 22 cm from the lip, with an ETT cuff pressure of 25 cmH_2O. The initial ventilator setting was a volume control ventilation mode, delivering 500 ml of tidal volume in 16 breaths per minute, with a fraction of inspired oxygen of 100% and positive end-expiratory pressure of 5 cmH_2O. Post-intubation chest radiography showed that the ETT had been too advanced (1cm below the carina) and that the cuff had been overinflated (Figure 1). The ETT tube was then repositioned and the inflation of the cuff was adjusted.

On the next day, crepitus on palpation was noted on her neck and anterior chest wall, which indicated the development of subcutaneous emphysema. The emergency CT scan of the chest showed a tracheal defect involving the posterior wall of the middle portion of the trachea, with pneumomediastinum and subcutaneous emphysema (Figure 2). Bronchoscopy revealed a linear laceration wound of 4 cm in length at the membrane portion of the trachea and 2cm above the carina (Figure 3-A). Therefore, the ETT was advanced distally to the lesion with fixation at 24 cm from the lip, guided by the bronchoscope, and cuff pressure was reset to 20 cmH_2O.

Due to the high-risk underlying condition of heart failure and the recent arrhythmia event be-

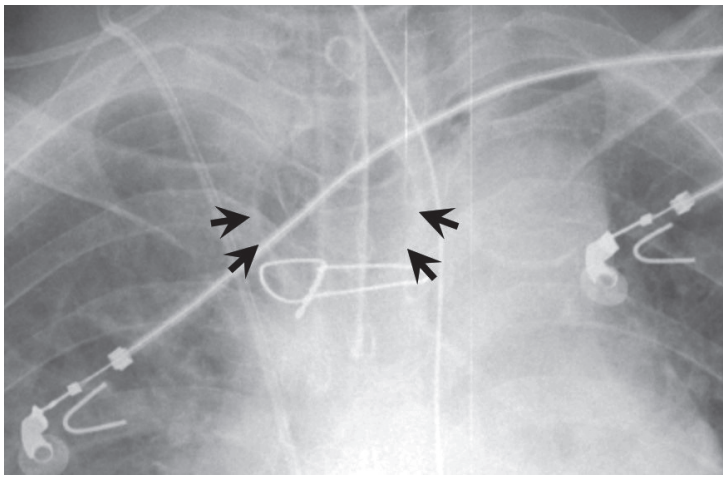

Fig. 1. Chest X-ray revealed a prominent endotracheal cuff (arrows).

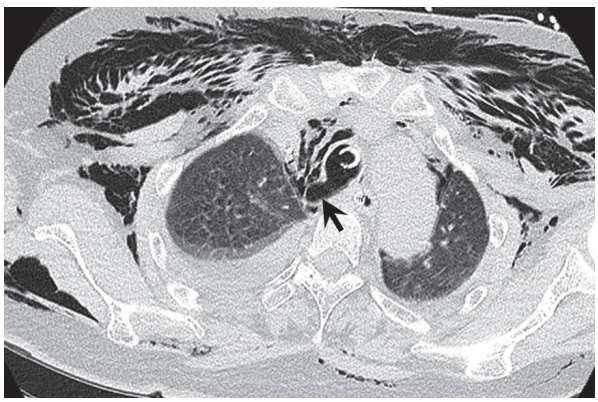

Fig. 2. Chest CT revealed rupture of the posterior tracheal wall (arrow) with pneumomediastinum and extensive subcutaneous emphysema.

fore CPR, a chest surgeon suggested maintaining conservative treatment. A broad-spectrum antibiotic, ceftazidime 2 g q8h, and antitussive agents were prescribed. Mechanical ventilation was set in a pressure control ventilation mode, delivering 400 ml (8 ml per kg) per breath, with an inspiratory and expiratory ratio of 1:2, in 20 breaths per minute, and with a peak pressure of 12 cmH_2O with a fraction of inspired oxygen of 70% and zero positive end-expiratory pressure. Afterward, the subcutaneous emphysema gradually resolved. The follow-up chest X-ray confirmed clinical improvement of the subcutaneous emphysema, and no pneumothorax or mediastinitis developed. The complete blood count and biochemistry of the patient revealed no evidence of systemic infection. As a result, we continued conservative treatment, and the weaning procedure was started on the 5th day after intubation, when the subcutaneous emphysema had almost resolved. On the 8th day after intubation, repeated bronchoscopic examinations showed that the tracheal rupture was in a healing process (Figure 3-B). The patient was weaned from mechanical ventilation, then successfully extubated without complications on the 20th day after intubation. The patient was discharged from the hospital 24 days after intubation.

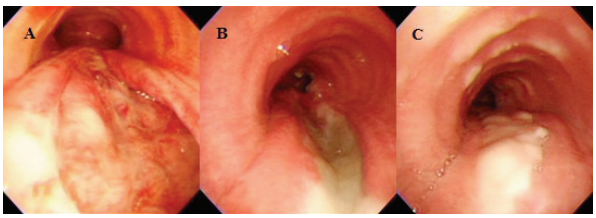

Fig. 3. (A) Bronchoscopy showed a linear wound at the membrane portion of the trachea (4 cm in length). (B) Bronchoscopy on the 8th day after intubation showed that the wound had healed, and (C) on day 15.

Discussion

Iatrogenic tracheal rupture is a severe complication of tracheal intubation, with an estimated incidence of 1/20,000 intubations [1]. Due to its rarity, it is often misdiagnosed as subcutaneous emphysema, pneumomediastinum, or barotrauma [2]. A delayed diagnosis can lead to mediastinitis and increased mortality [3].

The risk of tracheal intubation complications increases when the procedure is undertaken in an emergency setting and with an inexperienced technician. Patient risk factors for tracheal intubation complications include female gender, short stature, an anatomic variation of the airway, steroid use, chronic obstructive pulmonary disease, and an underlying connective tissue disease. Mechanical risk factors include multiple forced attempts, use of rigid stylets, an incorrectly sized ETT, and overinflated cuff pressure [4].

We cannot choose the patients who should be intubated, but there are several ways to avoid iatrogenic tracheal rupture due to mechanical factors. Training and familiarity with intubation skills is a key factor in avoiding this disaster. In a clinical situation, we estimate the proper cuff pressure through a pilot balloon. However, a study showed that this often leads to a much higher cuff pressure, even when performed by experienced technicians [5]. The recommended ETT cuff pressure to avoid tracheal mucosa damage while decreasing the risk of aspiration is 20–30 cm H2O. In our case, even though the ETT cuff pressure, measured using a manometer, was within a normal range, chest X-ray disclosed that the ETT cuff had been overinflated. Under such a circumstance, post-intubation tracheal rupture should be a concern, even if the ETT cuff pressure remained normal.

Clinical suspicion of a post-intubation tracheal rupture is based on the symptoms of dyspnea, hemoptysis, subcutaneous emphysema, pneumothorax, pneumomediastinum, and even pneumoperitoneum after intubation [2]. These signs often develop immediately or rapidly after intubation, but can sometimes take several days to appear. A CT scan may help in the early detection of subcutaneous emphysema, pneumothorax, pneumomediastinum, and mediastinitis. Direct visualization of tracheal wall injuries on CT has been reported in 71% of cases [6], and a horizontal ETT cuff diameter greater than 2.8 cm at the widest point on a CT scan has been reported to indicate a likely rupture [7, 8]. Bronchoscopy remains the gold standard diagnostic method, as it can directly visualize the tracheal injury, help in planning the therapeutic approach, and also be used to reposition the tube or reintubate the patient, if necessary [9].

There is currently no consensus on the optimal management. Surgical intervention may improve ventilation, prevent mediastinal infection, and avoid stenosis after spontaneous healing; however, the prognosis mostly depends on the underlying disease, rather than the size of the rupture [10, 11]. This may be because mortality is mainly associated with the reason for intubation, rather than with the tracheal rupture. A previous study tried to establish a classification for a treatment standard based on anatomical features [12], but this classification was not helpful in clinical decision-making since it did not consider the clinical status of the patient.

Although surgical repair has been suggested for lacerations of more than 2 cm [2], patients with critical illnesses (unstable hemodynamic status, arrhythmias) may not be suitable for surgery. However, if the rupture site is near the carina and/or bronchi, and the patient still needs mechanical ventilation support, conservative treatment often fails. Endoscopic treatments, such as intratracheal suture [13] and the use of fibrin glue on the tracheal lacerations, have been reported [14]; however, they have only been used in a small number of patients with small lacerations and without ventilation.

Conservative treatment includes tracheal stenting, and treatment with antitussive agents and broad-spectrum antibiotics. Conservative management is used for small lacerations and in the absence of mediastinal infections [2]. In patients requiring mechanical ventilation, surgical intervention is usually indicated. However, some previous studies have demonstrated that conservative treatment can still be beneficial for these patients, even if the rupture site is near the carina or bronchi [9, 15]. These studies have suggested driving the ETT through the rupture site under bronchoscopy. Surgical repair is still a solution in patients with a major air leak related to a tracheal laceration that may compromise ventilation and that can be improved only by closing the tear.

In our case, the tracheal rupture size was 4 cm in length and 2 cm above the carina, which indicates a large laceration. Usually, such a wound would require aggressive surgical exploration, but our patient had just had a cardiac dysrhythmia and was receiving CPR. In this situation, surgery would not have been appropriate. That was why we chose conservative treatment with antitussive agents, broad-spectrum antibiotics, driving the ETT through the rupture site, proper cuff pressure, and a proper ventilator setting. Fortunately, this patient had a favorable outcome after that.

We believe surgical exploration is highly recommended for those patients with a large

tracheal rupture. But, sometimes, a patient is at a high risk with surgical exploration, including the use of anesthesia, and conservative treatment should be considered. Therefore, further study is required to establish a treatment standard.

References

1. Lampl L. Tracheobronchial injuries. Conservative treatment. Interact Cardiovasc Thorac Surg 2004; 3(2): 401-5.
2. Carbognani P, Bobbio A, Cattelani L, *et al*. Management of postintubation membranous tracheal rupture. Ann Thorac Surg 2004; 77(2): 406-9.
3. Hashem B, Smith JK, Davis WB. A 63-year-old woman with subcutaneous emphysema following endotracheal intubation. Chest 2005; 128(1): 434-8.
4. Reilly JR, Pasquier M, Yersin B, *et al*. Blaming the balloon: the risk of post-intubation tracheobronchial rupture. Intern Emerg Med 2013; 8(8): 753-6.
5. Hoffman RJ, Parwani V, Hahn IH. Experienced emergency medicine physicians cannot safely inflate or estimate endotracheal tube cuff pressure using standard techniques. Am J Emerg Med 2006; 24(2): 139-43.
6. Chen JD, Shanmuganathan K, Mirvis SE, *et al*. Using CT to diagnose tracheal rupture. AJR Am J Roentgenol 2001; 176(5): 1273-80.
7. Rollins RJ, Tocino I. Early radiographic signs of tracheal rupture. AJR Am J Roentgenol 1987; 148(4): 695-8.
8. Mackenzie CF, Shin B, Whitley N, *et al*. Human tracheal circumference as an indicator of correct cuff size. Anesthesiology 1980; 53(3 Suppl): S414.
9. Deja M, Menk M, Heidenhain C, *et al*. Strategies for diagnosis and treatment of iatrogenic tracheal ruptures. Minerva Anestesiol 2011; 77(12): 1155-66.
10. Kumar SM, Pandit SK, Cohen PJ. Tracheal laceration associated with endotracheal anesthesia. Anesthesiology 1977; 47(3): 298-9.
11. Hofmann H, Rettig G, Radke J, *et al*. Iatrogenic ruptures of the tracheobronchial tree. Eur J Cardio-Thorac Surg 2002; 21(4): 649-52.
12. Cardillo G, Carbone L, Carleo F, *et al*. Tracheal lacerations after endotracheal intubation: a proposed morphological classification to guide non-surgical treatment. Eur J Cardiothorac Surg 2010; 37(3): 581-7.
13. Welter S, Krbek T, Halder R, *et al*. A new technique for complete intraluminal repair of iatrogenic posterior tracheal lacerations. Interact Cardiovasc Thorac Surg 2011; 12(1): 6-9.
14. Fiorelli A, Cascone R, Di Natale D, *et al*. Endoscopic treatment with fibrin glue of post-intubation tracheal laceration. J Vis Surg 2017; 3: 102.
15. Panagiotopoulos N, Patrini D, Barnard M, *et al*. Conservative versus surgical management of iatrogenic tracheal rupture. Med Princ Pract 2017; 26(3): 218-20.

Pulmonary Rehabilitation Facilitates Lung and Muscle Strength Recovery in a Critically Ill Patient with COVID-19 with Acute Respiratory Distress Syndrome

Hui-Chin Chen[1,2,9], Jui-Fang Liu[1,2,9], Ya-Chi Wang[3], Chun-Mei Huang[4], Shu-Hua Chi[5], Hwei-Ling Chou[6], Tien-Pei Fang[1,7], Hui-Ling Lin[1,7,8]

We presented the case of a critically ill COVID-19 patient with acute respiratory distress syndrome who received 6 weeks of pulmonary rehabilitation after being extubated. The patient was referred to the hospital for a severe acute respiratory syndrome Coronavirus-2 (SARS CoV-2) test due to close contact with confirmed COVID-19 cases. He presented with mild fever and a sore throat on the first day of admission. Tachypnea and desaturation were noted on day 6. A non-rebreathing mask was employed until day 10, when his dyspnea and tachypnea deteriorated into acute respiratory failure. He was then intubated and mechanically ventilated. After comprehensive treatments, he was weaned off ventilator support and then extubated on day 31. He received 6 weeks of pulmonary rehabilitation in the post-acute phase, beginning the day after extubation. The multiple-intervention pulmonary rehabilitation program included pursed-lip breathing, diaphragmatic breathing, cough training, upper and lower limb exercises, incentive spirometry, intermittent positive pressure breathing, inspiratory muscle training, and chest physiotherapy. The patient benefited from early post-acute phase pulmonary rehabilitation, as evidenced by improvement in muscle strength, peak inspiratory flow, lung volume, and the 6-minute walking test. ***(Thorac Med 2023; 38: 330-337)***

Key words: COVID-19, acute respiratory distress syndrome, pulmonary rehabilitation, pulmonary function, exercise capacity

[1]Department of Respiratory Care, Chang Gung University of Science and Technology, Chiayi, Taiwan. [2]Chronic Diseases and Health Promotion Research Center, Chang Gung University of Science and Technology, Chiayi, Taiwan, [3]Department of Respiratory Therapy, Chang Gung Memorial Hospital-Kaohsiung Medical Center and Chang Gung University College of Medicine, Kaohsiung, Taiwan. [4]Department of Respiratory Therapy, E-Da Hospital, Kaohsiung, Taiwan. [5]Respiratory Therapy Section for Adult, Changhua Christian Children's Hospital, Changhua, Taiwan. [6]Department of Respiratory Therapy, Kaohsiung Armed Forces General Hospital, Kaohsiung, Taiwan. [7]Department of Respiratory Therapy, Chiayi Chang Gung Memorial Hospital, Chiayi, Taiwan; [8]Department of Respiratory Therapy, Chang Gung University, Taoyuan, Taiwan. [9]Hui-Chin Chen and Jui-Fang Liu contributed to this work equally.

Address reprint requests to: Dr. Hui-Ling Lin, Department of Respiratory Therapy, Chang Gung University, 259, Wenhua 1st Rd., Guishan Dist., Taoyuan City, Taiwan

Introduction

Severe acute respiratory syndrome (SARS) Coronavirus-2 (SARS-CoV-2) has been classified as a viral pandemic since December 2019. In the acute state, coronavirus infectious disease-19 (COVID-19) induces damage to the vascular endothelium, and increases vascular permeability and pulmonary edema, resulting in decreased lung compliance and increased dead space, and then hinders oxygenation, known as acute respiratory distress syndrome (ARDS) [1,2]. The chest computed tomography of patients with COVID-19 showed diffused ground glass opacity of lung infiltrates and pulmonary consolidation [3]. A pathological study reported fibrin penetration into the alveolar region and interstitial fibrosis in patients with COVID-19 [4]. In patients infected with SARS complicated with ARDS in 2003, pulmonary fibrosis and reduced lung function, exercise intolerance requiring supplemental oxygen, and deconditioning at the post-acute stage have been reported [5-6]. Current case studies show that patients with COVID-19 and ARDS had reduced lung function, muscle power, and exercise capacity after extubation [7]. While most review articles and expert opinions have discussed the management of critical care for COVID-19 patients, little is known about the strategies for post-acute care. Previous studies have shown the benefits of pulmonary rehabilitation for patients with ARDS after they are weaned off mechanical ventilation (MV) [8]. We herein present a patient with COVID-19 with ARDS who benefited from a 6-week, post-acute pulmonary rehabilitation program.

Case Report

This 63-year-old man had traveled to Turkey with a tour group whose members had a fever and symptoms associated with COVID-19; therefore, he was sent by the Taiwan Centers for Disease Control for further testing. His nasal and oropharyngeal swabs tested positive for novel severe acute coronary virus-2 (SARS CoV-2). He was then admitted to a negative pressure isolation room in the hospital for further treatment.

He presented with mild fever and a sore throat on the first day of admission. Tachypnea and desaturation were noted on day 6. A non-rebreathing mask was employed until day 10, when his dyspnea and tachypnea deteriorated. His arterial blood gases revealed a pH of 7.299, $PaCO_2$ of 64.2 mmHg, PaO_2 of 64.4 mmHg, HCO_3 level of 30.8 mEq/L, SaO_2 at 89.9%, and P/F ratio of 64.4, and his chest X-ray (Fig. 1A) revealed diffused infiltrates. He was then intubated and mechanically ventilated. After comprehensive treatments, he was weaned off ventilator support and then extubated on day 31.

After being extubated, the patient appeared to have general weakness with a clinical frailty scale of 9, maximum inspiratory pressure (MIP) of 20 cmH_2O, and a muscle power assessment scale of 2 to 3 out of 5. He was diagnosed with intensive care unit (ICU)-acquired weakness. He then developed shortness of breath and tachypnea, with Borg scale scores of 3 at rest and 6 during active bedside sitting transfer. In addition, his SpO_2 was only 86% in room air, so an air-entrainment mask at 50% was used to maintain a SpO_2 of 94%. Chest X-ray (Fig. 1B) revealed chronic infiltration, pulmonary fibrosis, and atelectasis at the right base.

Due to his respiratory symptoms and muscle weakness, the medical team implemented

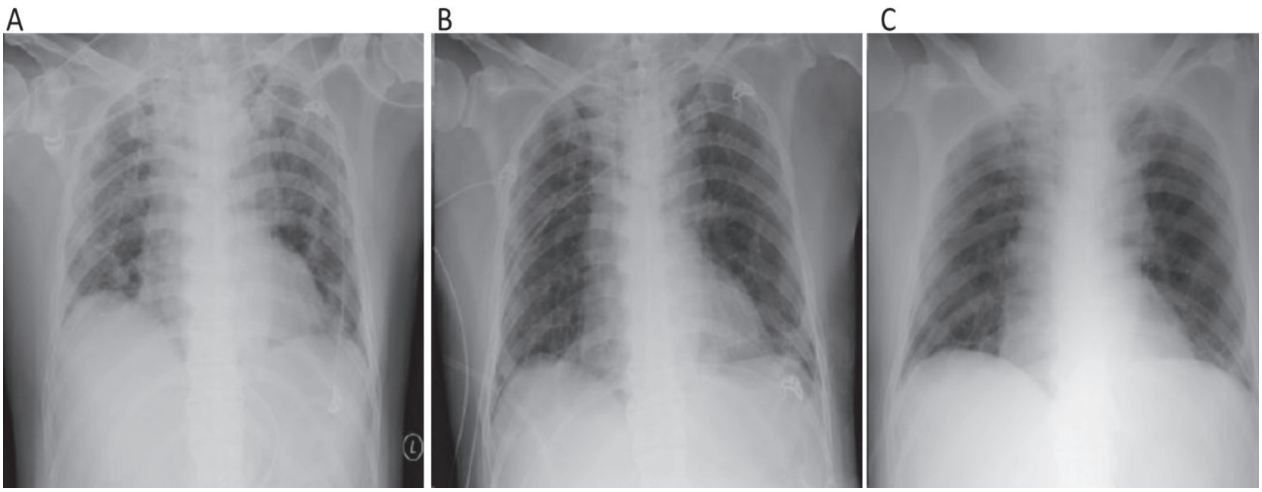

Fig. 1. Chest X-ray results at different stages. Panel A shows the X-ray result before intubation with diffused infiltrates. Panel B shows the X-ray result after extubation, with chronic infiltration, pulmonary fibrosis, and atelectasis. Panel C shows the X-ray result by the end of a 6-week pulmonary rehabilitation training, with a normal lung field.

a 6-week pulmonary rehabilitation program on the day after extubation. The program included breathing exercises, lung expansion therapy, inspiratory muscle training, and aerobic exercise. Multiple-intervention pulmonary rehabilitation consisted of breathing control education (pursed-lip breathing, diaphragmatic breathing, and cough training), upper and lower limb exercises from 30 min per day to patient tolerance, as determined using the modified Borg scale score, and incentive spirometry 3 times per day. **Table 1** shows the pulmonary rehabilitation protocol.

By the end of the 6th week of pulmonary rehabilitation training, on day 74, his muscle strength, dyspnea sensation, lung volume, and 6-minute walking test showed significant improvements. His Borg dyspnea scale scores were zero at rest and 2 during exercise, and he had 200% changes in MIP, 233% on peak expiratory flow rate, and 200% in lung volume. The muscle power of his extremities improved to a scale of 5 out of 5 e was able to perform a six-minute walking test for 50 meters. Figure 2 demotes the progress of by end of 6-week pulmonary rehabilitation training.

The X-ray image revealed a normal lung field (Fig 1C). The patient's nasal and oropharyngeal swabs turned negative on day 65, and he was discharged on day 75. Fig. 3 illustrates the timeline of patient disease progression and pulmonary rehabilitation interventions.

Discussion

Pulmonary rehabilitation has been proven to provide physiological benefits and a reduction in symptoms in patients with chronic obstructive pulmonary disease (COPD) [9]. However, performing pulmonary rehabilitation in patients with severe acute respiratory infections at a critical stage, such as with COVID-19, is difficult, due to the high risk of virus transmission to the health workers. Guidelines from China and Italy did not recommend pulmonary rehabilitation as a part of the COVID-19 management program, to avoid contamination of medical staff during the early phase of the pan-

Table 1. Pulmonary Rehabilitation Protocol

Clinical problem and assessment	**Goals**	**Prescriptions**	**1st stage (1-2 weeks)**	**2nd stage (3-4 weeks)**	**3rd stage (5-6 weeks)**
Problem: shallow breathing and dyspnea 1. Shallow breathing pattern 2. At rest ▸Moderate shortness of breath ▸Borg scale score: 3 ▸RR: 25 breaths/min 3. During activity ▸Severe shortness of breath ▸Borg scale score: 5 ▸RR: 32 breaths/min	1. Alleviate dyspnea 2. Slows respiratory rate 3. Reduce the work of breathing 4. Reduce stress	1. Pursed lip breathing 2. Diaphragmatic breathing 3. Positional release techniques	Frequency: 10 minutes, 3 times/day	Frequency: 10-15 minutes, 3 times/day	Frequency: 15-20 minutes, 3 times/day
Problem: hypoxemia 1. At rest ▸SpO_2 (Room Air):86% 2. During activity ▸SpO_2 (Room Air):86%	1. Treatment of hypoxemia 2. Keep SpO_2 >90%	Oxygen therapy	V-Mask 50%	1. V-Mask 35% 2. NC 3L	1. NC 2L prn 2. Room Air
Problem: reduced respiratory muscle strength MIP: 20cm H_2O	1. Increase the respiratory muscle strength 2. Build core strength	Inspiratory Muscle Training (IMT)	- IMT loads: 30%- 35% of MIP - 30 breaths/tid	IMT loads: 40-45% of MIP - 30 breaths/tid	IMT loads: 50-55% of MIP - 30 breaths/tid
Problem: atelectasis 1.CXR: RLL field with atelectasis	1. Aid lung expansion 2. Improvement in signs of atelectasis	IS	IS: 10 breaths every 1 to 2 hours while awake	IPPB: 10-15 min once a day. IS: 10 breaths every 1 to 2 hours while awake	IS: 10 breaths every 1 to 2 hours while awake
Problem: Decreased exercise capacity General weakness ▸Frailty scale: 9 Muscle weakness ▸mMRC Scale (right arm): 3 ▸mMRC Scale (left arm): 3 ▸mMRC Scale (right leg): 2 ▸mMRC Scale (left arm) 2 3. Bedridden 4. Not able to walk	1. Improve general muscle strength 2. Increased mobility 3. Walk without assistant	Sitting on a chair during the day Standing at bedside with assistant Walk with assistant Walk with a walker	1. Upper arm lifting 2. Upper arm lifting with water bottle 3. Sitting on a chair	1. Sitting on a chair 2. Standing for 5 minutes	Walking with a walker

Acronyms: RR: respiratory rate; SpO2: oxygen saturation by pulse oximetry; mMRC: Modified Medical Research Council; IS: incentive spirometer; V-Mask: venture mask; NC: nasal cannula; MIP: maximum inspiratory pressure

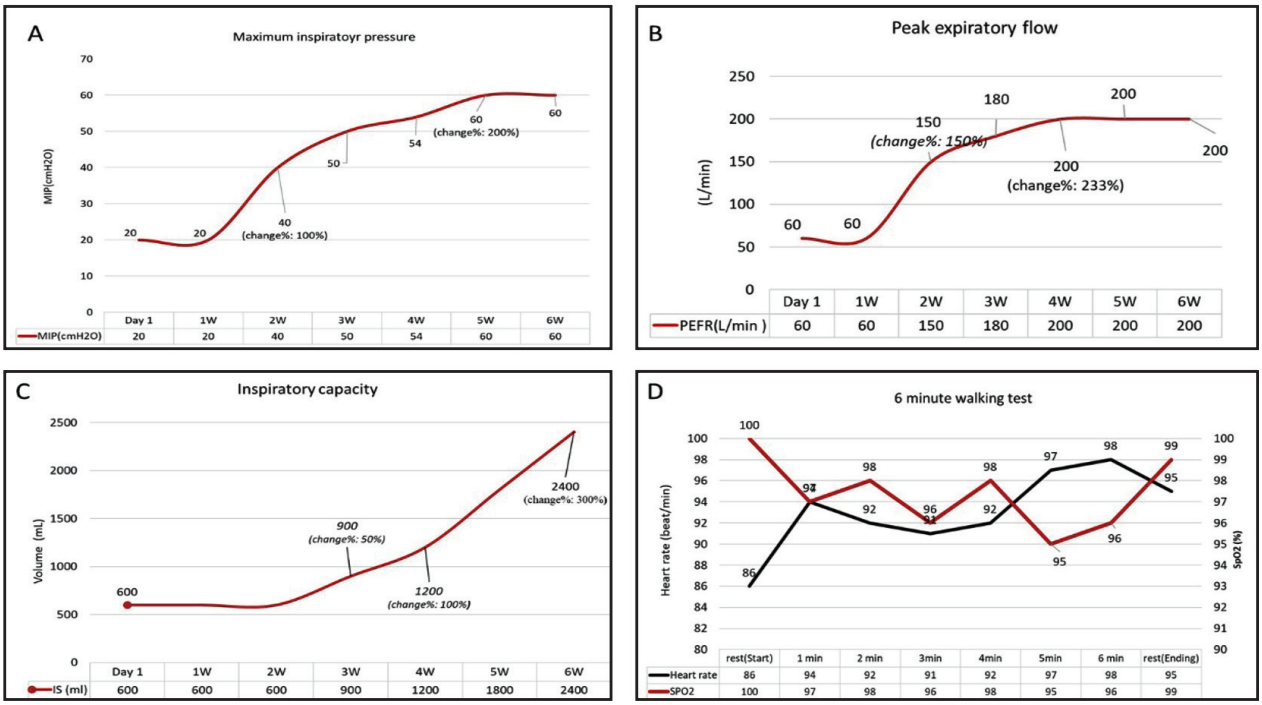

Fig. 2. Patient muscle strength recovery process during the course of pulmonary rehabilitation training. Panel A shows the maximum inspiratory pressure, which had 100% improvement at week 2 and 200% at week 5. Panel B shows improvement in peak expiratory flow, with a 233% change at week 4. Panel C shows the trend of inspiratory capacity, which had 100% change at week 4 and 300% change at week 6. MIP: maximum inspiratory pressure; IS: incentive spirometer; PEFR: peak expiratory flow rate.

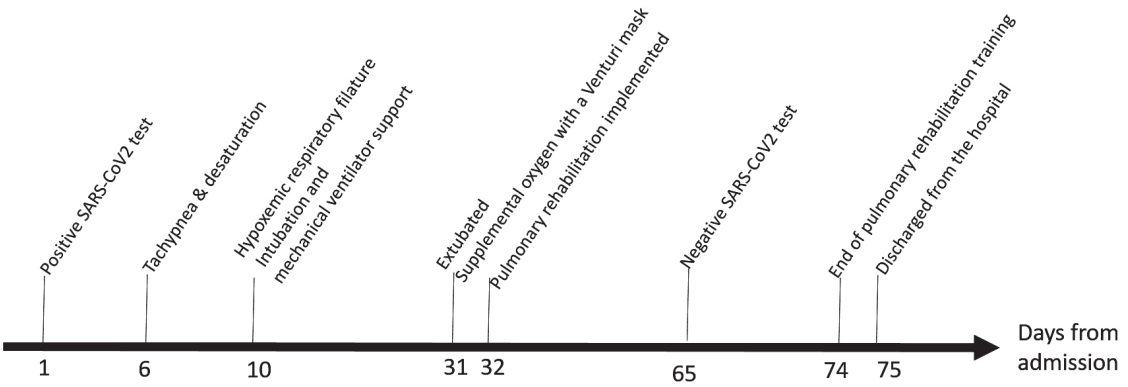

Fig. 3. Timeline of patient disease progression and pulmonary rehabilitation intervention.

demic [10-11]. However, systemic reviews and meta-analyses in 2022 have shown the benefit of pulmonary rehabilitation in patients with COVID-19. Fugazzaro *et al*. found that pulmonary rehabilitation in patients with post-acute COVID-19 at 4 to 12 weeks improves the level of dyspnea and anxiety, muscle strength, mobilization, and quality of life [12]. Yulin *et al*. reported in a systemic review that pulmonary rehabilitation should be considered, and initi-

ated within the first 30 days [13]. A randomized trial conducted with elderly patients with COVID-19 and normal pulmonary function found significant improvement in respiratory function, quality of life, and symptoms of anxiety [14].

Our patient developed ICU-acquired weakness, which was defined by critical illness polyneuropathy and critical illness myopathy, due to the use of neuromuscular blockers and being bed-ridden during MV. Pulmonary rehabilitation in patients with ICU-acquired weakness shortens the recovery time from general muscle weakness, muscle atrophy, and deconditioning [15-16]. Early implementation of a 6-week pulmonary rehabilitation program facilitated the recovery of both respiratory muscles and general muscle strength in our patient. To prevent medical staff from being infected with SARS-CoV-2 when the patient tested positive, everyone entering the negative pressure room was required to wear personal protective equipment. None of our team members were infected with SARS-CoV-2.

Breathing exercises improved the patient's symptoms of dynamic hyperinflation and dyspnea. This patient gradually developed pulmonary fibrosis and decreased vital capacity, and dyspnea on exertion. Breathing control prevented alveolar and airway collapse, resulting in minimized air trapping and improved oxygenation [8]. Therefore, we used diaphragmatic breathing and purse-lip breathing to prolong expiratory time. We observed that the patient had reduced dyspnea, lowered respiratory frequency, and increased SpO_2 while performing aerobic exercise, incentive spirometry training, and inspiratory muscle training with breathing control.

Incentive spirometry is usually prescribed for postoperative patients for lung expansion to treat or prevent atelectasis. The purpose of the therapy was to increase total lung capacity by deepening inspiration [10]. Since the chest X-ray of our patient revealed atelectasis at the time of extubation, we implemented spirometry training, and the X-ray showed resolved atelectasis by the end of the 6-week course. The inspiratory capacity measured during training improved from 600 mL to 1800 mL. The patient observed his own improvement using this visual feedback tool, which might motivate the patient to train himself more often when contained in an isolated negative-pressure room.

Previous studies have shown that aerobic exercise training improves exercise capacity, cardiopulmonary function, and immunity in critically ill patients [17]. For example, Bailey tried to train ventilated patients to sit at bedside, then move to a chair, and walk with a walker under assistance [18]. After training, 69% of patients could walk more than 30 meters without complications at the time of discharge from the ICU. Mohamed addressed the benefits of increasing aerobic capacity in terms of short-term and long-term improvements in the function of the immune and respiratory systems, particularly those specific to COVID-19 infections [19]. Our patient had dyspnea during active bedside sitting transfer on the first day, and was unable to perform a 6-minute walking test. However, he was able to walk 50 m during a 6-minute walking test after completion of the 6-week rehabilitation program. In addition, the patient was able to perform a walking test with a SpO_2 of 95%-100% without supplemental oxygen. The test was performed 1 day before being discharged, and his X-ray showed a normal lung field. The saturation levels indicated an intact oxygenation status for the patient post-COVID infection.

A minimum improvement of 30 meters in the 6-minute walking distance is considered significant for adult patients with COPD after receiving pulmonary rehabilitation training [20]. However, there is limited data to support a minimum improvement distance for patients with COVID infection.

In conclusion, we have reported the case of a critically ill patient with COVID-19 who benefited from early intervention with a 6-week pulmonary rehabilitation program, initiated from the second day of extubation. By the end of the training, he had fully recovered his respiratory muscle strength, peak inspiratory flow, lung volume, and general muscle strength. The medical staff were required to wear personal protective equipment, and none of the staff was infected with the novel coronavirus. We recommend early intervention with pulmonary rehabilitation in patients with COVID-19 and ARDS to hasten the recovery of pulmonary function and exercise capacity.

References

1. Ong KC, Ng AW, Lee LS, *et al*. Pulmonary function and exercise capacity in survivors of severe acute respiratory syndrome. Eur Respir J 2004; 24: 436-442.
2. Polak SB, Van Gool IC, Cohen D, *et al*. A systematic review of pathological findings in COVID-19: a pathophysiological timeline and possible mechanisms of disease progression. Mod Pathol 2020; 33: 1-11.
3. Zhao W, Zhong Z, Xie X, *et al*. Relation between chest CT findings and clinical conditions of coronavirus disease (COVID-19) pneumonia: a multicenter study. Am J Roentgenol 2020; 214: 1072-1077.
4. Tian S, Hu W, Niu L, *et al*. Pulmonary pathology of early-phase 2019 novel coronavirus (COVID-19) pneumonia in two patients with lung cancer. J Thorac Oncol 2020; 15: 700-704.
5. Hui DS, Joynt GM, Wong KT, *et al*. Impact of severe acute respiratory syndrome (SARS) on pulmonary function, functional capacity and quality of life in a cohort of survivors. Thorax 2005; 60: 401-409.
6. Ng CK, Chan JW, Kwan TL, *et al*. Six month radiological and physiological outcomes in severe acute respiratory syndrome (SARS) survivors. Thorax 2004; 59: 889-891.
7. Chinese Association of Rehabilitation Medicine; Respiratory Rehabilitation Committee of Chinese Association of Rehabilitation Medicine; Cardiopulmonary Rehabilitation Group of Chinese Society of Physical Medicine and Rehabilitation. Zhonghua Jie He He Hu Xi Za Zhi 2020; 43: 308-314.
8. Swigris JJ, Brown KK, Make BJ, *et al*. Pulmonary rehabilitation in idiopathic pulmonary fibrosis: a call for continued investigation. Respir Med 2008; 102: 1675-1680.
9. van Ranst D, Stoop WA, Meijer JW, *et al*. Reduction of exacerbation frequency in patients with COPD after participation in a comprehensive pulmonary rehabilitation program. Int J Chron Obstruct Pulmon Dis 2014; 9: 1059-1067.
10. Zhao HM, Xie YX, Wang C. Recommendations for respiratory rehabilitation in adults with COVID-19. Chin Med J 2020; 10: 1097/CM9.0000000000000848.
11. Lazzeri M, Lanza A, Bellini R, *et al*. Respiratory physiotherapy in patients with COVID-19 infection in acute setting: a Position Paper of the Italian Association of Respiratory Physiotherapists (ARIR). Monaldi Arch Chest Dis 2020; 90: 10.4081/monaldi.2020.1285.
12. Fugazzaro S, Contri A, Esseroukh O, *et al*. Rehabilitation interventions for post-acute covid-19 syndrome: a systematic review. J Environ Res Public Health 2022; 19: 5185.
13. Yelin D, Moschopoulos CD, Margalit I, *et al*. ESCMID rapid guidelines for assessment and management of long COVID. Clin Microbiol Infect 2022; 28: 955-972.
14. Liu K, Zhang W, Yang Y, *et al*. Respiratory rehabilitation in elderly patients with COVID-19: a randomized controlled study. Complement Ther Clin Pract 2020; 39: 101166.
15. Hermans G, Van den Berghe G. Clinical review: intensive care unit acquired weakness. Crit Care 2015; 19: 274.
16. Zorowitz RD. ICU-acquired weakness: a rehabilitation perspective of diagnosis, treatment, and functional management. Chest 2016; 150: 966-971.
17. Anekwe DE, Biswas S, Bussières A, *et al*. Early

rehabilitation reduces the likelihood of developing intensive care unit-acquired weakness: a systematic review and meta-analysis. Physiotherapy 2020; 107:1-10.

18. Bailey P, Thomsen GE, Spuhler VJ, *et al*. Early activity is feasible and safe in respiratory failure patients. Crit Care Med 2007; 35: 139-45.
19. Mohamed AA, Alawna M. Role of increasing the aerobic capacity on improving the function of immune and respiratory systems in patients with coronavirus (COVID-19): a review. Diabetes Metab Syndr 2020; 14: 489-496.
20. Holland AE, Spruit MA, Troosters T, *et al*. An official European Respiratory Society/American Thoracic Society technical standard: field walking tests in chronic respiratory disease. Eur Respir J. 2014; 44: 1428-46.
21. Gibbons WJ, Fruchter N, Sloan S, Levy RD. Reference values for a multiple repetition 6-minute walk test in healthy adults older than 20 years. J Cardiopulm Rehabil 2001; 21 (2): 87-93.

Hypercapnic Obstructive Sleep Apnea Caused by Straight Back Syndrome with Innominate Artery Compression of the Trachea

Ming-Sheng Shen[1,2], Yi-Chang Lin[3], Yu-Cheng Wu[4], Chia-Hsin Liu[2]

Straight back syndrome, a congenital deformity involving a loss of normal thoracic spinal curvature, can cause variable degrees of mediastinal compression, and is an easily overlooked cause of airway obstruction in adults. Herein, we report a case of acute hypercapnic respiratory failure in a 54-year-old man who was incidentally diagnosed with hypercapnic obstructive sleep apnea during hospitalization. Subsequent computed tomography and bronchoscopy of the thorax revealed severe tracheal stenosis caused by innominate artery compression of the trachea and straight curvature of the thoracic spine with a reduced anteroposterior diameter of the thoracic cavity. The patient underwent reconstruction of the innominate artery, and his symptoms were subsequently alleviated. These findings highlight the importance of thorough and timely diagnostic evaluations in order to efficiently recognize and treat straight back syndrome, thereby improving patient outcomes. ***(Thorac Med 2023; 38: 338-343)***

Key words: OSAS, hypercapnia, straight back syndrome (SBS), innominate artery compression, tracheal stenosis

Introduction

Hypercapnic obstructive sleep apnea (OSA) is characterized by hypercapnia during wakefulness in patients with OSA syndrome (OSAS) [1]. Many of these patients also have obesity, daytime hypercapnia, and sleep-disordered breathing, known collectively as obesity hypoventilation syndrome [2]. On rare occasions, airway compression caused by great vessel and spinal deformities could result in OSA with hypercapnia. Herein, we report an unusual case of

[1]Division of Pulmonary and Critical Care Medicine, Department of Internal Medicine, Taichung Armed-Forces General Hospital, Taichung, Taiwan. [2]Division of Pulmonary and Critical Care Medicine, Department of Internal Medicine, Tri-Service General Hospital, National Defense Medical Center, Taipei, Taiwan. [3]Division of Cardiovascular Surgery, Department of Surgery, Tri-Service General Hospital, National Defense Medical Center, Taipei, Taiwan. [4]Department of Radiology, Tri-Service General Hospital, National Defense Medical Center, Taipei, Taiwan.
Address reprint requests to: Dr. Chia-Hsin Liu, Division of Pulmonary and Critical Care Medicine, Department of Internal Medicine, Tri-Service General Hospital, National Defense Medical Center, 325, Cheng-Gung Road, Nei-Hu Dist. 114, Taipei, Taiwan.

tracheal compression caused by straight back syndrome (SBS) and innominate artery compression, with hypercapnic OSA complicated by acute respiratory failure secondary to bacterial infection.

Case Description

A 54-year-old man, a non-smoker, presented to the emergency department with a 3-day history of fever, productive cough, runny nose, and diarrhea. He had a history of idiopathic arterial hypertension (WHO functional class I), which had been managed with sildenafil by the outpatient department for 5 years. The patient's history also included chronic hypercapnia and non-pulsatile tingling headaches at the bilateral temporal region in the mornings, often accompanied by sensations of facial swelling. On physical examination, his vital signs were as follows: temperature, 38.8°C; heart rate, 123 beats/min; respiratory rate, 18 breaths/min; and blood pressure, 115/66 mmHg. The lung examination revealed loss of thoracic kyphosis, and chest auscultation revealed bilateral crackles in the lower lung fields without stridor or wheezes. Laboratory studies showed: a white cell count of 16.85 x 103/μl with 90.9% neutrophils, 4.0% lymphocytes, and 4.7% monocytes; hemoglobin, 14.1 g/dl; platelets, 126 x 103/μl; C-reactive protein, 25.19 mg/L; and D-dimer, 0.27 mg/L. Chest radiography revealed bilateral increased infiltrates in the lower lung fields. During hospitalization, a once-daily dose of 500 mg levofloxacin was prescribed as an empirical antibiotic treatment for bronchopneumonia. Nevertheless, acute on chronic hypercapnia (pH = 7.197, partial pressure of carbon dioxide [$PaCO_2$]: 101.9 mmHg, partial pressure of oxygen [PaO_2]: 84.7%, bicarbonate [HCO_3-]: 30.6 mmol/L, oxygen saturation [SaO_2]: 96.3%, and fraction of inspired oxygen [FiO_2]: 40%), and apnea with oxygen desaturation (SpO_2: 79-82%) were noted during sleep. Although the patient received non-invasive ventilation with bi-level positive airway pressure (BiPAP), there was only a partial correction of hypercapnia (pH = 7.24, $PaCO_2$: 95.7 mmHg, PaO_2: 97.0 %, HCO_3-: 40.1 mmol/L, SaO_2: 97.7, FiO_2: 40%), and the repetitive episodes of sleep apnea continued.

Upon further investigation, cervical radiography revealed a relatively straight curvature of the cervical spine (Fig. 1). Computed tomography (CT) of the chest showed that the innomi-

Fig. 1. Lateral neck radiograph revealing relatively straight curvature of the spine.

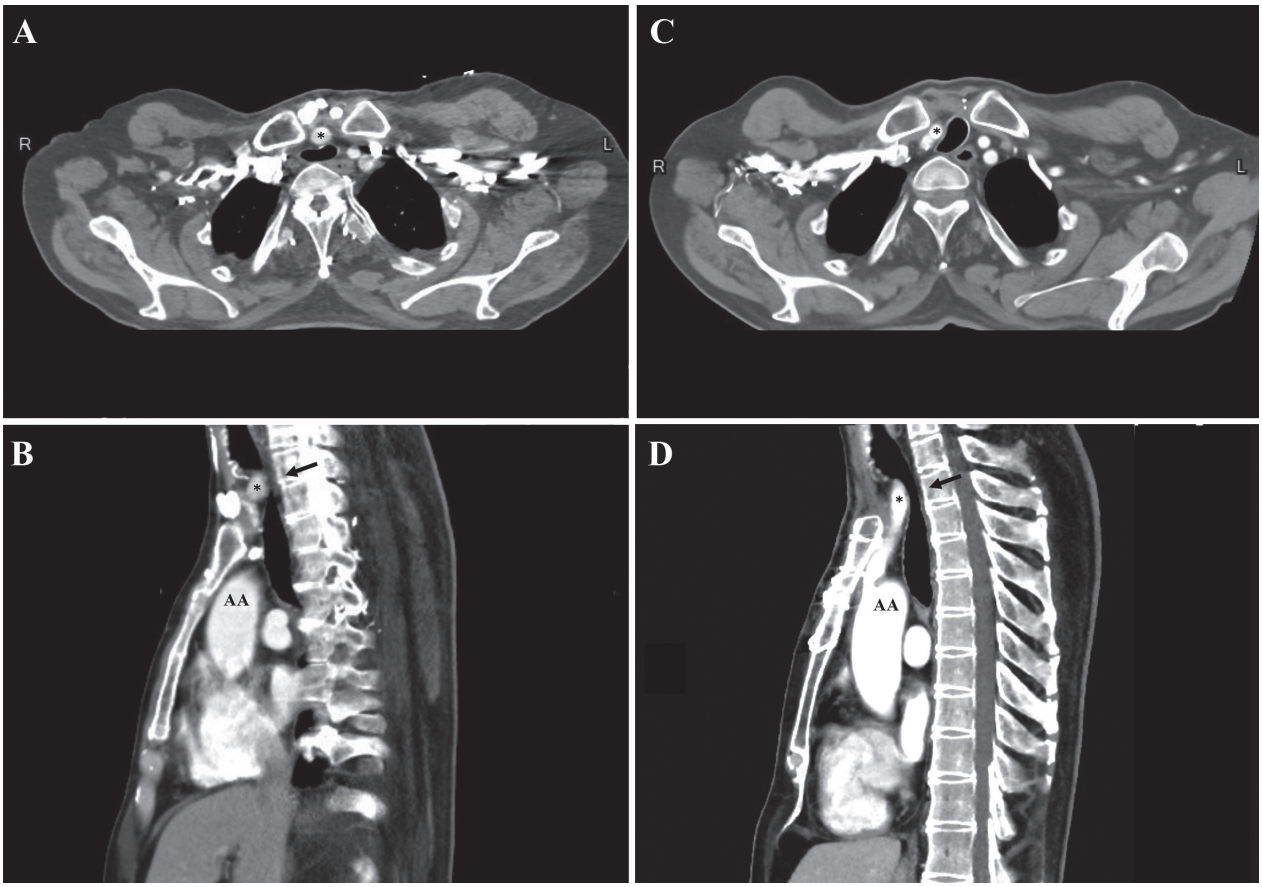

Fig. 2. Computed tomography scans before (A, B) and after (C, D) reconstruction: (A) preoperative axial view showing the innominate artery (star) located left of center and directly compressing the trachea, and a marked anteroposterior narrowing of the upper mediastinum; (B) preoperative sagittal view showing severe tracheal stenosis due to compression between the innominate artery (star) and the straight thoracic spine (black arrow); (C) postoperative axial view showing the reconstructed innominate artery (star) positioned further to the right and reduced tracheal compression; (D) postoperative sagittal view showing increased tracheal patency. AA = aortic arch.

nate artery was located further to the left with direct tracheal compression (Fig. 2A), while the tracheal lumen was further compromised due to the lack of normal dorsal curvature of the thoracic vertebral spine (Fig. 2B). Bronchoscopy revealed pulsatile anterior compression of the trachea, with severe luminal narrowing of the right anterior wall of the proximal trachea (Fig. 3). In addition, the result of a sputum test for Chlamydia pneumonia antigen was positive. We therefore diagnosed airway obstruction caused by SBS and innominate artery compression, with hypercapnic OSA complicated by acute

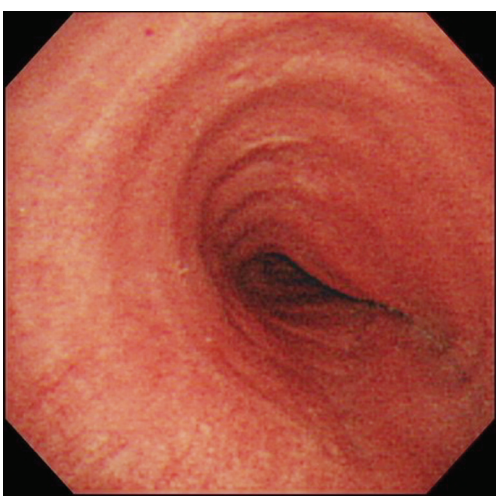

Fig. 3. Bronchoscopy showing extrinsic compression of the distal trachea, particularly on the right side.

hypercapnic respiratory failure secondary to Chlamydia pneumoniae infection.

The patient underwent a surgical cutdown and reconstruction of the innominate artery with a 10 mm InterGard Woven graft (InterVascular, La Ciotat, France) that was connected to the ascending aorta. Follow-up chest CT scans revealed that the reconstructed innominate artery was situated further to the right, resulting in reduced tracheal compression (Fig. 2C) and increased tracheal patency (Fig. 2D). The patient's hypercapnia was ameliorated (pH = 7.385, $PaCO_2$: 51.0 mmHg, PaO_2: 141.4 mmHg, HCO_3-: 30.8 mmol/L, FiO_2: 35%), and there were no further episodes of sleep apnea under nocturnal BiPAP ventilation. Furthermore, the patient's morning headaches and facial swelling sensations improved, and he was discharged uneventfully.

Discussion

Upper airway obstruction during sleep can be caused by several different conditions, among which OSAS is the most frequent [3]. The mechanism by which the upper airway collapses in patients with OSAS is multifactorial, and involves obesity, craniofacial changes, alterations in upper airway muscle function, pharyngeal neuropathy, and fluid shifts toward the neck [3]. Occasionally, extrinsic tracheal compression caused by goiters [4] or abnormalities in the innominate artery [5-7], aortic arch [8], chest wall structure [5], or spinal anatomy [5, 7-9] can cause respiratory obstruction and subsequent OSAS [10].

SBS is a skeletal deformity characterized by a lack of dorsal curvature of the upper thoracic spine, resulting in a reduced anteroposterior diameter of the thorax and subsequent compression of mediastinal structures [11]. Among various structures in the mediastinum, the heart and trachea are the 2 most frequently affected [8]; as a result, patients generally present with various conditions related to heart and tracheal compression, such as murmurs, mitral valve prolapse, pulmonary hypertension, exertional dyspnea, recurrent pulmonary infection, and respiratory failure [5, 12, 13]. Furthermore, nonspecific symptoms, such as fatigue, sleepiness, subtle changes in mental status, and headaches, have been reported in patients with hypercapnic OSA [1]. In the present case, repetitive apnea and worsening hypercapnia during sleep were due to severe tracheal stenosis caused by SBS with innominate artery compression, and the patient's condition was further compromised by the suppression of upper airway muscle tone during sleep and a concurrent lung infection.

Diagnosis of SBS is based on lateral chest radiographs drawing a horizontal line from the anterior aspect of T8 to a vertical line connecting T4 and T12; if the length of the horizontal line is less than 1.2 cm, SBS is confirmed [14]. Although the absence of thoracic spine kyphosis increases suspicion of a diagnosis of SBS, this condition is easily overlooked on physical examination, thereby leading to misdiagnosis. CT imaging with sagittal reconstruction quickly establishes an SBS diagnosis, and is a useful tool for evaluating the compression of mediastinal structures and the degree of tracheal obstruction. Furthermore, bronchoscopy may be used to evaluate SBS-associated tracheomalacia and facilitate treatment with stent implantation [6, 15].

Most patients with SBS have mild symptoms that manifest as simple cardiac or respiratory discomfort, which can be relieved with basic supportive measures. Tracheal stent implantation is a conservative treatment strategy

that can improve symptoms in selected cases. Nevertheless, stent insertion is usually not appropriate for long-term treatment [15], because life-threatening complications such as tracheo-innominate fistulas with fatal hemorrhaging secondary to tracheal compression between the innominate artery and tracheal stent have been reported [9]. Surgical intervention for SBS with airway obstruction is considered only if conservative treatment fails. The goals of surgical correction are to increase mediastinal space, restore the tracheal lumen, and improve tracheal stability. Techniques to widen the space between the spine and anterior chest wall include replacement and reconstruction of the central vessels, resection of the posterior border of the manubrium sterni, sternoplasty, and correction of any associated pectus excavatum [7]. Recently, surgical reconstruction of the anterior chest wall with digitally designed materials has enabled fundamental treatment of SBS by effectively increasing the accommodation space of the mediastinum and reducing pressure on vital structures [8]. Nevertheless, even after successful correction of mediastinal compression, tracheomalacia may persist and require further intervention [5]. Secondary treatments for tracheomalacia include resection and reconstruction of the malacic segment and posterior wall tracheal splinting [5]. In our case, the patient underwent innominate artery reconstruction with significant improvements in episodes of sleep apnea and daytime headaches; however, he continued to use nocturnal BiPAP for tracheomalacia with stable hypercapnia.

Conclusion

This case report highlights the need for increased awareness of SBS with innominate artery compression of the trachea as a differential diagnosis for patients with OSAS and straightening of the thoracic spine. Early diagnosis and prompt treatment of SBS are crucial to improve patient outcomes and minimize the morbidity and mortality associated with delayed diagnoses.

References

1. Zwillich C, Welsh CH. Hypercapnic obstructive sleep apnea: an underappreciated marker of severity. Chest 2007;132(6): 1729-30.
2. Masa JF, Pepin JL, Borel JC, *et al*. Obesity hypoventilation syndrome. Eur Respir Rev 2019;28(151): 180097.
3. Levy P, Kohler M, McNicholas, *et al*. Obstructive sleep apnoea syndrome. Nat Rev Dis Primers 2015;1: 15015.
4. Stang MT, Armstrong MJ, Ogilvie JB, *et al*. Positional dyspnea and tracheal compression as indications for goiter resection. Arch Surg 2012;147(7): 621-6.
5. Grillo HC, Wright CD, Dartevelle PG, *et al*. Tracheal compression caused by straight back syndrome, chest wall deformity, and anterior spinal displacement: techniques for relief. Ann Thorac Surg 2005; 80(6): 2057-62.
6. Liu CH, Huang WS, Wang HH, *et al*. Airway obstruction due to tracheomalacia caused by innominate artery compression and a kyphotic cervical spine. Ann Thorac Surg 2015; 99(2): 685-7.
7. Schmid S, Schibilsky D, Kalbhenn J, *et al*. Reconstruction of the mediastinum and tracheopexy for tracheomalacia in straight back syndrome. Ann Thorac Surg 2021;112(1): 41-e44.
8. Liu Y, Wang W, Long W, *et al*. Chest wall reconstruction with digitally designed materials for straight back syndrome with tracheal stenosis: a case report. Ann Transl Med 2021;9(16): 1357.
9. Beck KS, Lee BY, Kim HS, *et al*. Extrinsic tracheal compression caused by scoliosis of the thoracic spine and chest wall deformity: a case report. J Korean Soc Radiol 2014; 70(5): 343-346.
10. Muzumdar H, Nandalike K, Bent J, *et al*. Obstructive sleep apnea due to extrathoracic tracheomalacia. J Clin

Sleep Med 2013; 9(2): 163-4.
11. Rawlings MS. The "straight back" syndrome, a new cause of pseudoheart disease. Am J Cardiol 1960; 5: 333-8.
12. Deleon AC Jr, Perloff JK, Twigg H, *et al*. The straight back syndrome: clinical cardiovascular manifestations. Circulation 1965; 32: 193-203.
13. Leinbach RC, Harthorne JW, Dinsmore RE. Straight back syndrome with pulmonary venous obstruction. Am J Cardiol 1968; 21(4): 588-92.
14. Davies MK, Mackintosh P, Cayton RM, *et al*. The straight back syndrome. Q J Med 1980;49(196): 443-60.
15. Wood DE, Liu YH, Vallieres E, *et al*. Airway stenting for malignant and benign tracheobronchial stenosis. Ann Thorac Surg 2003; 76(1): 167-174.

Giant Cell Tumor of Bone with Lung Metastasis: A Case Report

Tien-Hsin Jeng[1], Yi-Han Hsiao[2,3,4]

Giant cell tumor of bone is a benign bone tumor with locally aggressive behavior that is usually curative after surgery, and rarely presents with distant metastasis. Herein, we presented a case of lung metastasis of giant cell tumor of the right phalanx, which had undergone surgical resection 18 months prior to presentation. The lung metastasis was treated by denosumab injection. Although giant cell tumor of bone has been considered a benign disease, our case showed the potential of both distant metastasis and the use of denosumab as a treatment option for patients with lung metastasis of giant cell tumor. ***(Thorac Med 2023; 38: 344-350)***

Key words: giant cell tumor of bone, lung metastasis, denosumab

Introduction

Giant cell tumor of bone (GCTB) is a benign neoplasm with locally aggressive and metastatic features that represents 5% of all primary bone tumors and 20% of all benign bone tumors. It is most commonly found in young adults between the ages of 20 and 40 years [1,2,3]. GCTB usually arises from the metaphysis and affects the epiphysis of long bones, with common locations including the long bones of the extremities, and the sacrum, pelvis, and spine [1]. According to a Swedish registry, the incidence of GCTB in the general population is 1.3 per million persons per year, although the incidence may be relatively higher in Asian populations [3]. Lung metastasis of GCTB is relatively rare, occurring in around 3% of all patients with GCTB and more commonly in the setting of a recurrence, and usually 2-3 years after the initial primary GCTB [4]. The most established risk factor for GCTB lung metastasis is the precedence or concurrence of local recurrence [5]. Other risk factors that have been mentioned in different studies include age at the time of diagnosis (younger, as opposed to

[1]Department of Chest Medicine, Taipei Veterans General Hospital, Taipei, Taiwan. [2]Department of Physiology, School of Medicine, National Yang Ming Chiao Tung University, Taipei, Taiwan. [3]Faculty of Medicine, School of Medicine, National Yang Ming Chiao Tung University, Taipei, Taiwan. [4]Division of General Chest Medicine, Department of Chest Medicine, Taipei Veterans General Hospital, Taipei, Taiwan.
Address reprint requests to: Dr. Yi-Han Hsiao, Division of General Chest Medicine, Department of Chest Medicine, Taipei Veterans General Hospital, 201 Shih-Pai Road, Section 2, Taipei 11217, Taiwan.

older), location of the primary tumor (axial, as opposed to appendicular location; distal radial bone if appendicular), and Campanacci stage 3 disease [4,6,7]. However, there is a lack of consensus among studies; thus, currently, the only established risk factor for lung metastasis is precedence or concurrence of local recurrence.

Case Presentation

A 49-year-old Asian woman who was otherwise healthy and without known systemic disease presented to our outpatient clinic with complaints of a dry cough and exertional dyspnea for 1 month. The patient had no fever, sputum production, hemoptysis, chest pain, cold sweating, decreased appetite, or body weight loss. Physical examinations were unremarkable. Chest x-ray (CXR) showed a giant right upper lung mass with a clear border and homogenous density (Figure 1A). Chest computed tomography (CT) revealed a solitary 8.8 x 7.6 cm heterogeneously enhancing mass at the right upper lobe of the lung, with direct attachment to the trachea, superior vena cava, and right pulmonary artery (Figure 1B). Serum levels of tumor markers, including carcinoembryonic antigen, β-human chorionic gonadotropin, and α-fetal protein, were within normal ranges. Real-time ultrasound-guided biopsy then was performed. The pathology report revealed that the specimen was composed of closely packed polyhedral cells with many giant cells dispersed among them. The tumor cells were positive for H3F3AG34W, SATB2, and p63, compatible with giant cell tumor (Figure 2). Further review of her medical and surgical history indicated she had had a giant cell tumor of the right index

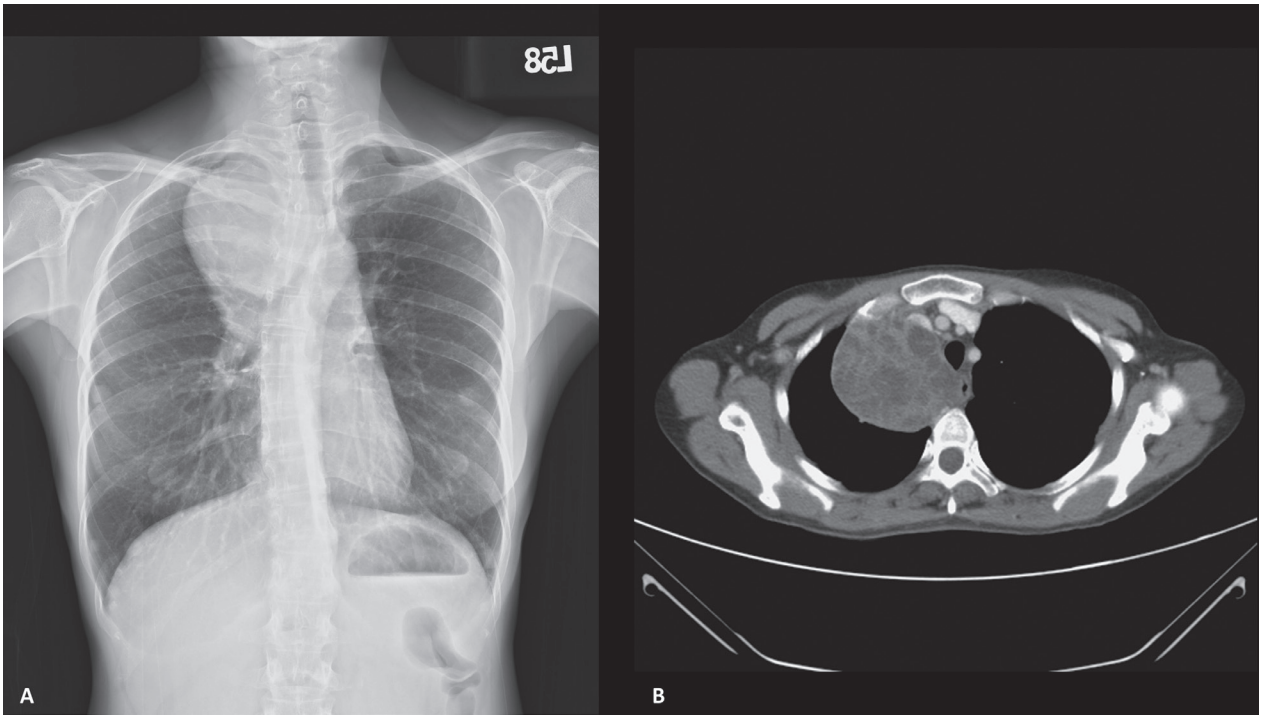

Fig. 1. Chest radiography (A) and chest computed tomography (B). Images show a mass lesion, measuring 8.8x6.7 cm, in the right upper lobe with direct attachment to the trachea, superior vena cava, and right pulmonary artery, using heterogeneous contrast enhancement.

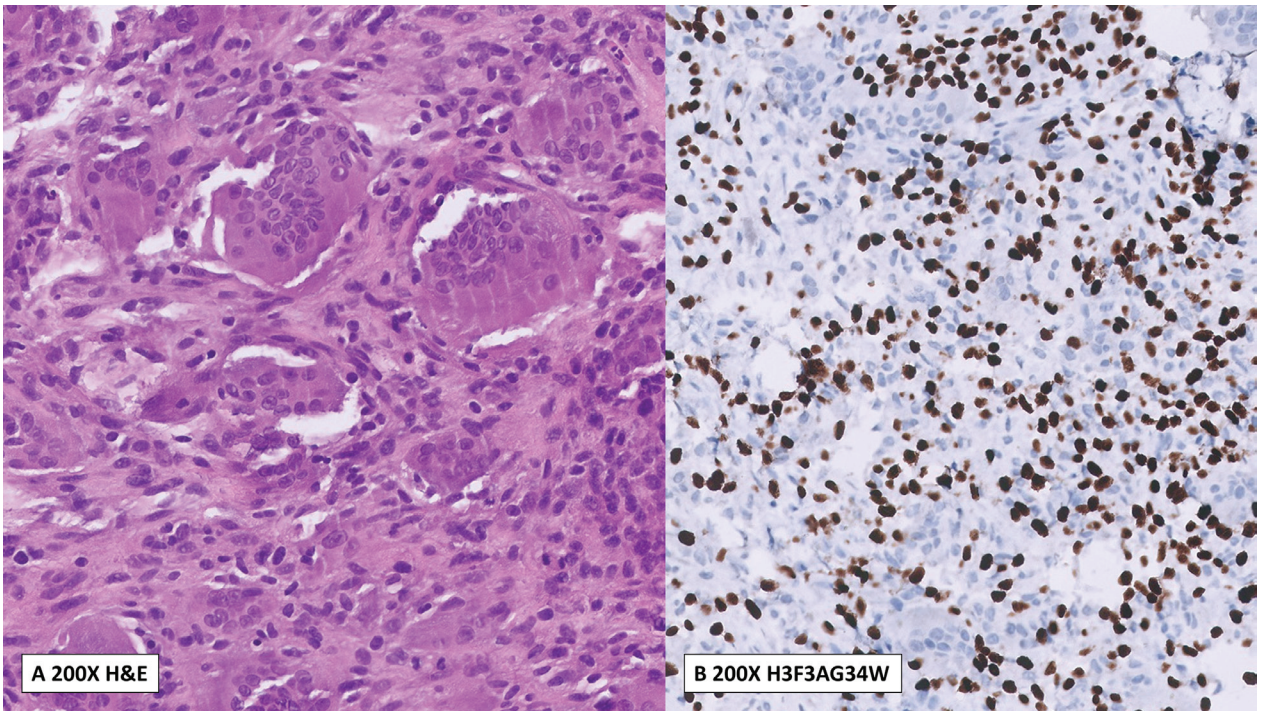

Fig. 2. Histology of lung tumor obtained by ultrasound-guided biopsy. (A) Closely packed polyhedral cells with many giant cells dispersed among them (hematoxylin and eosin, 200×). (B) The tumor cells were immunoreactive for H3F3AG34W (200×).

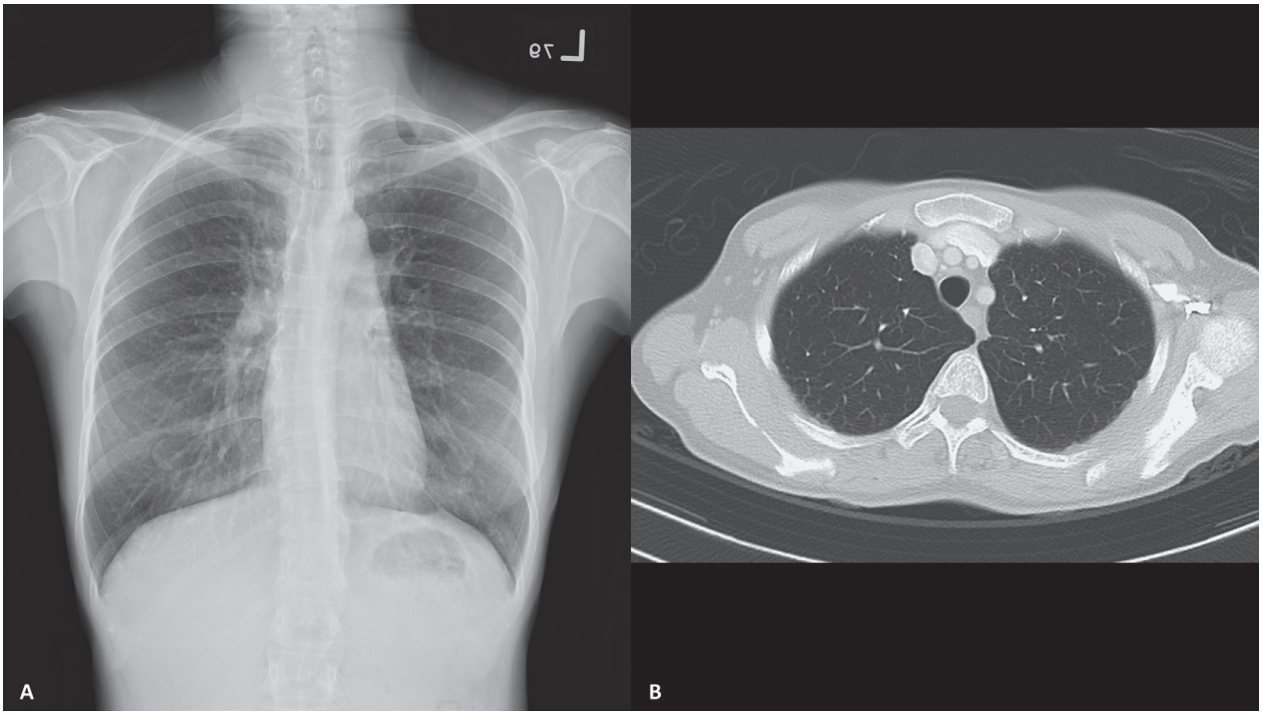

Fig. 3. Chest radiography (A) and chest computed tomography (B) at initial presentation of the primary GCTB. At that time, chest images showed no visible lung lesion.

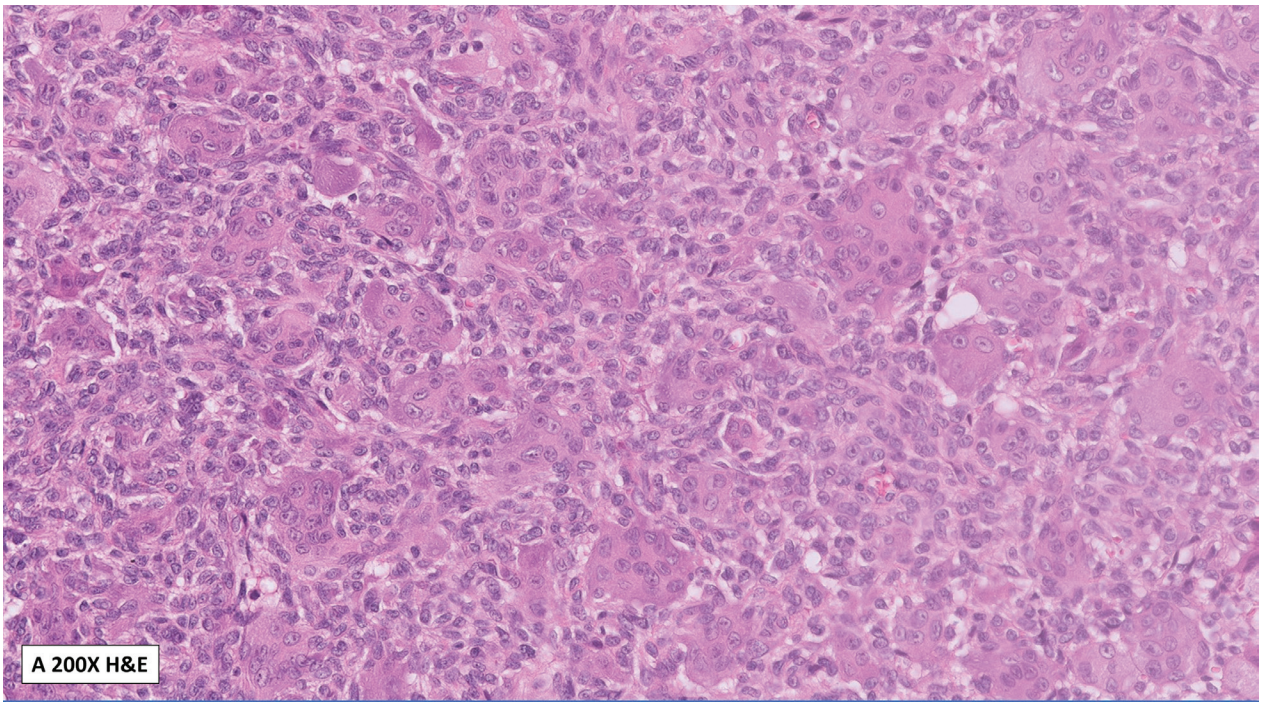

Fig. 4. Histology of the right phalanx specimen from surgical resection showed closely packed polyhedral cells with many giant cells dispersed among them (hematoxylin and eosin, 200×).

proximal pharynx and received tumor excision and bone grafting 18 months prior to this presentation. CXR and chest CT at that time showed no pulmonary nodule (Figure 3). The pathologist reviewed the bone tumor specimen and found that the lung and bone lesions shared similar histopathologic morphological features (Figure 4). Thus, a diagnosis of GCTB with lung metastasis was confirmed. After discussion with the patient about her treatment options, she received denosumab administration with 3 loading doses of 120 mg 7 days apart, followed by 1 dose every 4 weeks, and was closely followed up at our outpatient clinic. At 2 months after treatment, a decrease in tumor size was noted (Figure 5) and her symptoms had significantly improved. After 5 months of denosumab, a further decrease in tumor size was seen (Figure 6), and curative therapy with surgical tumor excision was planned.

Discussion

We reported the case of a patient with GCTB of the right phalanx in whom distant lung metastasis occurred 18 months after surgical resection, and was managed with regular denosumab injection followed by surgery.

Histologically, a GCTB is characterized by neoplastic mononuclear stromal cells with a monotonous appearance mixed with mononuclear histiocytic cells and osteoclast-like multinucleated giant cells with a benign spindle cell background. The mononuclear stromal cells, which are thought to constitute the neoplastic cells, are of osteoblastic origin. The mononuclear histiocytic cells (possible precursors of the giant cells) and multinucleated giant cells,

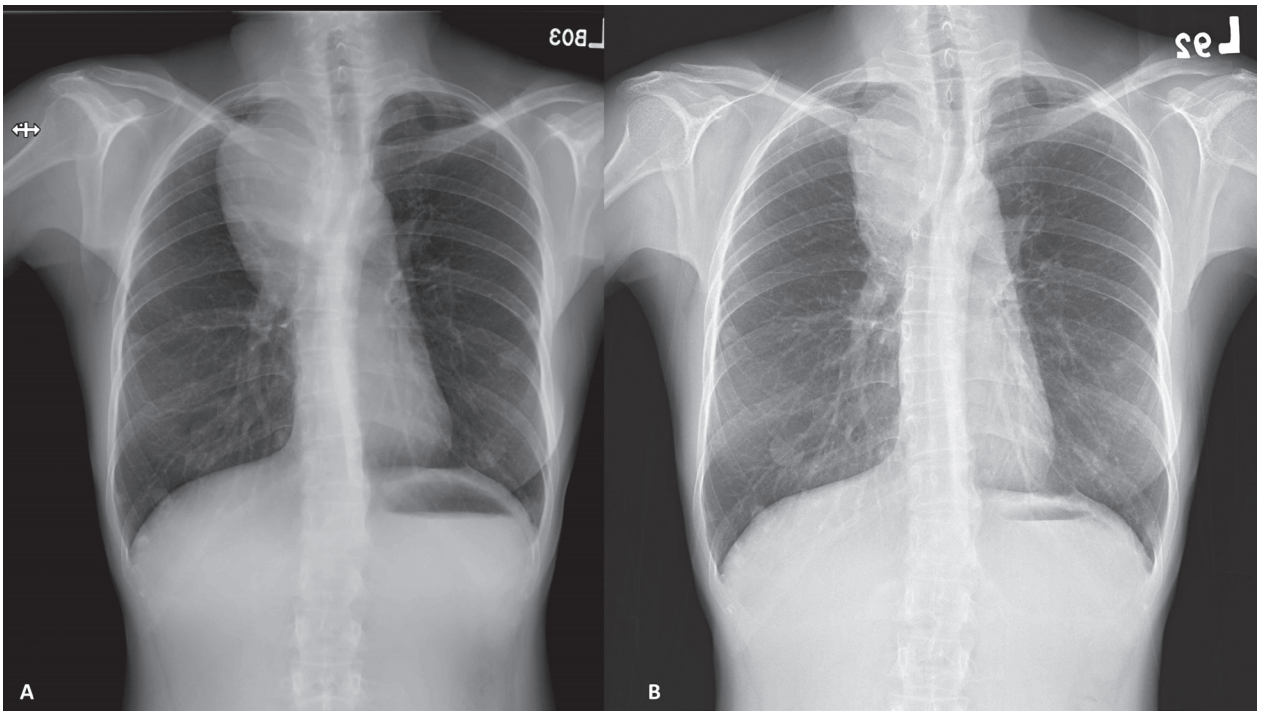

Fig. 5. A comparison of chest radiography before denosumab use (A) and 2 months after denosumab initiation (B). Images showed a decrease in the size of the right upper lobe lesion.

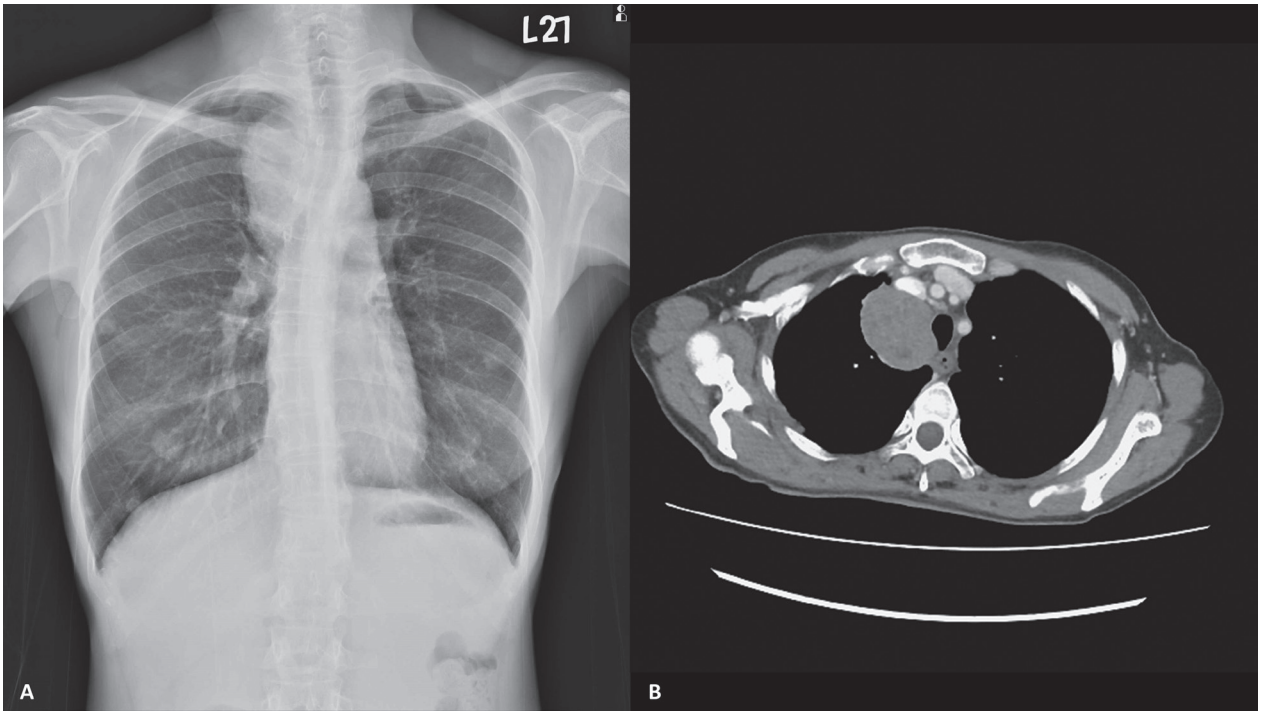

Fig. 6. Chest radiography (A) and chest computed tomography (B) after 5 months of denosumab treatment. Images showed a mass lesion, measuring 5.1 cm, decreased in size compared to the previous images.

in contrast, are thought to be recruited from peripheral blood and are non-neoplastic in nature [1]. Immunochemical stains will show positive to the special stain of H3F3AG34W for neoplastic stromal cells. The gene H3F3A encodes histone H3.3 and is essential in maintaining genome integrity. Mutation in the H3F3A gene, especially H3F3AG34W, is highly correlated to the formation of GCTB [8]. RANKL is highly expressed by the stromal cells within GCTB. It is believed that the osteoblast-like mononuclear stromal cells express RANKL, and thus stimulate the recruitment of osteoclastic cells, forming osteoclastic giant cells that consequently absorb host bone [9]. The high RANKL expression in GCTB suggests the treatment potential of RANKL inhibitors such as denosumab [10-11].

In terms of treatment, surgical resection is curative for the majority of primary GCTB, and is therefore the standard treatment. Thus, surgical resection of the pulmonary metastasis is a reasonable approach and has been suggested by some physicians [5]. However, this aggressive approach for pulmonary metastases may not always be necessary. According to a systematic review of 242 cases of metastatic GCTBs managed conservatively, with a mean follow-up of 6.9 years, 4.5% of the metastases regressed spontaneously, and 45% remained stable [12]. In a case series published by Tsukamoto *et al*., 22 patients with lung metastasis were initially managed with observation; of this group, 10 patients remained stable during the 3-year follow-up period, and 12 patients that experienced progression were successfully managed with surgical resection or denosumab injection [13]. Thus, observation is a reasonable first-line treatment option, especially for nodules smaller than 5 mm in size.

However, for nodules of 5 mm in size or above, the risk of progression is high; in the same case series by Tsukamoto, all 5 patients with nodules 5 mm or above in size experienced initial progression [14]. This highlights the importance of serial chest imaging (CXR or chest CT) every 6-12 months to follow up patients with GCTB. Another treatment option is denosumab with 3 loading doses of 120 mg 7 days apart followed by 1 dose every 4 weeks [15]. This option has shown promising results in 2 case series following patients with GCTBs with pulmonary metastasis: all 54 patients who received denosumab achieved tumor control [16-17]. However, the optimal treatment duration with denosumab is unknown, with concerns of tumor progression after denosumab discontinuation. Furthermore, adverse effects such as osteonecrosis of the jaw, atypical bone fracture, and peripheral neuropathy are also a concern. One needs to be reminded that current experience with denosumab treatment in patients with GCTB is still limited, and its long-term safety and relationship with malignancy transformation of GCTB needs to be monitored cautiously [11]. Other treatment options include bisphosphonate or cytotoxic chemotherapy, but its utility in treating GCTB has been limited in the era of denosumab [18]. Surgical resection of metastasis is recommended if the patient experiences complications with conservative treatment such as denosumab [18].

To summarize treatment options, a reasonable strategy for pulmonary metastasis is close monitoring first, followed by denosumab or surgical resection if there is disease progression after initial observation [18]. Further research is needed to determine the best treatment strategy and a long-term follow-up strategy for these patients, even though the prognosis of GCTB lung

metastasis is generally good.

In conclusion, this patient was found to have distant lung metastasis 18 months after resection of her giant cell tumor of the right proximal phalanx, which emphasizes the importance of close follow-up of resected giant cell tumor with chest imaging and the use of RANKL inhibitor treatment as an option in cases of GCTB with lung metastasis.

References

1. Sobti A, Agrawal P, Agarwala S, *et al*. Giant cell tumor of bone-an overview. Arch Bone Jt Surg 2016;4(1): 2-9.
2. Turcotte RE. Giant cell tumor of bone. Orthop Clin North Am 2006;37(1): 35-51.
3. Sung HW, Kuo DP, Shu WP, *et al*. Giant-cell tumor of bone: analysis of two hundred and eight cases in Chinese patients. J Bone Joint Surg Am 1982;64(5): 755-61.
4. Yang Y, Huang Z, Niu X, *et al*. Clinical characteristics and risk factors analysis of lung metastasis from benign giant cell tumor of bone. J Bone Oncol 2017;7: 23-8.
5. Muheremu A, Niu X. Pulmonary metastasis of giant cell tumor of bones. World J Surg Oncol 2014;12(1): 1-9.
6. Chan CM, Adler Z, Reith JD, *et al*. Risk factors for pulmonary metastases from giant cell tumor of bone. JBJS Am 2015;97(5): 420-28.
7. Wang J, Liu X, Yang Y, *et al*. Pulmonary metastasis of giant cell tumour: a retrospective study of three hundred and ten cases. Int Orthop 2021;45(3): 769-78.
8. Kervarrec T, Collin C, Larousserie, *et al*. H3F3 mutation status of giant cell tumors of the bone, chondroblastomas and their mimics: a combined high resolution melting and pyrosequencing approach. Mod Pathol 2017; 30(3): 393-406.
9. Huang L, Xu J, Wood DJ, *et al*. Gene expression of osteoprotegerin ligand, osteoprotegerin, and receptor activator of NF-κB in giant cell tumor of bone: possible involvement in tumor cell-induced osteoclast-like cell formation. Am J Pathol 2000;156(3): 761-67.
10. Branstetter DG, Nelson SD, Manivel JC, *et al*. Denosumab induces tumor reduction and bone formation in patients with giant-cell tumor of bone. Clin Cancer Res 2012;18(16): 4415-24.
11. Li H, Gao J, Gao Y, *et al*. Denosumab in giant cell tumor of bone: current status and pitfalls. Front Oncol 2020;10: 580605.
12. Itkin B, Straminsky S, De Ronato G, *et al*. Prognosis of metastatic giant cell tumor of bone in the pre-denosumab era. A systematic review and a meta-analysis. Jpn J Clin Oncol 2018;48(7): 640-52.
13. Tsukamoto S, Ciani G, Mavrogenis AF, *et al*. Outcome of lung metastases due to bone giant cell tumor initially managed with observation. J Orthop Surg Res 2020; 15(1): 1-11.
14. Network, NCCN. Bone cancer (version 2.2022) [June 25, 2022]; Available from: https://www.nccn.org/professionals/physician_gls/pdf/bone.pdf.
15. Thomas D, Henshaw R, Skubitz K, *et al*. Denosumab in patients with giant-cell tumour of bone: an open-label, phase 2 study. Lancet Oncol 2010;11(3): 275-80.
16. Palmerini E, Chawla NS, Ferrari S, *et al*. Denosumab in advanced/unresectable giant-cell tumour of bone (GCTB): for how long? Eur J Cancer 2017; 76: 118-24.
17. Engellau J, Seeger L, Grimer R, *et al*. Assessment of denosumab treatment effects and imaging response in patients with giant cell tumor of bone. World J Surg Oncol 2018; 16(1): 1-9.
18. Tsukamoto, S., Mavrogenis AF, Kido A, *et al*. Current concepts in the treatment of giant cell tumors of bone. Cancers 2021;13(15): 3647.

Amiodarone Pulmonary Toxicity Mimicking Metastatic Lesions: A Case Report

Rou-Jun Chou[1], Ching-Yao Yang[1]

Amiodarone is a widely-used antiarrhythmic agent. One of the most serious and well-discussed adverse effects of amiodarone is pulmonary toxicity, which can lead to severe pulmonary fibrosis if not diagnosed and managed promptly. Here, we reported a patient with multiple pulmonary nodules over bilateral lower lungs, which was initially suspected to be malignancy. The lung biopsy confirmed the diagnosis of amiodarone pulmonary toxicity. The lung nodules were resolved after amiodarone discontinuation and corticosteroid treatment. ***(Thorac Med 2023; 38: 351-356)***

Key words: Amiodarone, drug-induced pulmonary toxicity, pulmonary nodule

Introduction

Amiodarone is a commonly-used antiarrhythmic agent, which is an iodine-containing compound. Through its lipophilic character, amiodarone tends to accumulate in organs with a high lipid content [1]. Extensive tissue binding of amiodarone results in a pharmacokinetic profile with a high volume of drug distribution and an extremely long elimination half-life (t½ = 30-108 days) [2]. Although amiodarone possesses a high level of effectiveness in treating supraventricular and ventricular arrhythmia, associated adverse effects continue to be observed in different organs, and amiodarone pulmonary toxicity is one of the most discussed. Interstitial pneumonitis, eosinophilic pneumonia, organizing pneumonia, acute respiratory distress syndrome, diffuse alveolar hemorrhage, pulmonary nodules and solitary masses, and pleural effusion had been ever reported [3]. In our case, amiodarone pulmonary toxicity presented as multiple pulmonary nodules and masses on the chest radiograph.

Case Report

A 70-year-old man presented to our hospital with symptoms of nausea, decreased appetite and weight loss of six kilograms in

[1]Division of Chest Medicine, Department of Internal Medicine, National Taiwan University Hospital, Taiwan.
Address reprint requests to: Dr. Rou-Jun Chou, Division of Chest Medicine, Department of Internal Medicine, National Taiwan University Hospital, Taiwan. No. 7, Zhongshan S. Rd., Zhongzheng Dist., Taipei City 100225, Taiwan.

three months (a 10.3% decrease in baseline body weight). He was an ever-smoker with a 10-pack-year history, and had quit cigarette smoking 20 years before this presentation.

One and a half years before this presentation, the patient had experienced an episode of atrial flutter with a rapid ventricular rate, followed by in-hospital cardiac arrest after bolus injection of verapamil in a total dose of 15 mg. Spontaneous circulation was restored after cardio-pulmonary-cerebral resuscitation for 15 minutes without neurologic sequelae. Persistent atrial flutter was diagnosed and amiodarone in a 200-mg daily dose was prescribed beginning during hospitalization. Due to the symptoms of palpitation and persistent atrial flutter on electrocardiogram during outpatient follow-up, the dose of amiodarone was up-titrated to 200 mg twice daily one year prior to this presentation.

On this presentation, the patient's temperature was 36.4°C, heart rate was 99 beats per minute, respiratory rate was 16 breaths per minute, and blood pressure was 102/72 mmHg. Inspiratory crackles were noticed at the bilateral lower lungs, and the remainder of the physical examination was unremarkable. Laboratory studies revealed leukocytosis, elevated C-reactive protein (CRP) level, abnormal liver function with high aspartate aminotransferase (AST), high alanine transaminase (ALT), and high carcinoembryonic antigen (CEA) and carbohydrate antigen 19-9 (CA-199) levels. White blood cell count was 10.880 k/uL, CRP was 7.57 mg/dL, AST was 132 U/L, ALT was 207 U/L, total bilirubin (T-bil) was 1.13 mg/dL, direct bilirubin (D-bil) was 0.15 mg/dL, alkaline phosphatase (ALP) was 159 U/L, gamma-glutamyl transferase (GGT) was 387 U/L, CEA was 15.84 ng/mL, and CA-199 was 51.45 U/mL. Thyroid function was within normal range.

The chest radiograph showed ill-defined opacities at the bilateral basal lungs with bilateral blunted costophrenic angles (Figure 1). The esophagogastroduodenoscopy and colonoscopy yielded unremarkable results. Computed tomography (CT) of the chest, abdomen, and pelvis revealed multifocal pleural-based irregular confluent nodules and masses at the bilateral lower lobes, and inferior lingual segment of the left upper lobe, with increased attenuation at the non-contrast phase, also contrast enhancement and central necrosis. Bilateral mild pleural effusion and suspicious pleural nodularity in the deep sulcus of the right inferior costophrenic angle, and increased attenuation of the liver parenchyma were also noticed (Figure 2). The attenuation value of the liver at the unenhanced phase was 80 to 110 Hounsfield units (HU) (normal liver: 55 to 65 HU), and the left lower

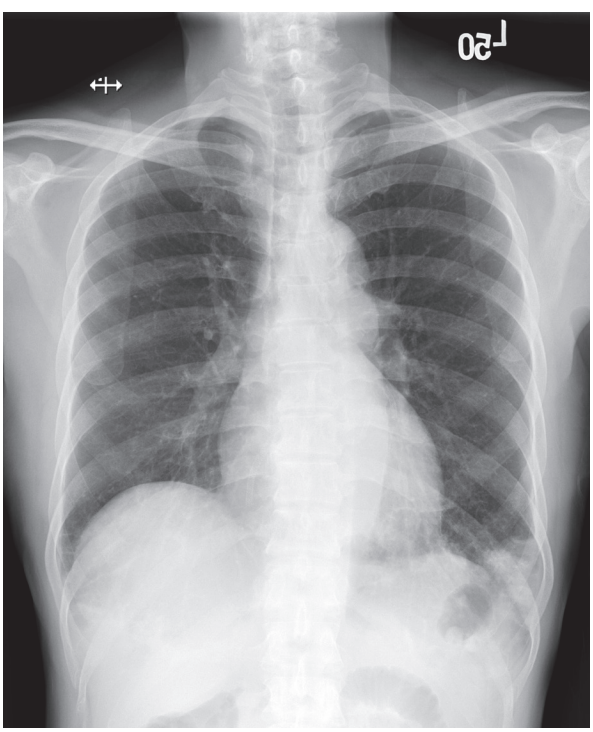

Fig. 1. Chest radiograph on admission.

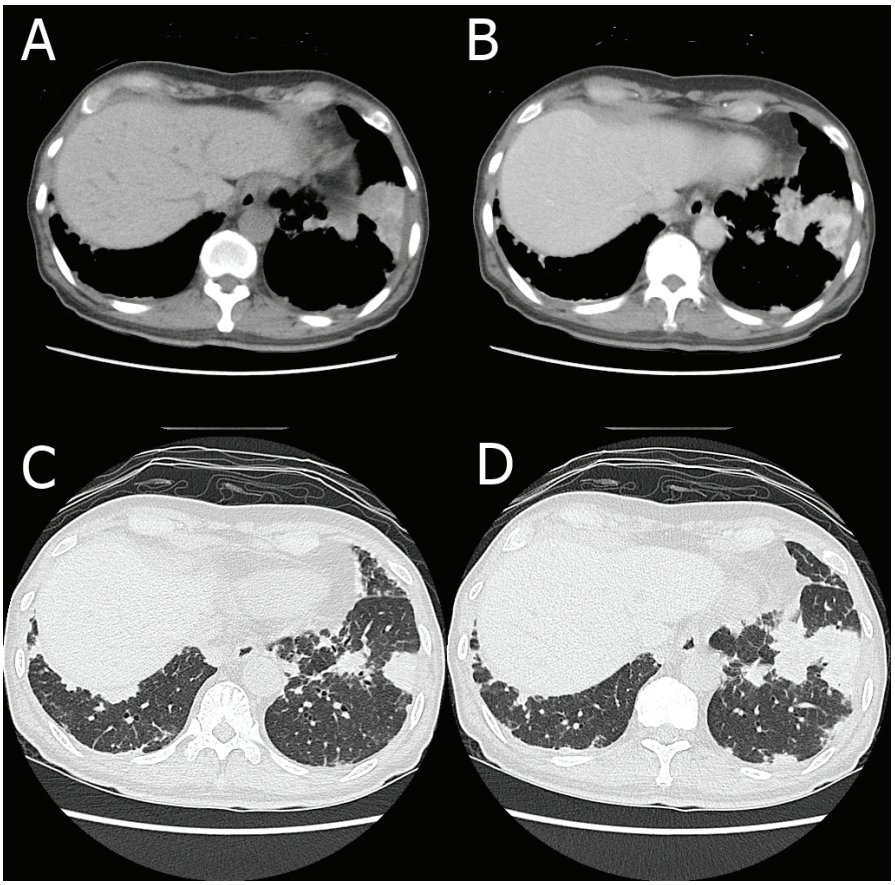

Fig. 2. Chest computed tomography: (A) Non-contrast phase, (B) contrast-enhanced phase, (C) and (D) lung window.

lung nodule was 50 to 100 HU, which were both higher than normal values. Given that the possibility of malignancy was not excluded, ultrasound-guided lung biopsy of the left lower lobe pleural-based nodule was performed. Pathology demonstrated abundant finely vacuolated foamy macrophages in the alveoli, with foci of fibrinous exudate, necrotic debris and fibrosis (Figure 3). The findings were morphologically compatible with amiodarone-induced pneumonitis.

Due to the diagnosis of amiodarone pulmonary toxicity, amiodarone was withdrawn and replaced with bisoprolol. Treatment with prednisone (25 mg per day, corresponding to

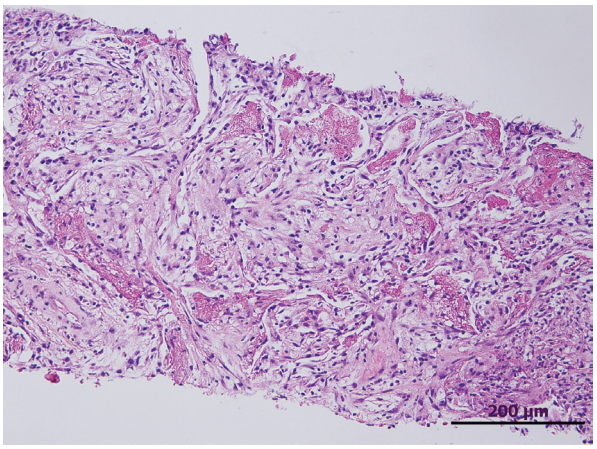

Fig. 3. Biopsy specimen of the lung reveals diffuse alveolar damage and vacuolated foamy macrophages in alveoli (hematoxylin and eosin stain).

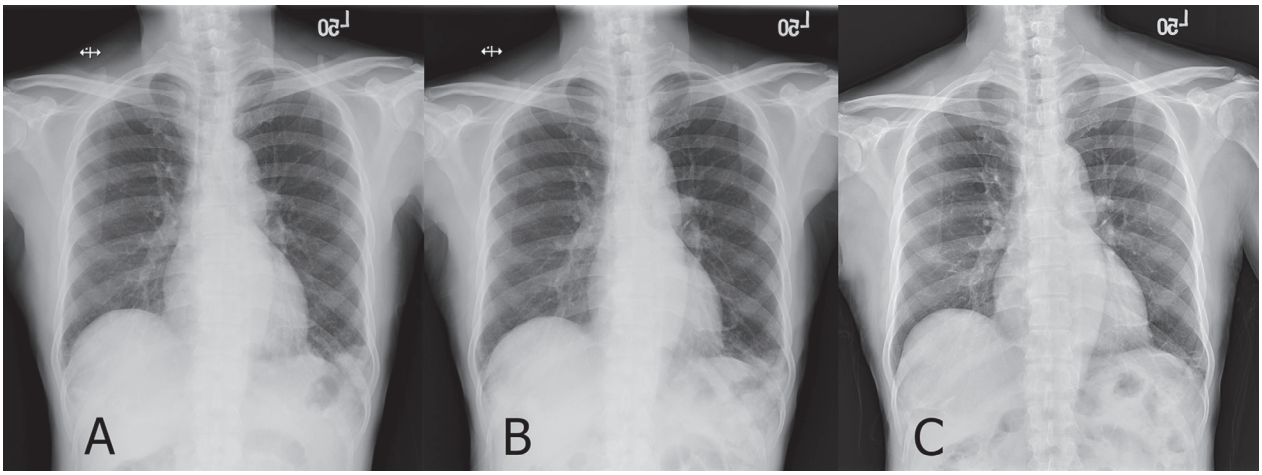

Fig. 4. Serial chest radiography: (A) On admission day, (B) three weeks after starting prednisolone treatment, (C) six months after starting prednisolone treatment.

≅0.5 mg/kg/day) was started, with a gradual taper within six months. Fever resolved after two days of prednisolone treatment. The chest radiograph repeated three weeks after starting prednisolone treatment showed partial resolution of the parenchymal opacity in the bilateral lower lung field. After six months of treatment, almost all lung fields were clear, with only mild ground glass opacity at the left costophrenic angle (Figure 4). Electric cardioversion of atrial flutter was performed under anticoagulant later, and the patient's cardiac rhythm returned to sinus rhythm.

Discussion

The incidence of amiodarone pulmonary toxicity has varied in past studies. A retrospective cohort study conducted in Japan reported the epidemiology of amiodarone pulmonary toxicity, which was defined as a new onset of pulmonary symptoms such as dyspnea, cough, pleuritic chest pain, and fever, in combination with new radiographic findings in patients without evidence of congestive heart failure, infectious disease or malignancy that subside with drug withdrawal. In this study, the incidence was 4.2%, 7.8%, and 10.6% at 1, 3, and 5 years, respectively, under a mean maintenance dose of 141 mg daily [4]. Of note, the duration and intensity of amiodarone treatment are important risk factors. A cumulative dose above 10 g, and up to 150 g, per se, increases the risk for pulmonary toxicity. Age is also a risk factor. Amiodarone pulmonary toxicity increases 3-fold for every 10 years of age in patients aged >60 years compared with those aged <60 years [5].

Amiodarone pulmonary toxicity usually develops after a few months or up to years into treatment. The clinical manifestations of amiodarone pulmonary toxicity, such as nonproductive cough, dyspnea, fever, body weight loss, and pleuritic pain, are usually insidious, evolving and nonspecific [6]. Physical examinations sometimes reveal bilateral inspiratory crackles. The most common presentation on a chest radiograph is subacute patchy or diffuse infiltrates that involve the lung bilaterally [7].

Chest radiograph plays an important role in the diagnosis of amiodarone pulmonary toxicity, and high-resolution CT (HRCT) is often utilized to clarify the radiographic pattern and distribution of abnormalities. Interstitial pneumonitis is the most common presentation of amiodarone pulmonary toxicity, and reveals itself as diffuse or localized, reticular, consolidative or mixed opacities, changes that may be migratory and asymmetric [8, 9, 10]. Other HRCT findings related to amiodarone pulmonary toxicity include diffuse ground glass opacities, septal thickening, honeycombing, traction bronchiectasis, pleural thickening, and less commonly pleural effusions.

A distinctive feature of amiodarone pulmonary toxicity on chest radiograph is the presentation of focal, homogenous pulmonary opacities, which typically are peripheral in distribution and of high attenuation on CT. The area of high attenuation may present in the lungs, as well as in the liver and spleen, due to the accumulation of iodinated amiodarone in tissue macrophages [11-12]. The finding of high attenuation is specific for amiodarone use, but is more considered as an indicator of amiodarone exposure rather than toxicity, which may be present in patients without pulmonary toxicity.

The histopathologic findings of amiodarone pulmonary toxicity include septal thickening, interstitial edema, nonspecific inflammation and fibrosis, and intra-alveolar accumulation of foamy macrophages. The foamy macrophage is due to amiodarone-phospholipid complexes, which is a unique feature of amiodarone pulmonary toxicity. The macrophages have finely vacuolated cytoplasm at the light microscopic level and contain distinctive cytoplasmic lamellar inclusions ultrastructurally [13]. Foamy alveolar macrophages are also seen in patients without toxicity who are taking amiodarone, and are considered as a marker of amiodarone exposure rather than toxicity [14]. Other findings include organizing pneumonia, acute organizing and fibrinous pneumonia, diffuse alveolar damage, hyperplasia of type II cells and acute respiratory distress syndrome (ARDS) [6, 13].

Lung biopsy is helpful in establishing a confident diagnosis of amiodarone pulmonary toxicity; however, it is not indicated for every patient. The diagnosis of amiodarone pulmonary toxicity is a diagnosis of exclusion. While lung biopsy is the gold standard for diagnosis, a clinical diagnosis can often be made when the clinical and radiologic findings are consistent, other possibilities have been excluded, and the patient improves with amiodarone cessation with or without a trial of glucocorticoid therapy.

Patients with mild symptoms and normal oxygenation can be observed off amiodarone without glucocorticoids. There is no current guideline or evidence to guide the dosing and duration of corticosteroid therapy. Generally, prednisolone is started in doses of 40 to 60 mg daily, and tapered slowly. Because of the long elimination half-life of amiodarone, pulmonary toxicity may progress initially despite amiodarone cessation. Prolonged therapy with glucocorticoids, on the order of months, may be required [10, 15]. The prognosis of amiodarone lung disease is generally favorable when diagnosed early. In one study, three-fourths of patients stabilized or improved after withdrawal of amiodarone with or without glucocorticoid treatment [16]. However, more advanced disease may result in pulmonary fibrosis. Mortality is highest among those who develop ARDS.

Conclusion

Given the frequency and potential severity of amiodarone pulmonary toxicity, early detection is desirable. The current guideline suggests obtaining a baseline and annual chest radiography for screening as long as patients remain on amiodarone treatment [15]. Clinicians should be alert to unexplained cough, dyspnea, or abnormal chest radiograph findings in patients, especially in those who are older and on a higher dose of amiodarone. With prompt diagnosis, most patients respond favorably to the withdrawal of amiodarone and the administration of corticosteroids.

References

1. Adams PC, Holt DW, Storey GC, *et al*. Amiodarone and its desethyl metabolite: tissue distribution and morphologic changes during long-term therapy. Circulation. 1985; 72: 1064-1075
2. Papiris SA, Triantafillidou C, Kolilekas L, *et al*. Amiodarone: review of pulmonary effects and toxicity. Drug Saf. 2010; 33(7): 539-558.
3. Mason JW. Amiodarone. N Engl J Med. 1987; 316(8): 455-466.
4. Yamada Y, Shiga T, Matsuda N, *et al*. Incidence and predictors of pulmonary toxicity in Japanese patients receiving low-dose amiodarone. Circ J. 2007; 71(10): 1610-1616.
5. Ernawati DK, Stafford L, Hughes JD. Amiodarone-induced pulmonary toxicity. Br J Clin Pharmacol. 2008; 66(1): 82-87.
6. Camus P, Martin WJ, Rosenow EC. Amiodarone pulmonary toxicity. Clin Chest Med. 2004; 25(1): 65-75.
7. Rossi SE, Erasmus JJ, McAdams HP, *et al*. Pulmonary drug toxicity: radiologic and pathologic manifestations. Radiographics. 2000; 20(5): 1245-1259.
8. Dean PJ, Groshart KD, Porterfield JG, *et al*. Amiodarone-associated pulmonary toxicity. A clinical and pathologic study of eleven cases. Am J Clin Pathol. 1987; 87(1): 7-13.
9. Standertskjöld-Nordenstam CG, Wandtke JC, Hood WB Jr, *et al*. Amiodarone pulmonary toxicity. Chest radiography and CT in asymptomatic patients. Chest. 1985; 88(1): 143-145.
10. Wolkove N, Baltzan M. Amiodarone pulmonary toxicity. Can Respir J. 2009; 16(2): 43-48.
11. Kuhlman JE, Teigen C, Ren H, *et al*. Amiodarone pulmonary toxicity: CT findings in symptomatic patients. Radiology. 1990; 177(1): 121-125.
12. Siniakowicz RM, Narula D, Suster B, *et al*. Diagnosis of amiodarone pulmonary toxicity with high-resolution computerized tomographic scan. J Cardiovasc Electrophysiol. 2001; 12(4): 431-436.
13. Bedrossian CW, Warren CJ, Ohar J, *et al*. Amiodarone pulmonary toxicity: cytopathology, ultrastructure, and immunocytochemistry. Ann Diagn Pathol. 1997; 1(1): 47-56.
14. Schwaiblmair M, Berghaus T, Haeckel T, *et al*. Amiodarone-induced pulmonary toxicity: an under-recognized and severe adverse effect? Clin Res Cardiol. 2010; 99(11): 693-700.
15. Goldschlager N, Epstein AE, Naccarelli GV, *et al*. A practical guide for clinicians who treat patients with amiodarone: 2007. Heart Rhythm. 2007; 4(9): 1250-59.
16. Coudert B, Bailly F, Lombard JN, *et al*. Amiodarone pneumonitis. Bronchoalveolar lavage findings in 15 patients and review of the literature. Chest. 1992; 102(4): 1005-12.

Think Outside the box in Cases of Severe Asthma Attack-Refractory Pulmonary Embolism in Severe Asthma: A Case Report and Literature Review

Yang Li[1], Ruei-Lin Sun[1], Kang-Cheng Su[1,2]

The interplay between thrombosis and inflammation has been recognized in the past decade. Asthma, one of the most common chronic inflammatory diseases, may increase the risk of pulmonary embolism (PE), particularly in those with higher asthma severities and coexisting risks for PE. While asthmatics may present to an emergency department with acute dyspnea, PE is not usually considered an attributable cause at first. However, PE can be life-threatening if timely diagnosis and management are delayed. We reported an obese female with severe asthma presenting with acute dyspnea due to coexisting PE, which was unrecognized initially and resulted in cardiopulmonary compromise requiring advanced life support with extracorporeal membrane oxygenation. Although emergency reperfusion therapy with ultrasound-assisted catheter-directed thrombolysis and concurrent infusion of thrombolytic agents failed, she was rescued with a 2nd course of thrombolytic therapy. The association between PE and asthma, as well as the risks and treatment for PE are reviewed in this article. ***(Thorac Med 2023; 38: 357-365)***

Key words: pulmonary embolism; severe asthma; thrombolytic therapy; ultrasound-assisted catheter-directed thrombolysis

Introduction

The interplay between thrombosis and inflammation has been recognized in the past decade 1. Asthma is one of the most common chronic inflammatory diseases and growing evidence has shown that the balance between coagulation and fibrinolysis is disturbed in asthma 2. Epidemiologic studies have reported that asthma is associated with an increased risk of pulmonary embolism (PE), in both European 3 and Asian 4 countries, and severe asthma further enhances the risk of PE 3,4. Obesity poses a shared risk for severe asthma, cancer, and cardiovascular and venous thromboembolic disease 5. Dyspnea is a common presentation of asthma and PE, but PE is not usually considered as the first tentative diagnosis when asthma patients present to an emergency department (ED) with acute dyspnea. However, delayed diagno-

[1]Department of Chest Medicine, Taipei Veterans General Hospital, Taipei, Taiwan, R.O.C. [2]School of Medicine, College of Medicine, National Yang Ming Chiao Tung University, Taipei, Taiwan.
Address reprint requests to: Dr. Kang-Cheng Su, Department of Chest Medicine, Taipei Veterans General Hospital, No. 201, Sec. 2, Shipai Road, Beitou District, Taipei City 11217, Taiwan, ROC

sis of PE may result in a catastrophic outcome. We report an obese female with severe asthma who presented to our ED with acute dyspnea. Coexisting PE was not diagnosed initially, and once it was diagnosed, the PE was refractory to emergency reperfusion therapy. However, the patient was finally rescued by a 2nd course of thrombolytic therapy. The pitfalls of delayed diagnosis and treatment of refractory PE are discussed below.

Case Report

This 54-year-old, non-smoking, obese (body mass index (BMI): 36.8) woman had a medical history of hypertension, gastroesophageal reflux disease and allergic rhinitis in past years. At the age of 51, she was diagnosed as having severe, allergic asthma in our pulmonary clinics, based on the manifestations of uncontrolled asthma symptoms and frequent unscheduled visits. She was allergic to cockroaches with an initial blood total immunoglobulin E level of 120 IU/mL (reference < 200 IU/mL). Thereafter, she received regular triple therapy (high doses of inhaled corticosteroids/long-acting beta-agonist plus long-acting muscarinic antagonist) for asthma control. During the past 3 years, she had constant but low forced expiratory volume in the first second (FEV_1, ranging from 60% to 65% of the predicted value), and intermediate peripheral blood eosinophils (between 100 and 200 cells/μL). She was exacerbation-free, with an asthma control test score of 22 to 24 in the absence of biological treatment.

Three days prior to this admission (day -3), she called our ED due to an episode of syncope and acute dyspnea lasting for hours. On arrival, she was hemodynamically stable, and room-air pulse oximetry (SpO_2) was 90-93% during this ED stay (baseline 98% at our pulmonary clinic). Her chest X-ray (CXR) showed cardiomegaly with slightly more prominent perihilar vasculature with interstitial infiltration, compared with the previous CXR (Fig. 1A and 1B). Her electrocardiogram (ECG) showed new changes in the S1T3Q3 pattern and right ventricle strain (vs. the previous ECG, Fig. 2A and 2B). Physical examinations showed no significant abnormalities, except mild bilateral leg pitting edema and transient wheezing in bilateral lungs. Serial workups, including a brain computed tomog-

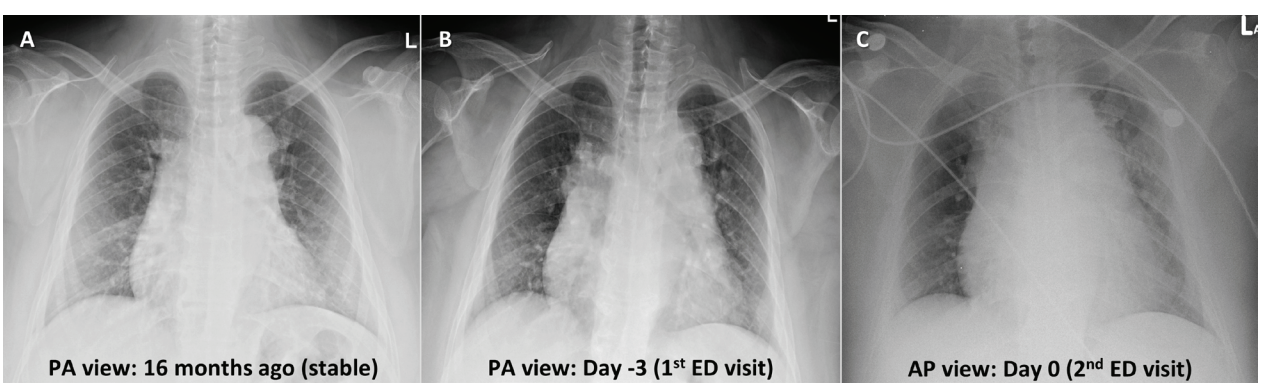

Fig. 1. Serial CXR findings. Compared with the previous CXR showing a stable status (A), the CXR taken 3 days prior to this admission (day -3) reveals stationary cardiomegaly, but more prominent perihilar vascularity (B). On admission day (day 0), the CXR shows findings similar to those of day -3 (C). CXR, chest X-ray; ED, emergency department; AP, anterior posterior; PA, posterior anterior.

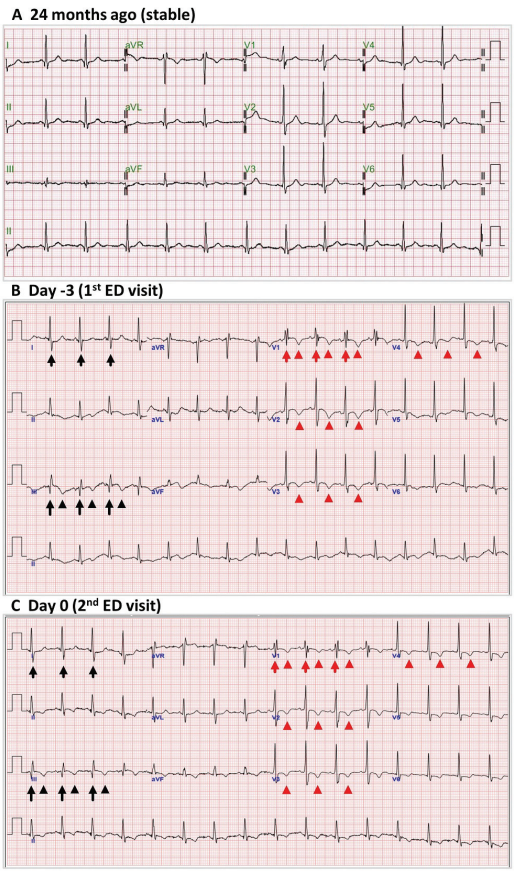

Fig. 2. Serial ECG findings. Compared with the previous ECG with the patient in a stable status (A), the ECG 3 days prior to this admission (day -3) reveals S1 (deep S wave in lead I, short black arrow), Q3 (deep Q wave in lead III, black arrow), T3 (T wave inversion in lead III, black arrowhead), RBBB in lead V1 (short red arrow) and T-inversion in leads V1 to V4 (red arrowhead) (B). On admission day (day 0), the ECG shows similar findings (vs. day -3) (C). ECG, electrocardiogram; RBBB, right bundle branch block.

raphy (CT), hemograms, biochemistry and repetitive cardiac enzyme tests were all negative, except for elevated NT-pro-BNP (1754 pg/mL, reference value < 450 pg/mL).

She was managed as having had an asthma attack and heart failure with fluid overloading, monitored closely for 1 day, and then discharged in stable condition after relief of symptoms on the next day. Unfortunately, she called our ED again 2 days after discharge (day 0) due to dyspnea recurrence and chest tightness for 2 hours. At arrival, she presented with stable hemodynamics, but developed respiratory distress and significant hypoxemia (arterial blood oxygen 153 mmHg under 100% oxygen supplement). Physical examinations revealed no significant abnormalities (neither wheezing nor cardiac murmur), except for mild bilateral lower leg pitting edema. The CXR and ECG showed findings similar to those of the previous tests on day -3 (Fig. 1C and 2C). All blood test results were within normal limits, except for elevated levels of D-dimer (20.12 μg/mL, reference < 0.5 μg/mL) and NT-pro-BNP (4036 pg/ml).

The emergency chest CT pulmonary angiography (CTPA) revealed massive bilateral PE in bilateral main pulmonary arteries and their proximal branches (Fig. 3A1 to 3A4). Moreover, the lower limb Doppler echo found deep vein thrombosis (DVT) formation in the right-side popliteal and femoral veins and left-side popliteal vein. She was immediately admitted to the intensive care unit (ICU) for respiratory support with non-invasive positive pressure ventilation and reperfusion therapy on the same day (day 0). She received emergency ultrasound-assisted catheter-directed thrombolysis (UACDT) , using the Ekosonic Endovascular System (EKOS, BTG International Ltd, London, United Kingdom), on day 0, and concurrent thrombolytic therapy with continuous intravenous (IV) urokinase (UK) infusion for 3 days (days 0-2). The inferior vena cava (IVC) filter was not placed due to her personal issues of the patient.

However, she developed profound hypoxemia, hypercapnia and cardiogenic shock on day 1, and was rescued with mechanical ventilation and venoarterial extracorporeal membrane oxygenation (VA-ECMO) for cardiopulmonary

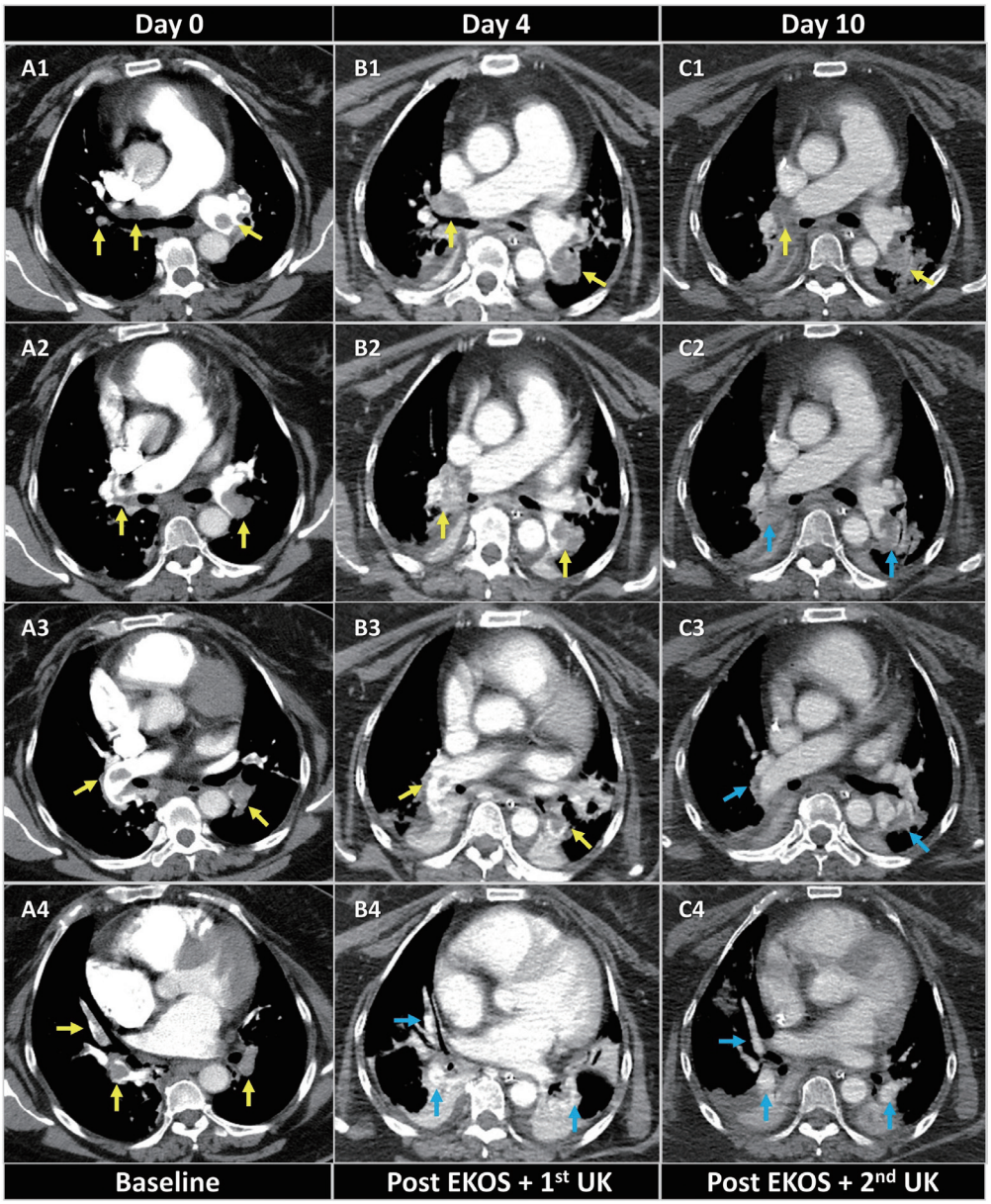

Fig. 3. Serial chest CTPA findings. The chest CTPA taken on day 0 reveals significant filling defects in bilateral main pulmonary arteries and their proximal branches (yellow arrow, A1 to A4). Three days after the initial ultrasound-assisted catheter-directed thrombolysis, using the Ekosonic Endovascular System (EKOS) and the first course of continuous intravenous infusion of urokinase (UK), the CTPA on day 4 shows no significant resolution of the previous filling defects (yellow arrow, B1 to B3), except for the lower lobe arterial branches (blue arrow, B4). On day 10, the CTPA shows partially regressive changes in some branches (blue arrow, C2 to C4) during the 2nd course of prolonged UK infusion. CTPA, computed tomographic pulmonary angiography.

support. On day 3, the thrombolytic agent was shifted to recombinant tissue plasminogen activator (rt-PA, Actilyse) 50 mg because there was little improvement in the cardiopulmonary compromise. On day 4, a CTPA was repeated, which showed non-resolved PE (Fig. 3B1 to 3B3), except for bilateral lower arterial branches (Fig. 3B4). Therefore, she received a 2nd

course of IV UK infusion from day 4 to day 8.

On day 5, the patient experienced deterioration of hypoxemia and unstable hemodynamics while on VA-ECMO. Consequently, the ECMO support was upgraded to veno-arterial-venous (VAV)-ECMO. Fortunately, her oxygenation and hemodynamics gradually improved. On day 9, VAV-ECMO was shifted to venovenous (VV)-ECMO, followed by the successful removal of ECMO on day 13. Anticoagulant therapy with a heparin pump was maintained until removal of ECMO. On day 10, repeated CTPA revealed gradual resolution of the previous PE (Fig. 3D2-3D4). The serial changes in the P/F ratio (the ratio of arterial oxygen partial pressure [PaO_2 in mmHg] to fractional inspired oxygen [FiO_2]) and the treatment course are illustrated in Figure 4. During the systemic thrombolytic course, several bleeding complications occurred, and then subsided after adjustment of the UK doses and supportive care. Subsequently, her anticoagulation therapy was shifted to long-term use of a direct oral anticoagulant (DOAC, edoxaban). After stabilization of the cardiopulmonary compromise, her consciousness level was clear (Glasgow Coma Scale score: E4VtM6). A cancer survey was performed due to refractory PE, and high-grade endometrial carcinoma was diagnosed. After intensive treatment, she was discharged with tracheostomy and ventilator support due to difficult weaning and readmission for cancer treatment was scheduled.

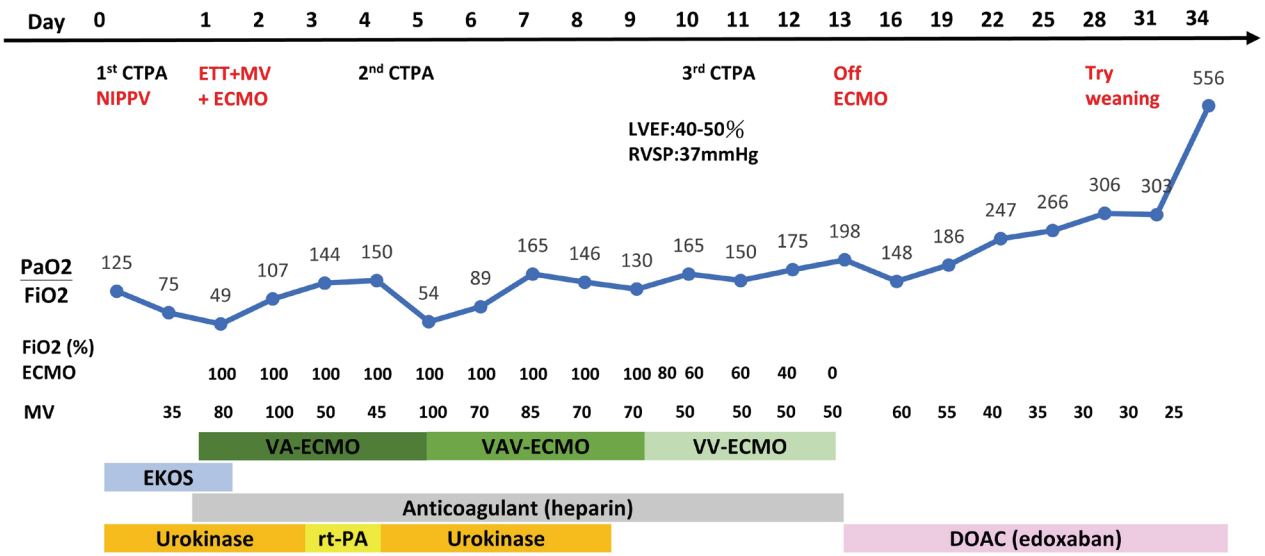

Fig. 4. Main clinical course. The ratio of PaO_2 to FiO_2 did not improve after the emergency ultrasound-assisted catheter-directed thrombolysis by EKOS (day 0) and the concurrent first course of UK infusion. The patient was supported by the MV and VA-ECMO on day 1. Thrombolytic therapy was used with UK for the first course (day 0 to day 2), followed by rt-PA on day 3, and the 2nd course of UK (day 4 to day 8). The VA-ECMO was changed to VAV-ECMO on day 5. The patient's oxygenation and hemodynamic status gradually improved. The ECMO was changed to a VV-mode on day 9, and removed successfully on day 13. Anticoagulant therapy was applied, using a heparin pump from day 0 to day13, followed by long-term oral DOAC with edoxaban. CTPA, computed tomographic pulmonary angiography; DOAC, direct oral anticoagulant; ETT, endotracheal intubation; LVEF, left ventricular ejection fraction; NIPPV, non-invasive positive pressure ventilation; MV, mechanical ventilation; RVSP, right ventricular systolic pressure; VA-ECMO, venoarterial extracorporeal membrane oxygenation; VAV, veno-arterial-venous; VV, venovenous.

Discussion

We have learned important lessons from this case, regarding the association between asthma and PE, the diagnosis of PE in asthma patients, and the treatment of massive and refractory PE.

The association between asthma and PE

Increasing evidence suggests that asthma is been associated with dysregulated procoagulant and antifibrinolytic activities in the airways. The mechanisms include enhanced coagulation driven by overexpressed tissue factor, impaired anticoagulation through reduced activity of the protein C system, and suppressed fibrinolysis through decreased activity of plasminogen [2,6,7]. In particular, plasminogen can be transformed to plasmin to exert a fibrinolytic process through tissue-type plasminogen activator (tPA) or UK-type plasminogen activator [2]. In severe asthma, this dysregulation can further progress [8].

However, the mechanism linking the locally dysregulated coagulation in the airways to systemic thromboembolic disease, such as PE and DVT, remains largely unknown. Notably, airway inflammation is associated with circulatory hemostatic activation, based on the findings that asthma patients (vs. non-asthmatics) have presented elevated blood markers of endothelial injury [9], pro-coagulation [9-12], and reduced markers of fibrinolysis [10-11]. In additional, a nationwide cohort study by Chung *et al*. found that asthma patients had a 3.24-fold increase in the risk of developing PE compared with that in the general population [4]. Majoor *et al*. also showed a higher incidence of PE in severe asthma patients than in mild-to-moderate asthmatics, and concluded that oral corticosteroid (OCS) use and severe asthma were independent risk factors for PE (hazard ratio: 2.82 and 3.33, respectively) [3].

Moreover, a significant relationship between the frequency of ED visits for asthma exacerbations and the incidence of PE has been reported [13]. Alzghoul *et al*. reported that around one-fifth of patients with exacerbating asthma patients had coexisting acute PE proven by CTPA [14]. The overall in-hospital mortality for asthma exacerbations has been 0.5% in the United States [15]. However, compared with PE-free exacerbating asthmatics, those with coexisting PE had higher ICU admission rates, longer hospitalization periods, and a significantly elevated mortality rates, up to 4% [14]. Factors associated with acute PE included previous history of PE or DVT, high CHA2DS2-VASc scores, heart failure, malignancy, chronic OCS use, high BMI, and atrial fibrillation [14]. In this case, the risk factors for PE included severe asthma, obesity, heart failure, and occult endometrial cancer. Therefore, physicians should recognize that asthma patients are at higher risk of PE, and they must be aware of the possibility of the existence of PE while treating exacerbating asthma patients, particularly in those with higher severity and coexisting risks for PE.

Diagnosis of PE in asthma patients

Distinguishing PE from asthma exacerbation based on symptoms and signs is challenging since both diseases share some common manifestations, such as dyspnea, tachycardia, chest tightness, and cough, and CXR findings are usually unreliable for differential diagnosis. Wheezing is a typical sign of asthma exacerbation, but 10% of PE patients might also present wheezing [16]. Some manifestations, such as pre-syncopal or syncopal episode associated

with hypoxia, are more likely to be ascribed to PE; in addition, oxygen is often preserved in asthma exacerbation, but might be reduced in PE, even in the absence of an additional acute lung pathology (e.g., pneumonia, pulmonary edema, pneumothorax, etc.) [17]. Blood D-dimer and BNP levels might be higher in asthmatics with PE (vs. without PE) [14]. Elevated levels of cardiac enzyme and D-dimer are frequently found in acute diseases or cofounded with coexisting cardiovascular diseases, thus providing little diagnostic value; however, a negative D-dimer test usually effectively rules out significant PE [17]. Twelve-lead ECG can provide useful but non-specific findings suggestive of PE, including sinus tachycardia, atrial dysrhythmia, a dramatic shift in R wave axis, incomplete or complete right bundle-branch block, a QR pattern in lead V1, inferolateral ST elevation or depression, inversion of T waves in leads V1–V4, and classic S1Q3T3 changes [17].

Pragmatic advice for early diagnosis of PE is always to maintain a high level of suspicion of PE as a cause of acute deterioration and/or less responsiveness to conventional asthma treatment. Subsequently, a CTPA will confirm the diagnosis of PE. In our patient's 1st ED visit, we retrospectively identified 3 pitfalls suggestive of PE, including syncope, a trivial but potentially important decline of SpO_2 (90-93% during her ED stay vs. 98% at baseline), and unawareness or neglect of the ECG abnormalities. PE might appear with obscure clinical manifestations. Physicians should always maintain a high level of clinical suspicion and familiarize themselves with the diagnostic clues for timely diagnosis and treatment.

Treatment of massive and refractory PE

Delayed diagnosis of PE is linked to a reduced response to thrombolysis. Acccording to a report, each additional day of symptoms before PE thrombolysis resulted in a decrement of 0.8% of lung tissue reperfusion on lung scanning [18]. This is of particular importance for both submassive (intermediate-risk) and massive (high-risk) PE, because they are associated with a substantial risk of death due to right ventricular failure and hemodynamic instability [19-20]. In hemodynamically unstable patients, reperfusion therapy with systemic thrombolytic agents, surgical embolectomy, or catheter-directed thrombolytic therapy (CDT) is mandatory. However, selection of appropriate treatment modalities remains challenging, when considering the risks of death from PE, bleeding from the thrombolytic agents, or surgical complications. CDT emerges a possible substitute for systemic thrombolysis and surgical embolectomy, especially in patients at intermediate-to-high risk of bleeding, because CDT can reduce the doses of thrombolytic agents [19]. Catheter-based therapy is also an option for those failing systemic thrombolysis. The overall procedural success rate has been reported to be up to 87% [21].

UACDT is an innovative catheter-based approach; it accelerates clot dissolution and drug dispersion by using ultrasonic waves. The aforementioned EKOS is a type of UACDT, and was approved for the treatment of PE in 2014. Several trials have demonstrated the efficacy and safety of UACDT for massive and submassive PE [22-24], and some unfavorable predictors for reduced UACDT efficacy have been reported, including obesity (such as our case), renal or hepatic dysfunction and active smoking [20]. However, the treatment strategy for non-responders to initial systemic thrombolysis or UACDT remains unclear. In

this context, the use of VA-ECMO in the management of high-risk PE as a bridge to definite reperfusion therapy, has increased worldwide in the last decade [25]. Surgical embolectomy or repeated systemic thrombolytic therapy can be considered as a rescue strategy for definite reperfusion therapy after weighing the risks and benefits.

So far, some case studies have reported that repeated systemic thrombolytic therapy such as rt-PA, acted as a successful treatment strategy to rescue initially refractory PE, but the patients had bleeding complications requiring intensively supportive care [26]. However, the optimal agents to be used and the dose of thrombolytic therapy in the scenario of coexisting bleeding complications or repeated administration is unclear and may vary case by case. In our case, we successfully rescued the refractory PE with prolonged and repeated thrombolytic therapy. The reasons for refractory PE are complicated, and are supposed to be associated with delayed diagnosis and treatment, obesity, undiagnosed active cancer, and lack of placement of an IVC filter.

In conclusion, asthma patients have elevated risks for PE, particularly those with a higher severity and certain coexisting risks. Delayed diagnosis and treatment of PE is life-threatening. Physicians should always maintain a high degree of suspicion of PE in acute asthma patients, and must be familiarize with the diagnostic clues (e.g., S1Q3T3 in an ECG) of PE to avoid fatal outcomes.

References

1. Stark K, Massberg S. Interplay between inflammation and thrombosis in cardiovascular pathology. Nat Rev Cardiol. 2021;18(9):666-682.
2. de Boer JD, Majoor CJ, van 't Veer C, Bel EH, van der Poll T. Asthma and coagulation. Blood. 2012;119(14): 3236-44.
3. Majoor CJ, Kamphuisen PW, Zwinderman AH, *et al*. Risk of deep vein thrombosis and pulmonary embolism in asthma. Eur Respir J. 2013;42(3): 655-61.
4. Chung WS, Lin CL, Ho FM, *et al*. Asthma increases pulmonary thromboembolism risk: A nationwide population cohort study. Eur Respir J. 2014;43(3): 801-7.
5. Australian institute of health and welfare. Impact of overweight and obesity as a risk factor for chronic conditions- australian burden of disease study 2017; https://www.aihw.gov.au/getmedia/f8618e51-c1c4-4dfb-85e0-54ea19500c91/20700.pdf.aspx?inline=true.
6. Lee PH, Fu PK. Pulmonary embolism and severe asthma: Case report and literature review. Medicina (Kaunas). 2019;55(10): 647.
7. Corbett V, Hassouna H, Girgis R. In situ thrombosis of the pulmonary arteries: An emerging new perspective on pulmonary embolism. Med Student Res J. 2015;4(Winter): 54-58.
8. Brims FJ, Chauhan AJ, Higgins B, Shute JK. Coagulation factors in the airways in moderate and severe asthma and the effect of inhaled steroids. Thorax. 2009;64(12): 1037-1043.
9. Bazan-Socha S, Kuczia P, Potaczek DP, *et al*. Increased blood levels of cellular fibronectin in asthma: Relation to the asthma severity, inflammation, and prothrombotic blood alterations. Respir Med. 2018;141: 64-71.
10. Bazan-Socha S, Mastalerz L, Cybulska A, *et al*. Asthma is associated with enhanced thrombin formation and impaired fibrinolysis. Clin Exp Allergy. 2016;46(7):932-944.
11. Bazan-Socha S, Mastalerz L, Cybulska A, *et al*. Prothrombotic state in asthma is related to increased levels of inflammatory cytokines, il-6 and tnfalpha, in peripheral blood. Inflammation. 2017;40(4):1225-1235.
12. Sneeboer MMS, Majoor CJ, de Kievit A, *et al*. Prothrombotic state in patients with severe and prednisolone-dependent asthma. J Allergy Clin Immunol. 2016;137(6): 1727-1732.
13. Zoller B, Pirouzifard M, Memon AA, Sundquist J, Sundquist K. Risk of pulmonary embolism and deep venous thrombosis in patients with asthma: A nationwide

case-control study from sweden. Eur Respir J. 2017; 49(2).

14. Alzghoul BN, Reddy R, Chizinga M, *et al*. Pulmonary embolism in acute asthma exacerbation: Clinical characteristics, prediction model and hospital outcomes. Lung. 2020;198(4): 661-669.
15. Krishnan V, Diette GB, Rand CS, *et al*. Mortality in patients hospitalized for asthma exacerbations in the united states. Am J Respir Crit Care Med. 2006;174(6): 633-8.
16. Calvo-Romero JM, Perez-Miranda M, Bureo-Dacal P. Wheezing in patients with acute pulmonary embolism with and without previous cardiopulmonary disease. Eur J Emerg Med. 2003;10(4): 288-9.
17. Somasundaram K, Ball J. Medical emergencies: Pulmonary embolism and acute severe asthma. Anaesthesia. 2013;68 Suppl 1: 102-116.
18. Daniels LB, Parker JA, Patel SR, Grodstein F, Goldhaber SZ. Relation of duration of symptoms with response to thrombolytic therapy in pulmonary embolism. Am J Cardiol. 1997;80(2): 184-8.
19. Harvey JJ, Huang S, Uberoi R. Catheter-directed therapies for the treatment of high risk (massive) and intermediate risk (submassive) acute pulmonary embolism. Cochrane Database Syst Rev. 2022; 8(8): CD013083.
20. Sardar P, Piazza G, Goldhaber SZ, *et al*. Predictors of treatment response following ultrasound-facilitated catheter-directed thrombolysis for submassive and massive pulmonary embolism: A seattle ii substudy. Circ Cardiovasc Interv. 2020;13(6): e008747.
21. Bajaj NS, Kalra R, Arora P, *et al*. Catheter-directed treatment for acute pulmonary embolism: Systematic review and single-arm meta-analyses. Int J Cardiol. 2016;225: 128-39.
22. Pei DT, Liu J, Yaqoob M, *et al*. Meta-analysis of catheter directed ultrasound-assisted thrombolysis in pulmonary embolism. Am J Cardiol. 2019;124(9): 1470-77.
23. Kucher N, Boekstegers P, Muller OJ, *et al*. Randomized, controlled trial of ultrasound-assisted catheter-directed thrombolysis for acute intermediate-risk pulmonary embolism. Circulation. 2014;129(4): 479-86.
24. Avgerinos ED, Jaber W, Lacomis J, *et al*. Randomized trial comparing standard versus ultrasound-assisted thrombolysis for submassive pulmonary embolism: The sunset spe trial. JACC Cardiovasc Interv. 2021; 14(12): 1364-73.
25. Assouline B, Assouline-Reinmann M, Giraud R, *et al*. Management of high-risk pulmonary embolism: What is the place of extracorporeal membrane oxygenation? J Clin Med. 2022;11(16).
26. Poor AD, Poor HD. Successful treatment of refractory massive pulmonary embolism with repeated administration of systemic thrombolysis. Tanaffos. 2018;17(2): 127-31.